The Geological Society of America
Special Paper 552

New tectonic model and division of the Ubendian-Usagaran Belt, Tanzania: A review and in-situ dating of eclogites

Nelson Boniface*
University of Dar es Salaam, P.O. Box 35052, Dar es Salaam, Tanzania, and
Center for Northeast Asian Studies, Tohoku University, Aoba, Sendai 980-8576, Japan

Tatsuki Tsujimori
Center for Northeast Asian Studies, Tohoku University, Aoba, Sendai 980-8576, Japan, and
Department of Earth Science, Tohoku University, Aoba, Sendai 980-8578, Japan

ABSTRACT

Records of high-pressure/low-temperature (H*P*-L*T*) metamorphic interfaces are not common in Precambrian orogens. It should be noted that the association of H*P*-L*T* metamorphic interfaces and strongly deformed ocean plate stratigraphy that form accretionary prisms between trenches and magmatic arcs are recognized as hallmark signatures of modern plate tectonics. In East Africa (Tanzania), the Paleoproterozoic Ubendian-Usagaran Belt records a H*P*-L*T* metamorphic interface that we consider as a centerpiece in reviewing the description of tectonic units of the Ubendian-Usagaran Belt and defining a new tectonic model. Our new U-Pb zircon age and the interpretations from existing data reveal an age between 1920 and 1890 Ma from the kyanite bearing eclogites. This establishment adds to the information of already known H*P*-L*T* metamorphic events at 2000 Ma, 1890–1860 Ma, and 590–520 Ma from the Ubendian-Usagaran Belt. Arc–back-arc signatures from eclogites imply that their mafic protoliths were probably eroded from arc basalt above a subduction zone and were channeled into a subduction zone as mélanges and got metamorphosed. The Ubendian-Usagaran events also record rifting, arc and back-arc magmatism, collisional, and hydrothermal events that preceded or followed H*P*-L*T* tectonic events. Our new tectonic subdivision of the Ubendian Belt is described as: (1) the western Ubendian Corridor, mainly composed of two Proterozoic suture zones (subduction at 2000, 1920–1890, Ma and 590–500 Ma) in the Ufipa and Nyika Terranes; (2) the central Ubendian Corridor, predominated by metamorphosed mafic-ultramafic rocks in the Ubende, Mbozi, and Upangwa Terranes that include the 1890–1860 Ma eclogites with mid-ocean ridge basalt affinity in the Ubende Terrane; and (3) the eastern Ubendian Corridor (the Katuma and Lupa Terranes), characterized by reworked Archean crust.

*nelson.boniface@udsm.ac.tz, nelson_boniface@yahoo.co.uk

Boniface, N., and Tsujimori, T., 2021, New tectonic model and division of the Ubendian-Usagaran Belt, Tanzania: A review and in-situ dating of eclogites, *in* Wakabayashi, J., and Dilek, Y., eds., Plate Tectonics, Ophiolites, and Societal Significance of Geology: A Celebration of the Career of Eldridge Moores: Geological Society of America Special Paper 552, p. 133–175, https://doi.org/10.1130/2021.2552(08).

1. INTRODUCTION

Precambrian orogenic belts have significant records of hallmark signatures of subduction proxies, e.g., dismembered ocean plate stratigraphy and possible ophiolites, thrust-fold belts, arc magmas geochemical signatures, low-grade foreland basin sediments (Cawood et al., 2006, 2018; Kusky, et al., 2018). It should be noted that Wakita and Metcalfe (2005) defined the ocean plate stratigraphy as an idealized stratigraphic succession of the ocean floor, reconstructed from the protoliths of mélanges or ancient accretionary complexes. Ancient accretionary wedges, especially from the Phanerozoic orogenic belts, provide a comprehensive history of ocean plate subduction and have been recognized by the presence of blueschist, radiolarian chert, and mélanges (Wakita and Metcalfe, 2005). On the contrary, Precambrian orogenic belts have poor records of high-pressure–low-temperature (H*P*-L*T*) subduction interface metamorphism (eclogite–blueschist facies metamorphism) when compared with the Phanerozoic orogenic belts (e.g., Windley, 1995; Maruyama et al., 1996; Windley, 1998; Stern et al., 2013; Tsujimori and Ernst, 2014). Global example records of Precambrian H*P*-L*T* metamorphism in Africa include those found at the margins of the Congo Craton (Democratic Republic of Congo), in the Paleoproterozoic Nyong Complex (Cameroon), in the Paleoproterozoic Ubendian-Usagaran Belt (Tanzania) and others from Namibia, Mali, and Algeria (see Fig. 1; Möller et al., 1995; Collins et al., 2004; Schenk et al., 2006; Boniface and Schenk, 2007; Boniface et al., 2012; François et al., 2018). Precambrian eclogites or blueschists, mostly of the Neoproterozoic Era, are also reported from North America (Molson Lake and Snowbird) Asia (Delhi, Aksu, Banxi, and Heilongjiang) and Russia (Kola-Karelia) (Fig. 1; Volodichev et al., 2004; Mints et al., 2014).

In Tanzania, the Paleoproterozoic H*P*-L*T* metamorphic events (subduction) are recorded at the margins of the Tanzania Craton along the Ubendian and Usagaran Belts (Fig. 2). The Usagaran subduction event refers to a record of 2000 Ma H*P*-L*T* eclogites with MORB affinity at the southeastern margins of the Tanzania Craton whereas the Ubendian subduction event means

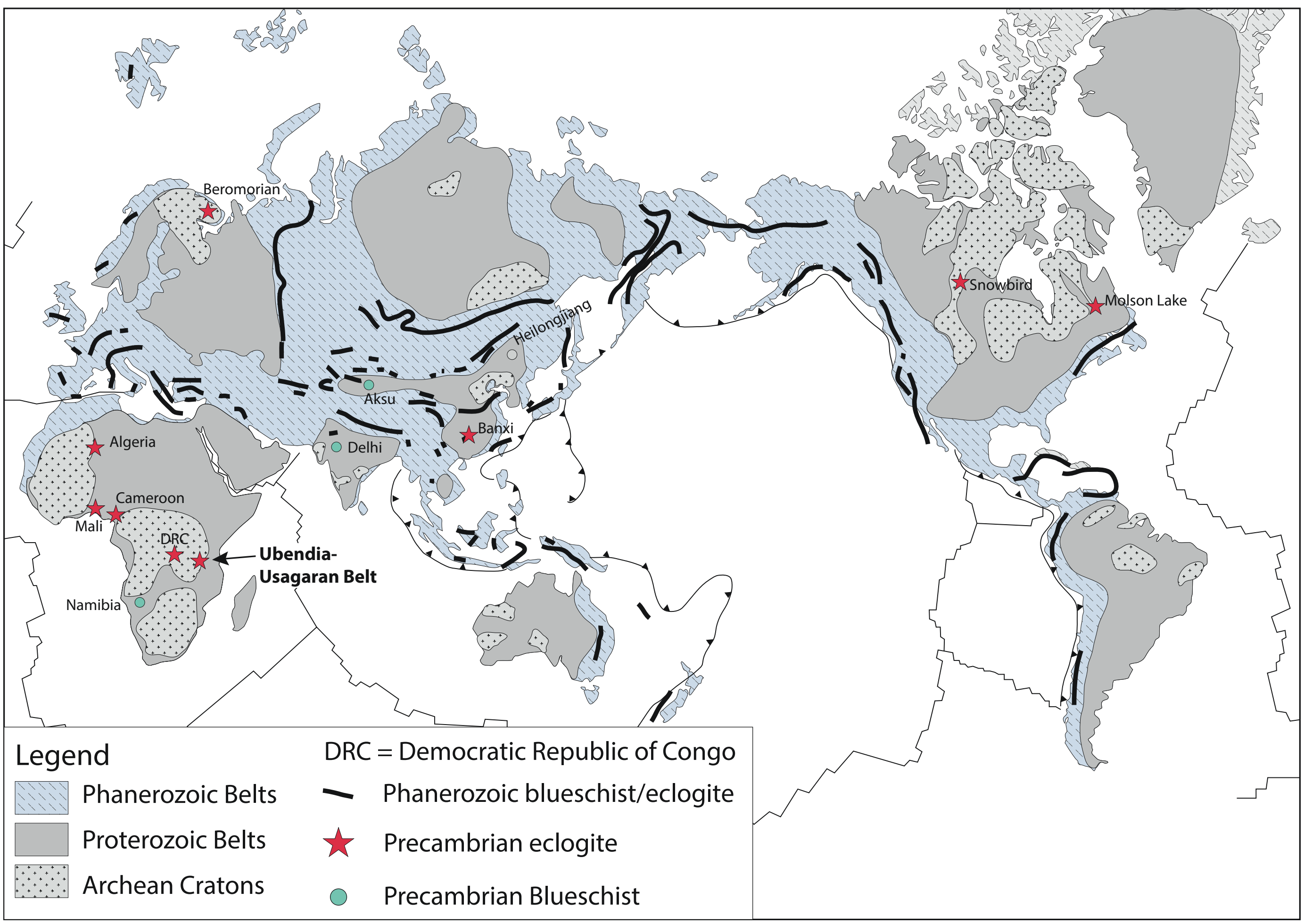

Figure 1. Global distribution Precambrian and Phanerozoic eclogite/blueschist and the location of the Ubendian-Usagaran Belt in Tanzania. The geological map was modified after Maruyama et al. (1996).

a record of 1890–1860 Ma H*P*-L*T* eclogites with MORB affinity at the southwestern margins of the Tanzania Craton (Fig. 2; Möller et al., 1995; Boniface et al., 2012). Interestingly, the Ubendian Belt records the recurrence of H*P*-L*T* metamorphic interface in the Neoproterozoic Era, ca. 590–500 Ma (Boniface and Schenk, 2012).

Records of the Paleoproterozoic and Neoproterozoic H*P*-L*T* metamorphic events at the margins of the Tanzania Craton provide a chance of strengthening our understanding about the operation of global Proterozoic geodynamic regimes. The Ubendian-Usagaran Belt also records tectonothermal events like volcanic arc magmatism and collisional metamorphism dated between 2000 and 500 Ma along with back-arc–related pillow basalts displacement, collisional metamorphism, deformation and reworking of older crusts, and rifting tectonics. These events were accompanied by the formation of metallic deposits like gold, base metals, platinum, and rare earth elements (REE) (see Cahen and Snelling, 1966; Stendal et al., 2004; Maier et al., 2007; Lawley et al., 2013a, 2013b; Kazimoto et al., 2014; Tulibonywa et al., 2015; Legler et al., 2015; Bahame et al., 2016; Manya and

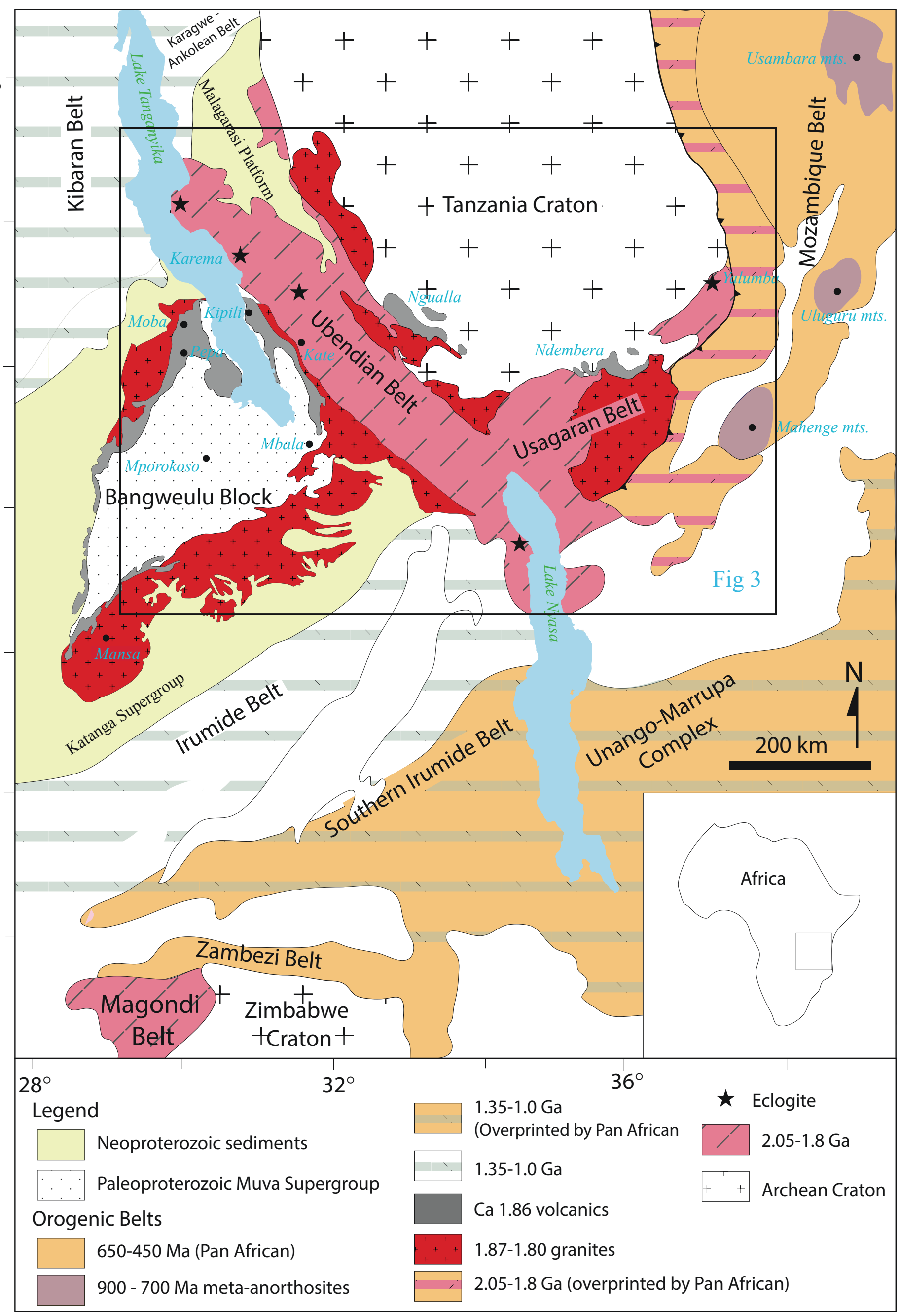

Figure 2. Precambrian geological map of central and eastern Africa. Map modified after Hanson (2003); Andersen and Unrug (1984); Pinna et al. (2004); De Waele et al. (2006a).

Maboko, 2016; Thomas et al., 2016; Boniface and Appel, 2017; Tulibonywa et al., 2017; Boniface and Appel, 2018). The presence of H*P*-L*T* and associated tectonic events in the Ubendian-Usagaran Belt implies that Proterozoic tectonic regimes in the Ubendian-Usagaran Belt reflect analogous operations of Phanerozoic mobile-lid tectonics in the Precambrian. Therefore, the Proterozoic tectonic events in the Ubendian-Usagaran Belt have global interest as they shed light to a complete record of Wilson Cycle in Precambrian i.e., rifting, subduction, arc and back-arc magmatism, and collision.

Daly (1988) developed a conceptual model that describes the tectonic evolution of the Ubendian-Usagaran Belt such that the Usagaran Belt thrusted onto the southeastern Tanzania craton ca. 2000 Ma and this thrusting event was followed by a series of lateral accretions ca. 1860 Ma to form the Ubendian Belt at the southwestern margins of the Tanzania Craton. Since the publication of Daly's work ~30 years ago, a large amount of geochronological, geochemical, petrological, and geotectonic data has been collected. The data depict the Ubendian-Usagaran Belt as a more complex zone, and its evolution cannot be explained by the existing thrusting-accretion model. Therefore, the major aim of this article is to find a link between the H*P*-L*T* events and the subsequent tectonothermal events, e.g., rifting, arc magmatism, collision, and reworking of older crusts in the Ubendian-Usagaran Belt. In this article, we present new petrographic and geochronological data from eclogites of the Ubendian Belt, and we review and interpret the existing published data. Finally, we describe the state-of-the-art conceptual tectonic model of the evolution of the Ubendian-Usagaran Belt in the Proterozoic.

2. REGIONAL GEOLOGY

The Paleoproterozoic Ubendian-Usagaran Belt borders the Archean Tanzania Craton along with the Paleoproterozoic Bangweulu Block, the Neoproterozoic Mozambique Belt and Malagarasi Platform, and the Mesoproterozoic Belts (Kibaran, Karagwe-Ankolean, Irumide, and Southern Irumide Belts) (Fig. 2). Key geological features of the geologic units that surround the Ubendian-Usagaran Belt are summarized in the sections below.

2.1. The Bangweulu Block and Tanzania Craton

The Ubendian-Usagaran Belt is sandwiched between the Bangweulu Block and the Tanzania Craton. The contacts of the Ubendian-Usagaran Belt, Tanzania Craton, and Bangweulu Block are characterized by the presence of voluminous Paleoproterozoic volcano-plutonic complex (explosive volcanics, mafic and felsic plutons). The volcano-plutonic rocks form a corona-like pattern around the core of the Bangweulu Block, which is covered by the Paleoproterozoic Mporokoso Group (part of the Muva Supergroup) (Fig. 2; Daly and Unrug, 1982; Pinna et al., 2004; Legler et al., 2015).

Geochronological and geochemical data acquired through time from the rhyolitic tuff, basalts, and granites at the margins of the Bangweulu Block in the areas of Mansa, Moba, Pepa, and Kate-Kipili indicate their eruption in volcanic arc tectonic settings that existed between 1871 ± 24 and 1832 ± 32 Ma (Fig. 2; Schandelmeier, 1983; Unrug, 1984; Kabengele et al., 1991; Lenoir et al., 1994; Kapenda et al., 1998; De Waele et al., 2006a, 2006b; De Waele and Fitzsimons, 2007; Debruyne et al., 2014). Similarly, the southern margins of the Tanzania Craton comprise slightly older volcano-plutonic suites exposed in the Ngualla and Ndembera areas (Fig. 2). The volcano-plutonic suites the southern margins of the Tanzania Craton erupted between 1921 ± 14 and 1871 ± 5 Ma in the continental arc tectonic settings (Fig. 2; Gabert and Wendt, 1974; Sommer et al., 2005; Bahame et al., 2016; Tulibonywa et al., 2015, 2017).

2.2. Mesoproterozoic Orogenic Belts

The Mesoproterozoic orogenic belts that bound the northwest and southeast ends of the Ubendian Belt are the Kibaran Belt, the Karagwe-Ankolean Belt (NE Kibaran Belt) to the northwest, and the Irumide Belt, Southern Irumide Belt and Unango-Marrupa Complex to the southeast (Fig. 2).

The Kibaran and the Karagwe-Ankolean Belts are composed of shallow-water metasedimentary rocks (arenaceous and pelitic metasediments) overprinted by greenschist- to amphibolite-facies metamorphic conditions. Mafic-ultramafic layered igneous complexes (1403 ± 14 and 1392 ± 26 Ma) intruded the metasedimentary rocks along with the granitic magmas (S-type, minor A-type granites, and tin-granites) (Tack et al., 1994; Fernandez-Alonso and Theunissen, 1998; Duchesne et al., 2004; Tack et al., 2010). The bimodal magmatism, i.e., mafic-ultramafic and granitic magmas, are considered to have intruded the long-lived shallow-water intracratonic basins (aulacogens) between 1400 and 1200 Ma (Meert et al., 1994; Maier et al., 2007; Tack et al., 2010). The greenschist- to amphibolite-facies metamorphic imprints on Supracrustal rocks dated at 1079 ± 14 Ma (U-Pb zircon) is considered to reflect a Mesoproterozoic collisional event associated with the emplacement of tin-granitoids magmatism (Kokonyangi et al., 2006).

The Irumide Belt and the Southern Irumide Belt separate the Bangweulu Block and the Zimbabwe Craton along with the Neoproterozoic Zambezi Belt (Fig. 2). The Kibaran Belt is characterized by reworked Archean and Paleoproterozoic rocks intruded by two distinct episodes of plutons, which include biotite granitoids (1665–1630 Ma) and the voluminous granitic magmatism dated between 1053 ± 14 and 942 ± 9 Ma (U-Pb zircon; De Waele et al., 2009). Therefore, the Irumide Belt is regarded as a passive continental margin of the Bangweulu Block that was metacratonitized during the Irumide Orogeny (e.g., Liégeois et al., 2013) while the Southern Kibaran Belt is predominantly late Paleoproterozoic basement intruded by arc-related magmas dated between 1.09 and 1.04 Ga and is regarded as an active continental margin of the Irumide Orogeny (Johnson et al., 2006; Liégeois et al., 2013).

The Unango-Marrupa Complex to the south is composed of Mesoproterozoic supracrustal gneisses and ortho-gneisses that are overprinted by amphibolite- to granulite-facies Neoproterozoic events dated between 569 ± 9 and 527 ± 8 Ma (U-Pb zircon; Bingen et al., 2009; Boyd et al., 2010).

2.3. Neoproterozoic Mozambique Belt

The Mozambique Belt hosts juvenile Neoproterozoic rocks, and the reworked crusts of Archean and Paleoproterozoic time. The reworked Archean–Paleoproterozoic rocks are locally known as the Western Granulites, which define a prominent 580–550 Ma thrust zone to the Usagaran Belt and the Tanzania Craton (Mruma, 1989; Johnson et al., 2003; Cutten et al., 2006; Fritz et al., 2009). The Neoproterozoic juvenile rocks (meta-anorthosites and meta-enderbites) crop out at the Usambara, Uluguru, and Mahenge mountains (Fig. 2). The meta-anorthosites and meta-enderbites have emplacement ages ranging between 900 and 700 Ma and are grouped as the Eastern Granulites in Tanzania and Cabo-Delgado Nappe Complex in Mozambique (Lenoir et al., 1994; Maboko and Nakamura, 1996; Tenczer et al., 2006; Fritz et al., 2013). Metasedimentary rocks (marble, metapelites, semipelitic, etc.) overlie the Eastern Granulites and were metamorphosed during the East African Orogeny (650–620 Ma) (Möller et al., 2000; Hauzenberger et al., 2007).

3. THE UBENDIAN-USAGARAN BELT

3.1. The Existing Tectonic Model

McConnell (1950) firstly described the existence of separate geological structural entities in the Ubendian Belt and later on Sutton et al. (1954) interpreted the belt as a deep-seated zone of strike-slip movement. Further studies indicate that the Ubendian Belt is made up of NW-SE–oriented deeply seated lateral and ductile shear zones with dextral displacements that separate single tectonic blocks or terranes with distinguished lithological assemblages that overprint the E-W old structures (Fig. 3; Sutton and Watson, 1959; McConnell, 1967; Smirnov et al., 1973; Theunissen et al., 1996; Boven et al., 1999).

Based on previous studies and on their own structural analyses, Daly et al. (1985) divided the Ubendian basement rocks into eight lithotectonic terranes or blocks based on predominant geological units and internal fabric orientation as follows: Ubende (metabasites: ENE-WSW); Mbozi (metabasites and intermediate granulites with quartzite: NE-SW); Ufipa (gneissic granite: NW-SE); Upangwa (meta-anorthosite: NW-SE); Lupa (meta-volcanics); Nyika (cordierite granulites: EW); and Wakole (aluminosilicate schist) (Fig. 3A). Consequently, Daly (1988) developed a tectonic model that explained the evolution of the Ubendian and Usagaran Belts (Fig. 3). The model explains that, in the Paleoproterozoic Era, the Usagaran Belt developed as NW-directed thrust sheets and over-thrusts onto the Tanzanian Craton, and later the Ubendian terranes probably developed as a series of tectonic slivers that accreted laterally to the Tanzania Craton during a late stage in this thrusting event, the internal fabrics of the terranes being developed during the Usagaran orogeny (Fig. 3A; Daly, 1988).

Generally the Usagaran event is dated as an older orogenic event relative to the Ubendian event. The 2.0 Ga high-pressure granulite and eclogite facies metamorphism is associated with the E-W internal Usagaran Orogeny that developed between 2100 and 2050 Ma (Daly 1988; Lenoir et al., 1994; Möller et al., 1995; Theunissen et al., 1996; Boven et al., 1999). Whereas, the amphibolite facies NW-SE inter-terrane shear zones and subhorizontal linear fabrics define the anatomy of the Ubendian Belt (Figs. 3B–3D). The NW-SE massive structures of the Ubendian Belt are considered to have developed through dextral wrench faulting that was accompanied by the formation of the terrane bounding barroisite tectonites (high-pressure tectonite) and the emplacement of granites dated between 1864 ± 32 and 1847 ± 37 Ma (Lenoir et al., 1994; Theunissen et al., 1996; Boven et al., 1999).

Geochronological, geochemical, and petrological databases established in the past two decades indicate that the Ubendian-Usagaran Belt evolved through different episodes, which are mainly associated with oceanic crust subduction events in Orosirian Period (2000–1860 Ma) and Ediacaran–Cambrian Periods (590–500 Ma). The subduction events were followed by arc magmatism, collision, and reworking of older crusts. There is also a record of ancient rifting events that separate the Paleoproterozoic and Neoproterozoic subduction events. Based on this establishment, the following sections will be focused on presenting new petrological and geochronological data from eclogites, and on reviewing and interpreting the existing data from eclogites of the Ubendian-Usagaran Belt, along with describing subsequent tectonic events that follow or come before subduction for the purpose of describing the complex tectonic history which can no longer be addressed by Daly's Paleoproterozoic thrust and lateral accretion model.

3.2. New Digests on the Eclogites of the Ubendian Belt

Eclogites of the Ubendian Belt occur in the Ubende, Ufipa, and Nyika Terranes (Fig. 4). Ring et al. (1997, 2002), Sklyarov et al., 1998, Boniface et al. (2012), and Boniface and Schenk (2012) provide detailed petrography, geochemistry, and geochronology data of the Ubendian Belt eclogites. The Ubende Terrane hosts Paleoproterozoic (1890–1860 Ma) foliated eclogites with a MORB geochemical affinity (Boniface et al., 2012). The Nyika Terrane hosts Paleoproterozoic (2000 Ma) high-pressure granulites (enderbites) and Neoproterozoic (530–500 Ma) eclogites with affinity to plume basalts (Ring et al., 1997, 2002).

The Ufipa Terrane hosts two types of eclogites: the kyanite-free eclogites, which belong to the Neoproterozoic Era, and kyanite-bearing eclogites, which belong to the Paleoproterozoic Era. The kyanite-free eclogites have affinity to back-arc basalt and island-arc basalt, and they attained the eclogite facies metamorphism between 593 ± 20 and 524 ± 12 Ma (Boniface and Schenk, 2012). The arc signature from the kyanite-free eclogites implies

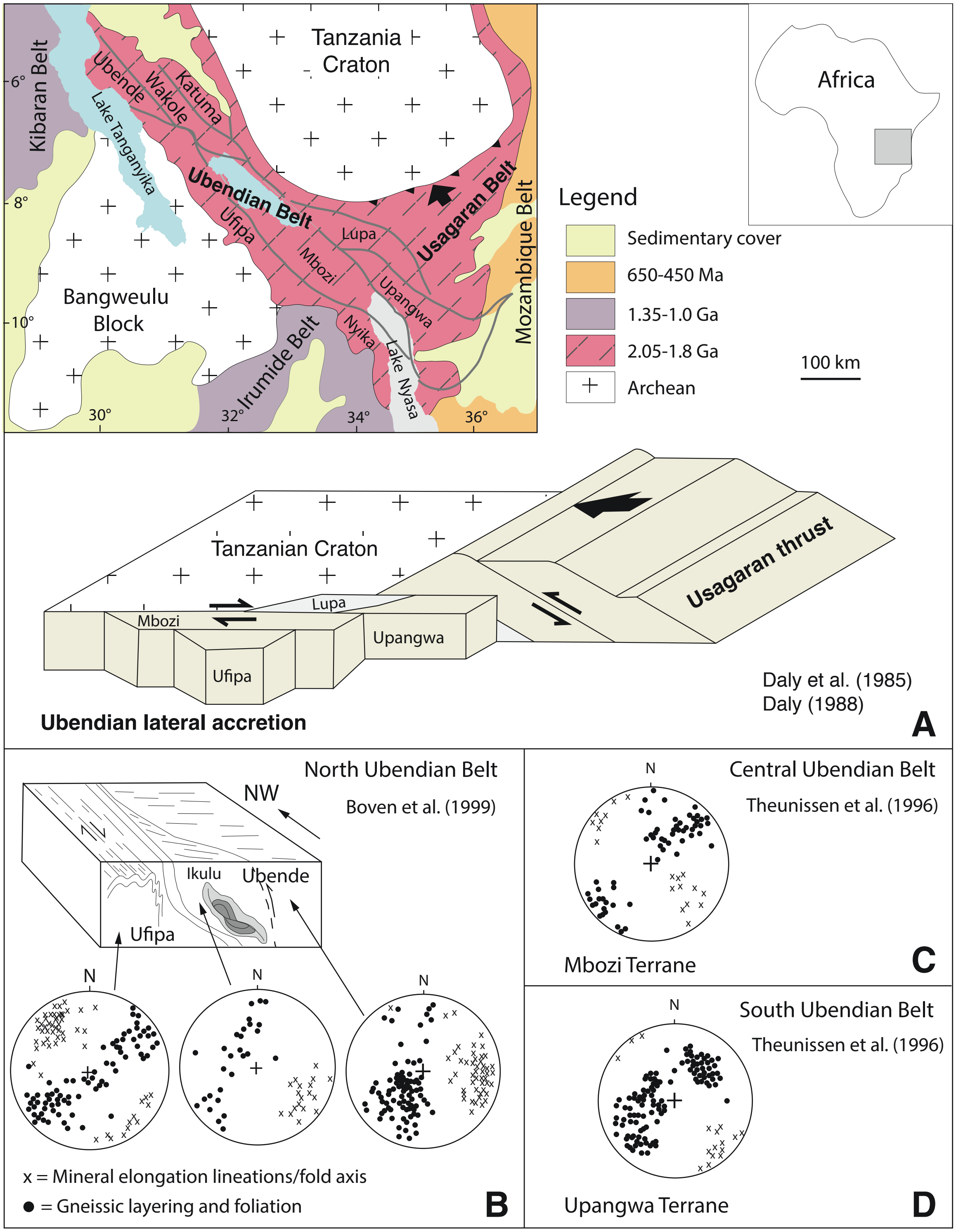

Figure 3. (A) Geological map of the Ubendian-Usagaran Belt illustrating the division of terranes and the tectonic model for the evolution of the Ubendian-Usagaran Belt, adapted from Daly (1988). (B, C, and D) Stereographic projections (equal-area, lower hemisphere) are outcrop data by Theunissen et al. (1996) and Boven et al. (1999); attitude of gneissic layering and foliation for planar fabrics (dot plots) and mineral lineation and fold axes (x plots) are from northern, central, and southern Ubendian Belt, respectively.

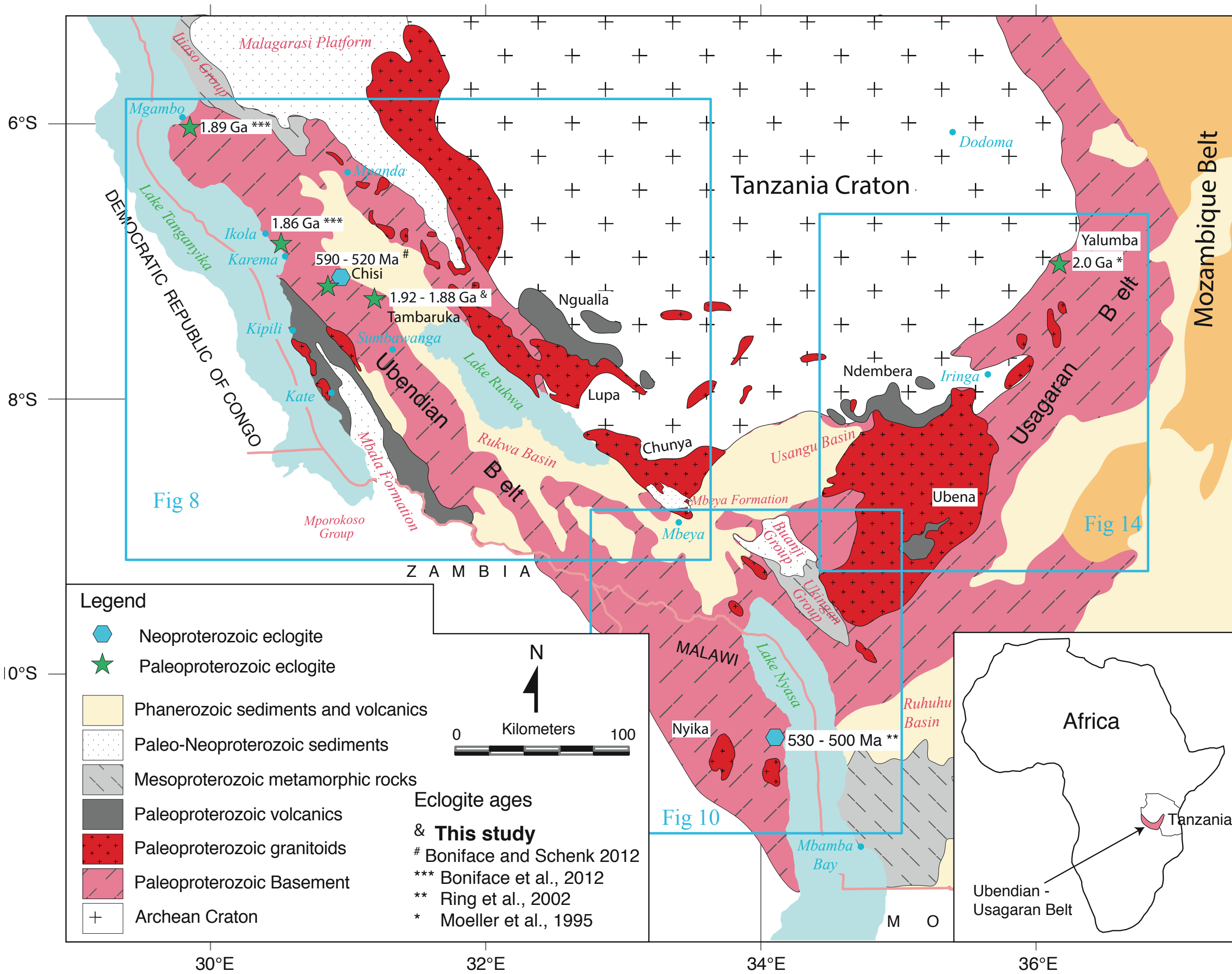

Figure 4. The Paleoproterozoic Ubendian-Usagaran Belt and the eclogite localities with ages (Möller et al., 1995; Ring et al., 2002; Boniface et al., 2012; Boniface and Schenk, 2012). The map was modified after Pinna et al. (2004).

that their mafic protoliths formed above a subduction zone and were probably channeled into a subduction zone as olistostromal blocks in mélanges that recrystallized and deformed to eclogites. *P-T* conditions at *P* = 1.5–1.7 GPa and *T* = 610–690 °C for the kyanite-free eclogites of the Ufipa Terrane indicate a relatively warm subduction with geothermal gradient of ~11 °C/km (Boniface and Schenk, 2012).

The kyanite-bearing eclogites of the Ufipa Terrane give a different story. Boniface and Schenk (2012) obtained a concordant age of 1877 ± 20 Ma from zircon mantle of the kyanite-bearing eclogites of the Ufipa Terrane along with a lower intercept age at 548 ± 39 Ma from the same rocks. Due to lack of mineral growth textures that relate zircon and other metamorphic minerals (garnet-omphacite), the kyanite-bearing eclogites were interpreted as being derived from the Paleoproterozoic aluminous mafic crust that were subducted in Neoproterozoic Era. Therefore, detailed petrography and *P-T* conditions (1.5–1.9 GPa/610–790 °C: equivalent to 10–11 °C/km; i.e., deep and relatively warm subduction) obtained from the kyanite-bearing eclogites of the Ufipa Terrane were attributed to the 593 ± 20 to 524 ± 12 Ma subduction event derived from the kyanite-free eclogites. However, recent studies done by Boniface and Tsujimori (2014, 2016) indicate that the kyanite-bearing eclogites attained their eclogite facies conditions during the Paleoproterozoic subduction event, and they were reworked to granulite facies conditions in the Neoproterozoic Era when the kyanite free eclogites formed. In the following section, we present new comparative petrographic descriptions of the kyanite-bearing eclogites of the Ufipa Terrane and the foliated eclogites (from the neighboring Ubende Terrane), both of which yield Paleoproterozoic eclogite facies ages. Geochronological data of the kyanite-bearing eclogite are available in the conference abstracts of Boniface and Tsujimori (2014,

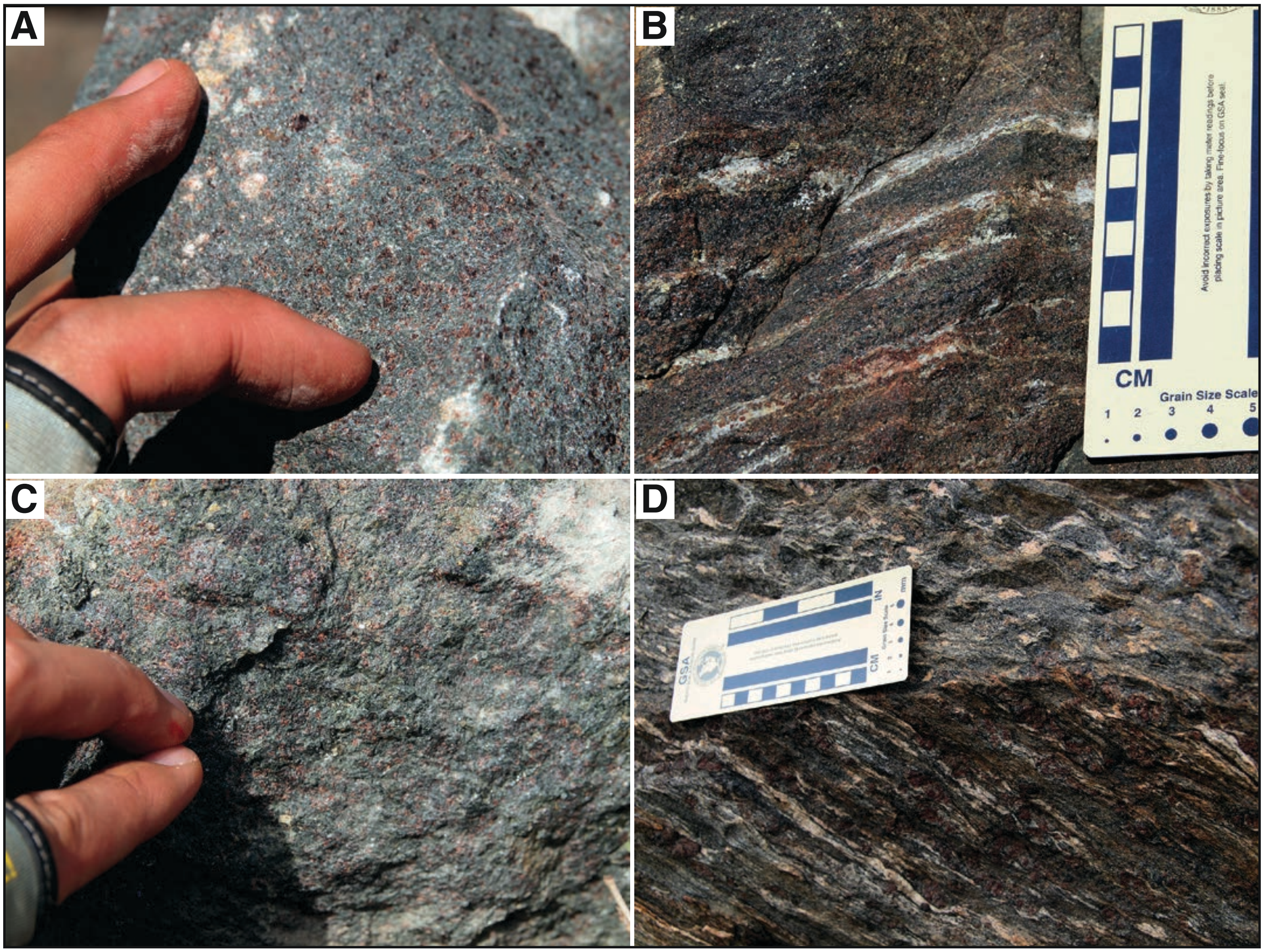

Figure 5. Field photographs of the Ubendian Belt eclogites. (A) Eclogite from the Ubende Terrane without strong foliated fabric. (B) Eclogite from the Ubende Terrane with strong foliated fabric. (C) Kyanite-bearing eclogite from the Ufipa Terrane. (D) Migmatitic metapelite gneiss that host the Ufipa Terrane eclogites.

2016) that are also appended here as Supplementary Materials S1 and S2[1]. Boniface et al. (2012) provide ages of the foliated eclogites. We therefore, integrate the new petrographic descriptions and the available data and present new interpretations about the subduction events in the Ubendian Belt.

3.2.1. New Petrographic Comparison of the Ubendian Eclogites

Figure 5 illustrates the appearance of the Ubendian Belt eclogite from the Ubende and Ufipa Terranes. In the Ubende Terrane, eclogites occur as solitary blocks with dimensions of meter scale hosted in foliated amphibolites and granulites. Some eclogites are strongly foliated, whereas others are better preserved, therefore exhibiting a much weaker fabric (Figs. 5A and 5B). In the Ufipa Terrane, the outcrops of kyanite-free and kyanite-bearing eclogite occur in area covering more than 100 m, appearing as massive, isolated blocks with meter-scale dimensions, hosted in migmatitic metapelite gneiss (Figs. 5C and 5D). It should be noted that both kyanite-bearing (with Paleoproterozoic ages) and kyanite-free eclogites (with Neoproterozoic ages) of the Ufipa Terrane are massive, and they do not display deformational fabrics, contrary to the foliated eclogites throughout the Ubende Terrane.

The foliated eclogites of the Ubende Terrane are composed of garnet porphyroclasts surrounded by recrystallized plagioclase and clinopyroxene. Ilmenite is also abundant (Figs. 6A and 6B).

[1]Supplemental Material: conference abstracts of Boniface and Tsujimori (2014, 2016). Please visit https://doi.org/10.1130/SPE.S.15108738 to access the supplemental material; contact editing@geosociety.org with any questions.

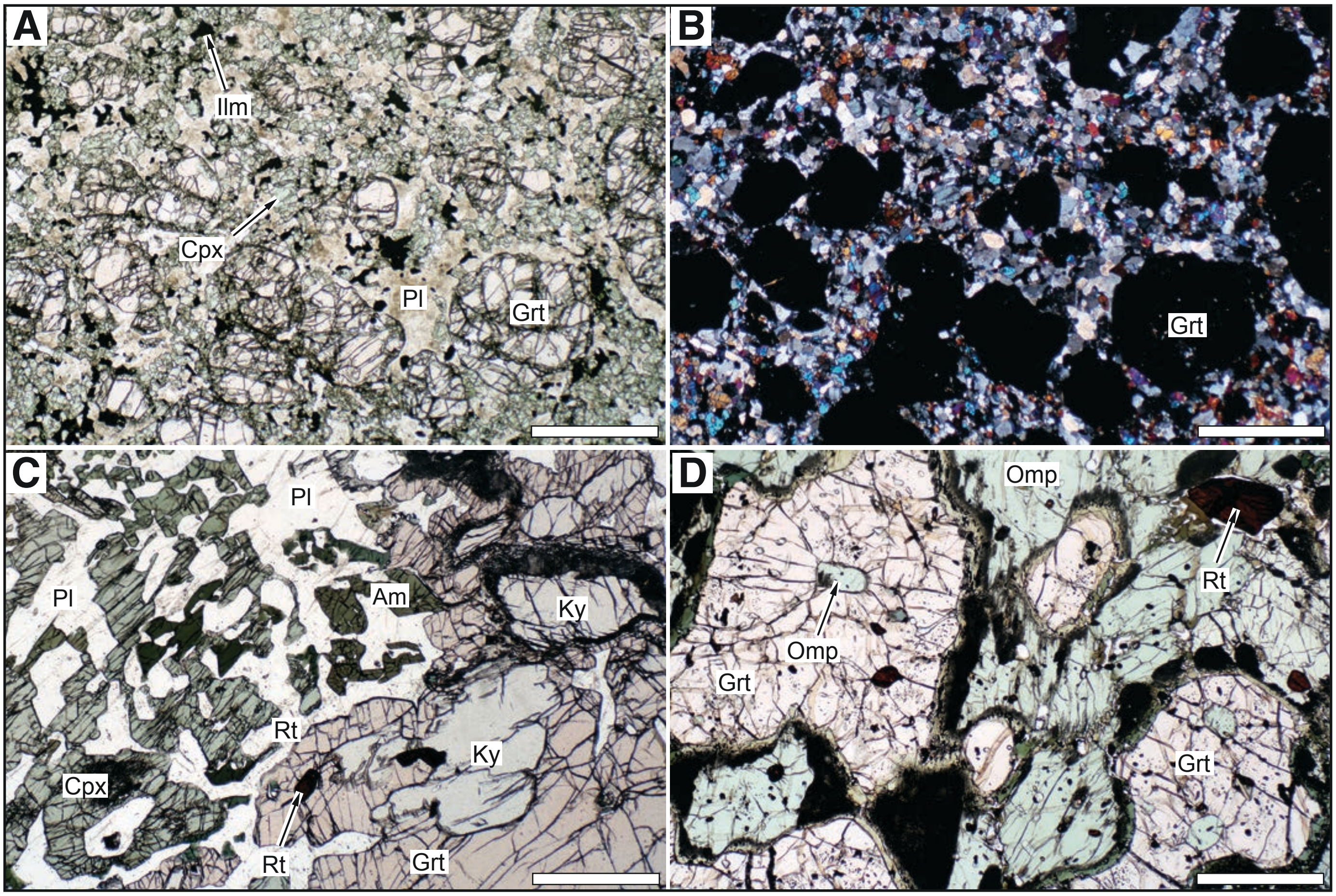

Figure 6. Microphotographs of the Ubendian Belt eclogites. Bar scale is 1 mm. (A, B) Foliated eclogite of Ubende Terrane with recrystallized plagioclase (Pl) and clinopyroxene (Cpx) around garnet (Grt), plane-polarized light and crossed polar, respectively. Ilm—ilmenite. (C) Paleoproterozoic kyanite-bearing eclogite from the Ufipa Terrane showing kyanite (Ky) surrounded by garnet and garnet coronas and matrix omphacite retrogressed to amphiboles (Am), clinopyroxene, and plagioclase. Rt—rutile. (D) Neoproterozoic kyanite-free eclogite from the Ufipa Terrane composed mainly of garnet, rutile, and omphacite (Omp).

The kyanite-free eclogite of the Ufipa Terrane is mainly composed of garnet porphyroblasts and rutile included in omphacite. The garnet margins are sometimes surrounded by amphibole coronas and omphacite has broken down to form symplectitic diopside and plagioclase (Fig. 6D; Boniface and Schenk, 2012). In contrast, the kyanite-bearing eclogite is composed of garnet porphyroblast, rutile, kyanite, and omphacite inclusions as peak mineral assemblage that is overgrown by a granulite facies mineral assemblage. The granulite facies mineral assemblage includes clinopyroxene, garnet corona around kyanite, amphibole and plagioclase forming a sieve-like texture (Fig. 6C). Zircon was found as inclusions in garnet coronas around kyanite, therefore providing the opportunity to date the age of the peak mineral assemblage and the granulite facies overprint.

3.2.2. Kyanite-Bearing Eclogite: In Situ U-Pb Zircon Ages

Zoned metamorphic zircons contain cores with fluid inclusions formed at eclogite-facies conditions (Fig. 7B; Boniface and Tsujimori, 2014, 2016). A discordant upper intercept age at 1924 ± 74 Ma suggests fluid infiltration and consequent mineral crystallizations during eclogite-facies metamorphism. Therefore, the zircon core age yields the timing of growth of omphacite, garnet porphyroblast, and kyanite mineral assemblages that were overgrown by granulite-facies metamorphism at 563 ± 46 Ma (zircon rims age; Fig. 7A). The zircon rims are surrounded by garnet corona that grew during granulite facies metamorphism with a mean $^{206}Pb/^{238}Pb$ age of concordant analyses of 577 ± 6.4 Ma, which yields the timing of the growth of the garnet corona and the associated mineral assemblages of clinopyroxene, amphibole, and plagioclase.

The eclogite crystallization age at 1924 ± 74 Ma is equivalent to the age of 1877 ± 20 Ma obtained by Boniface and Schenk (2012) from the same kyanite-bearing eclogites. Th-U data indicate that the Th/U ratios of zircon cores in the kyanite-bearing eclogite overlap with those of the mantles (ranging from 0.24 to 1.72) (Boniface and Schenk, 2012). Low content of Th/U ratios

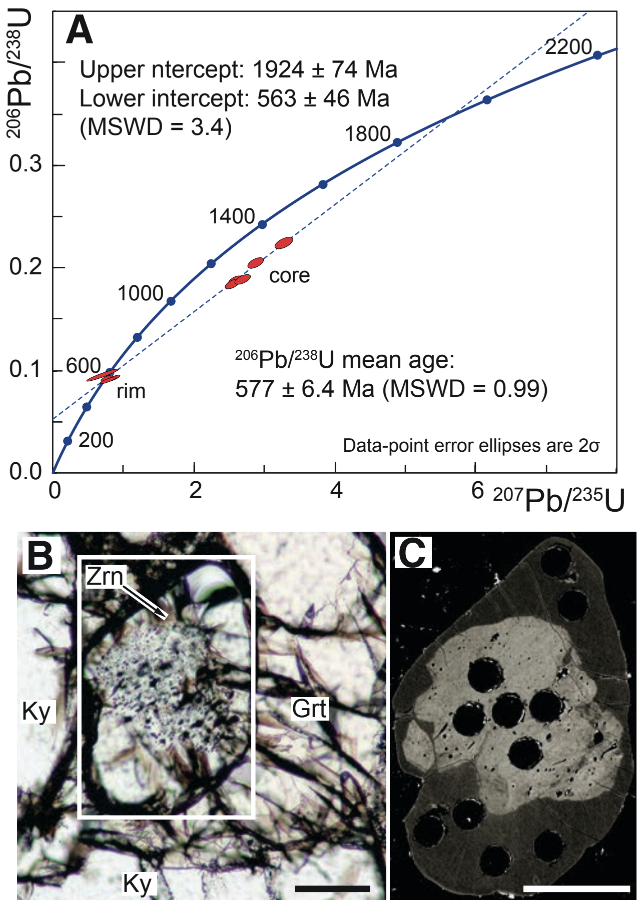

Figure 7. New in situ U-Pb dating of a large zoned zircon from the kyanite-bearing eclogite. (A) A concordia diagram showing zircon core data plotting along a discordia with intercepts at 1924 ± 74 and 563 ± 46 Ma. The mean ^{206}Pb/^{238}Pb age of concordant rim analyses is 577 ± 6.4 Ma. MSWD—mean square of weighted deviates. (B) A photomicrograph illustrating dated zircon (Zrn) inclusion in garnet (Grt) corona around kyanite (Ky). (C) Back-scattered electron image illustrating a zoned zircon after laser ablations; black circles on the zircon are pits after the dating.

in zircon may indicate growth of cores and rims during metamorphism (Rubatto, 2002; Corfu et al., 2003). Therefore, zircon textures data conform to the U-Th composition and support the interpretation that the zircon mantle and the analyzed cores grew in metamorphic conditions. Based on these observations, we conclude that the eclogite facies conditions of the kyanite-bearing eclogite in the Ufipa Terrane were attained between 1924 ± 74 and 1877 ± 20 Ma. This time window overlaps with the time ages of the foliated eclogites of the Ubende Terrane that formed between 1890 and 1860 Ma (Boniface et al., 2012).

3.3. Eclogites in Usagaran Belt

Eclogites of the Usagaran Belt form outcrops at the Yalumba Hill (Fig. 4). The eclogites have MORB affinity and they formed in a subduction zone that existed ca. 2000 Ma (Möller et al., 1995; Collins et al., 2004).

3.4. How *P-T* Conditions Were Determined in Eclogites

Different authors have used various thermobarometric methods to determine the *P-T* condition of eclogites from the Ubendian-Usagaran Belt (see Möller et al., 1995; Sklyarov et al., 1998; Ring et al., 2002; Boniface and Schenk, 2012; Boniface et al., 2012). It should be noted that different thermobarometric techniques commonly yield different *P-T* results therefore it is important to communicate to our readers the information of all *P-T* estimates and various thermobarometric methods that were used by different authors to determine subduction zone metamorphic conditions of the Ubendian-Usagaran Belt. For example, a global comparison of pressure determined by Ab = Jd + Qtz equilibria commonly yields a minimum pressure which is much less than that estimated by Grt-Cpx-Phengite thermobarometry. Mineral abbreviations throughout the article are according to Kretz (1983) and Whitney and Evans (2010).

Sklyarov et al. (1998) and Boniface et al. (2012) determined the *P-T* conditions of the Paleoproterozoic eclogites from the Ubende Terrane. Sklyarov et al. (1998) used the THERMOCALC technique to estimate range of P = 1.7–1.9 GPa and T = 609–724 °C (calibrations of Powell and Holland, 1988). Boniface et al. (2012) estimated a range of P = 1.5 GPa (Ab = Jd [17] + Qtz equilibria: calibrations of Newton and Perkins [1982]; Powell and Holland [1988]) and T = 603–742 °C (Zr-in-rutile thermometry: calibration of Ferry and Watson [2007]).

Boniface and Schenk (2012) estimated the *P-T* conditions of the Neoproterozoic and Paleoproterozoic eclogites from the Ufipa Terrane Jadeite, GASP (garnet-plagioclase-Al2SiO5-quartz) and other reactions. The Paleoproterozoic kyanite bearing eclogite yielded overlapping P = 1.5–2.0 GPa under the equilibria of Ab = Jd + Qtz and GASP equilibria (Holland, 1980; Koziol 1989) and T = 700 - 785 °C (Powell and Holland 1988). The pressure at 1.7 GPa was obtained under the equilibria of Ab = Jd + Qtz and GASP equilibria for the Neoproterozoic kyanite-free eclogite along with the T = 609–684 °C (Zr-in-rutile thermometry: calibration of Ferry and Watson [2007]).

Ring et al. (2002) used the Grt-Cpx thermometry to obtain the temperatures between 660 and 780 °C (calibrations of Krogh, 1988; Ellis and Green, 1985) from eclogites in Malawi (Nyika Terrane) obtained minimum pressures of 17–18 kbar (Ab = Jd + Qtz equilibria; Holland, 1980).

Möller et al. (1995) estimated the *P-T* conditions of Paleoproterozoic eclogites from the Usagaran Belt and obtained P = 1.55–1.79 GPa (Ab = Jd + Qtz and GASP equilibria; Holland, 1980) and P = 1.89–1.90 GPa (equilibria: Grt-An-Di-Qtz; Eckert et al., 1991, and Grs-aluminosilicate-Qtz-Pl; Holland, 1979) along with T = 745–780 °C (Fe-Mg exchange in Grt and Cpx or Opx: Harley, 1984; Krogh, 1988).

4. SUBDUCTION AND TECTONICS IN THE UBENDIAN BELT

This chapter will be focused on the H*P*-L*T* metamorphic events of the Ubendian-Usagaran Belt as a centerpiece for the discussion of all the tectonothermal events that affected the same region in space and time, e.g., arc-magmatism, collision, and rifting events. Therefore, tectonic settings of the lithologies of the Ubendian Belt and their time constraints are summarized in Tables 1, 2, and 3. Table 1 provides a summarized geology of different lithotectonic terranes of the Ubendian Belt that was extracted from different sources, e.g., quarter degree sheets and geological reports, and Tables 2 and 3 summarize metamorphic and magmatic ages of all dated lithological assemblages, which indicate the tectonothermal events of the Ubendian Belt making distinct clusters that span from the Orosirian Period to the Cambrian Period.

By considering similarities in geology and age distribution, we group the Ubendian Belt terranes into three corridors: the Western Corridor (Ufipa and Nyika), the Central Corridor (Ubende, Mbozi and Upangwa), and the Eastern Corridor (Katuma and Lupa) (Fig. 3A). The Mesoproterozoic Wakole Terrane will be discussed as a high-grade metamorphic equivalent of the Mesoproterozoic Itiaso sedimentary basins and the termination of the NE Kibaran Belt in Tanzania (refer Boniface et al., 2014).

4.1. Ufipa and Nyika Terranes

The Ufipa and Nyika Terranes have common geologic features and evolutional trends that we here define as the Western Ubendian Corridor. The Ufipa and Nyika Terranes are predominated by high-grade metasedimentary rocks (Bt granitic gneisses, Bt-Grt-Ky/Sil gneiss/schist, migmatites, rare Crd-Grt-Sil granulites) interlayered with lenses of H*P*-L*T* metamorphosed mafic rocks (enderbite/charnockites and eclogites), and the intrusions of Bt-Hbl granites and granodiorites (Fig. 8; Iskahakov et al., 1970; Miyashev et al., 1970; Thatcher, 1974). But the most striking feature of the Ufipa and Nyika Terranes (or the Western Ubendian Corridor) is the presence in both terranes of the Paleoproterozoic and Neoproterozoic H*P*-L*T* metamorphic units (eclogites and high-pressure granulite) as described below.

4.1.1. Neoproterozoic eclogites in the Western Ubendian Corridor

The Ufipa Terrane hosts kyanite-free eclogites as lenses enclosed in Grt-Bt-Ky gneisses. More information about these rocks is given in section 3.2 above. But in summary, the kyanite-free eclogites have affinity to back-arc basalt and island-arc basalt, and they attained eclogite facies metamorphic conditions at P = 1.5–1.7 GPa and T = 610–690 °C between 593 ± 20 and 524 ± 12 Ma (Boniface and Schenk, 2012).

The Nyika Terrane in southern Ubendian Belt hosts eclogites with affinity to plume basalts (Ring et al., 2002). The Nyika Terrane eclogites formed between 530 and 500 Ma in a subduction zone under P-T conditions at P = 1.7–1.8 GPa and T = 660–780 °C (Fig. 9D; Ring et al., 2002). The precursors of the Nyika Terrane eclogites are basaltic rocks with a magmatic age of 1010 ± 22 Ma (U-Pb zircon) (Ring et al., 2002). Neoproterozoic eclogites within the same age range in the Ufipa Terranes are considered to be proxies of back-arc and volcanic-arc geologic environments that separated the Tanzania Craton from the Bangweulu Block before their collision during the final amalgamation of Gondwana (Boniface and Schenk, 2012).

4.1.2. Paleoproterozoic Eclogites in the Western Ubendian Corridor

The Paleoproterozoic eclogites from the Ufipa Terrane are the kyanite-bearing eclogites, which have been described in sections 3.2 and 3.2.2. In summary the Ufipa Terrane kyanite-bearing eclogites attained their eclogite facies conditions between 1924 ± 74 and 1877 ± 20 Ma in a subduction zone under the metamorphic conditions of P = 1.5–1.9 GPa and T = 610–790 °C (Fig. 9A1; Boniface and Schenk, 2012).

Like in the Ufipa Terrane, the Nyika Terrane hosts metasedimentary rocks (Crd-Grt-Sil granulite, Grt-Bt gneisses, migmatitic locally), which enclose lenses of high-pressure granulite (enderbites) and eclogites (Fig. 10; Thatcher, 1974; Ring et al., 1997, 2002). The high-pressure granulites with a protolith Pb-Pb zircon age of 2093 ± 0.6 Ma were metamorphosed at 2002 ± 0.3 Ma under conditions of P = 0.9–1.1 GPa and T = 850–880 °C (Fig. 9C), which was interpreted by Ring et al. (1997) to be a subduction zone environment and as a coeval event with the 2000 Ma subduction in the Usagaran Belt (subduction of eclogites with a MORB affinity) (Möller et al., 1995).

4.1.2. Metapelitic Gneisses of the Western Ubendian Corridor

Geochronological and petrological data from metapelites (Grt-Bt-Ky/Sil gneisses) of the Ufipa Terrane indicate that these rocks have clearly recorded collisional metamorphic events that postdated the subduction events in the Paleoproterozoic and Neoproterozoic Eras. The kyanite-bearing eclogite recorded a subduction event between 1920–1890 Ma, which is reflected as metamorphic overprint at 1949 ± 16 and 1901 ± 37 Ma (U-Pb zircon) in zircons that were separated from the Ufipa Terrane pelitic rocks (Boniface and Appel, 2018). However, zircons from metapelites have neither clear younger metamorphic ages nor Neoproterozoic rim overgrowth. Contrary to zircon records, monazite from the same rocks, recorded the Paleoproterozoic post subduction metamorphic event along with the younger Neoproterozoic ages dated between 566 ± 8 and 556 ± 5 Ma (U-Th-Pb monazite metamorphic ages). The monazite Neoproterozoic ages record collisional event that succeed the Neoproterozoic subduction event that was recorded in the kyanite-free eclogite (Boniface and Appel, 2018). Garnet and the associated minerals yield high-pressure metamorphic P-T conditions (P = 9–12 kbar; T = 760–820 °C) for the Neoproterozoic collisional event in the Ufipa Terrane (Boniface and Appel, 2018).

TABLE 1. BRIEF GEOLOGY OF DIFFERENT LITHOTECTONIC TERRANES OF THE UBENDIAN BELT SUMMARIZED FROM PUBLISHED QUARTER DEGREE SHEETS AND GEOLOGICAL REPORTS

Terrane	Paleoproterozoic lithology	Mesoproterozoic lithology	Neoproterozoic lithology
Ubende	(1) Metabasites: Amphibolite; Hb-Bt gneiss; interlayered with quartzite; lenses of mylonitic eclogite; meta-ultrabasite; Px gneisses (granulite) (2) Metasediments: Grt-Bt-Ms gneiss/schist, interlayered with quartzite (3) Intrusives (foliated): Bt granite, gabbro-norite, ultrabasites (pyroxenites), serpentinized peridotite (4) Tectononites: mylonite, ultramylonites	(1) Carbonatite (dolomitic, calcitic) (2) Syenite–Porphyry	
Wakole	(1) Metasediments: Alumino-silicate schists (Ky-Grt-Ms/Bt schist); bands quartzites (2) Quartzite amphibolite sequence (amphibolite-amphibolite schist-quartzite)	(1) Itiaso Group: quartzite, sandstone, siltstone (2) Layered mafic-ultramafic igneous complex	Dolerites
Katuma	(1) Metabasites: Amphibolite, Hbl schist/gneiss, Grt-Px gneiss, Grt metabasite, with quartzite layers, migmatitic Bt gneiss layers, Bt-Ms ± Sil gneiss/schist layers (2) Intrusive: Bt granite, leucogranite (alaskites), metabasite	(1) Itiaso Group: quartzite, sandstone, siltstone (2) Syenite—dykes? (NE trend direction)	Malagarasi platform (sandstone, siltstone, mudstone, conglomerate) Dolerite dykes cut the Malagarasi Platform
Ufipa	(1) Orthogneiss: Gneissic granite and granodiorite (2) Metasediments: Bt gneiss, Bt-Grt-Ky/Sil gneiss/schist, migmatites, quartzite, amphibolite layers, metabasite layers, Ky-eclogite lenses, charnokites (3) Intrusives: granite, Bt granite, granodiorite, syenogranite (4) Volcanics: dacite, rhyolites	(1) Mbala Formation (sandstone, siltstone, mudstone, conglomerate)	Metabasite layers, eclogite lenses in gneisses
Mbozi	(1) Metabasites: Hbl-Opx gneiss, Grt-Opx gneiss (2) Metasediments: Grt-Bt± Sil gneiss (quartzo-feldspathic), quartzite layers (3) Tectonites: phyllonites, mylonite, mortar gneiss, acidic cataclasites		
Lupa	(1) Orthogneiss: granitic migmatite gneiss, Hb-Px migmatites, (2) Metasediments: Hbl-Px-Ep migmatite (Calc-silicates), (3) Volcanics: Meta-andesite, meta-agglomerate, meta-rhyolite, meta-dacite (4) Intrusives (foliated): Granite, Hbl-Bt granite, Diorites, granodiorite, gabbro	(1) Carbonatite (calcitic), fenite	Malagarasi platform (quartzite, limestone, sandstone conglomerate)
Upangwa	(1) Meta-gabbroic group: Anorthosite, gabbro, norite, gabbro-norite, Iron ore, diorite mafic–ultramafic (Nkenja) (2) Metasedimentary: Bt gneiss, Grt-Sil-Bt gneiss, migmatites, calc-silicate, marble Ukingan Group: Phyllite Buanji Group: quartzite, sandstone, siltstone, shale, dolomite, cut by andesite (3) Orthogneisses: granitic migmatites, amphibolite (4) Intrusives: Granite, granodiorite, tonalite	syenite?	Granite
Nyika	(1) Metasediments: Crd-Sil granulites, Grt-Sil-Bt gneiss/schist, migmatites, quartzite, Hb-gneisses/schists (2) Orthogneiss: Enderbite (charnokites) interlayered with Crd-Sil gneisses (3) Intrusions: Bt-Hbl granite, granodiorite, diorite dykes, syenite	Basalts (eclogite protolith)	Eclogite

Note: Data sources: Harpum (1952); Morris (1952); Haldemann (1953); Harpum and Brown (1958); Harpum (1958); Teale et al. (1958); Halligan and Birch (1961b, 1961a); Kennerley (1962); van Loenen and Kennerley (1962b,1962a); van Loenen and Kabengele (1962); Mudd (1962); Orridge (1962); Macfarlane and Macdonald (1962); Macfarlane et al. (1962); Macfarlane (1963, 1965, 1966); Iskahakov et al. (1970); Miyashev et al. (1970); Smirnov et al. (1970); Semyanov et al. (1970); Smirnov et al. (1971b, 1971a); Biyashev et al. (1971); Iskhakov et al. (1971); Trifan et al. (1972); Tolochko et al. (1972); Semyanov et al. (1972c, 1972a, 1972b); Smirnov et al. (1973); Harkin and Harpum (1978).

TABLE 2. ARCHEAN TO NEOPROTEROZOIC MAGMATIC AGES OF FROM UBENDIAN LITHOTECTONIC TERRANES

Terrane	Magmatic ages (Ma)	Analytical technique	Lithology	Authors
Archean ages				
Katuma	2553 ± 10, 2638 ± 5, 2643 ± 4, 2645 ± 34, 2651 ± 5, 2677 ± 29, 2713 ± 11	U-Pb zircon, LA-ICP-MS	Metabasites, granitoids	Kazimoto et al. (2014)
Lupa	2723 ± 10, 2739 ± 10, 2758 ± 9	U-Pb zircon, LA-MC-ICP-MS	Granite	Lawley et al. (2013a)
	2682 ± 10 Ma	U-Pb zircon, SHRIMP	Granite	Tulibonywa et al. (2015)
	2688	Nd ages	Granite	Manya (2011)
	2731 ± 29	U-Pb zircon, LA-SC/MC-ICP-MS	Granite	Thomas et al. (2016)
Paleoproterozoic ages				
Katuma	1936 ± 20, 1952 ± 7, 1993 ± 6, 2021 ± 11	U-Pb zircon, LA-ICP-MS	Metabasite, granitoids	Kazimoto et al. (2014)
	1847 ± 37	Rb-Sr whole rock, TIMS	Granite	Lenoir et al. (1994)
Lupa	1934.5 ± 1, 1942 ± 14, 1958.5 ± 1.3, 1959.6 ± 1.1	U-Pb zircon, ID-TIMS, LA-MC-ICP-MS	Granodiorite, syenogranite, monzogranite	Lawley et al. (2013a)
	1921 ± 7, 1930 ± 3	U-Pb Titanite, ID-TIMS	Granodiorite, granite	Lawley et al. (2014)
	1891 ± 17, 1880 ± 17	U-Pb zircon, LA-MC-ICP-MS	Quartz diorite, Gabbroic dyke	Lawley et al. (2013a)
	1878 ± 15	U-Pb zircon, SHRIMP	Porphyritic dacites to rhyodacites	Tulibonywa et al. (2015)
	1943 ± 32	U-Pb zircon, SHRIMP	Basaltic andesite	Tulibonywa et al. (2015)
	1871 ± 5	U-Pb zircon, SHRIMP	Granite	Tulibonywa et al. (2015)
	1929 ± 20, 1919 ± 37, 1896 ± 16	U-Pb zircon, LA-SC/MC-ICP-MS	Bt granites	Thomas et al. (2016)
Mbozi	1876 ± 20, 1871 ± 8	U-Pb zircon, LA-SC/MC-ICP-MS	Biotite-bearing granitic orthogneiss	Thomas et al. (2016)
Nyika	1970 ± 30	U-Pb zircon	Granite	Dodson et al. (1975)
	1871 ± 16, 1876 ± 20	U-Pb zircon, LA-SC/MC-ICP-MS	Granite	Thomas et al. (2016)
	1969 ± 0.4, 2048 ± 0.7, 2093 ± 0.6	$^{207}Pb/^{206}Pb$ zircon	Granite, enderbite (protolith)	Ring et al. (1997)
Ufipa	1838 ± 86	Rb-Sr	Granite	Schandelmeier (1983)
	1723 ± 41, 1725 ± 48, 1864 ± 32	U-Pb zircon, TIMS	Granite	Lenoir et al. (1994)
Bangweulu Block	1832 ± 32, 1860 ± 13, 1862 ± 8, 1866 ± 9	U–Pb SHRIMP zircon	Granite	De Waele et al. (2006b)
	1856 ± 4, 1862 ± 19, 1868 ± 7, 1871 ± 24	U–Pb SHRIMP zircon	Rhyolitic tuff, basalt	De Waele and (2006b)
Upangwa	2084 ± 86	U-Pb zircon, TIMS	Tonalitic gneiss (protolith)	Lenoir et al. (1994)
	2026 ± 8	U-Pb zircon, TIMS	Granite	Lenoir et al. (1994)
	1984 ± 35	U-Pb zircon, LA-MC-ICP-MS	Hbl-Pl-Px gneiss (protolith)	Thomas et al. (2016)
	1674 ± 15	U-Pb zircon, SHRIMP	Andesite	Manya (2013)
	1960.7 ± 0.4	Pb-Pb zircon, evaporation	Biotite metatonalite	Vrána et al. (2004)
	1797 ± 44	U-Pb zircon, LA-MC-ICP-MS	Bt gneiss (protolith)	Thomas et al. (2016)
Ubena granitoids	1857 ± 19, 1877 ± 15, 1887 ± 11	U-Pb zircon, LA-MC-ICP-MS	Hbl Tonalites, Bt high-K granites	Manya and Maboko (2016)
	1820 ± 9 - 1824 ± 12	U-Pb zircon, SHRIMP	Faintly foliated granite	Sommer et al. (2005)
Mesoproterozoic ages				
Upangwa	991 ± 32, 1045 ± 24, 1083 ± 16	Pb-Pb zircon, evaporation	Nepheline syenite	Vrána et al. (2004)
	1329.1 ± 0.6	Pb-Pb zircon, evaporation	Biotite metagranite	Vrána et al. (2004)
Lupa	1040 ± 40	K - Ar mica	Carbonatite	Cahen and Snelling (1966)
Wakole	1392 ± 26	U-Pb zircon, SHRIMP	Ultramafic complex (Kapalagulu)	Maier et al. (2007)
	1403 ± 14	U-Pb zircon, SHRIMP	Ultramafic complex (Kabanga)	Maier et al. (2007)
Nyika	1010 ± 22	U-Pb zircon, SHRIMP	Eclogite protolith	Ring et al. (2002)
Bangweulu Block	1145 ± 20	Rb - Sr whole rock	Lusenga syenite	Brewer et al. (1979)
Neoproterozoic ages				
Upangwa	724 ± 6	U-Pb zircon, TIMS	Granite	Lenoir et al. (1994)
	724 ± 6	U-Pb zircon, TIMS	Granite	Theunissen et al. (1992)
	842 ± 80	U-Pb zircon, TIMS	Granite	Lenoir et al. (1994)
Mbozi	743 ± 30	K-Ar biotite	Syenite	Brock (1968)
	685 ± 62		Syenite	Ray (1974)

Note: ID-TIMS—isotope dilution-thermal. ionization mass spectrometry; LA-ICP-MS—laser ablation–inductively coupled plasma–mass spectrometry; SC/MC—single collector/multicollector; SHRIMP—sensitive high-resolution ion microprobe.

TABLE 3. METAMORPHIC AGES FROM THE UBENDIAN LITHOTECTONIC TERRANES

Terrane	Metamorphic ages (Ma)	Analytical technique	Lithology	Authors
Archean ages				
Katuma	2650 ± 8	U-Pb zircon, LA-ICP-MS	Metabasites	Kazimoto et al. (2014)
Paleoproterozoic ages				
Katuma	1902 ± 73	Rb-Sr whole rock, TIMS	Bt gneiss	Lenoir et al. (1994)
	1941 ± 8, 1958 ± 8, 1963 ± 14, 2025 ± 7, 2046 ± 11	U-Pb zircon, LA-ICP-MS	Metapelite, calc-silicate, granitoids	Kazimoto et al. (2014)
	1957 ± 10, 1967 ± 16	U-Th-Pb monazite, microprobe	Metapelite	Kazimoto et al. (2015a)
	1837 ± 6, 1848 ± 16	U-Th-Pb monazite, microprobe	Metapelite	Kazimoto et al. (2015a)
	1938 ± 11	U-Th-Pb monazite, microprobe	Metapelite	Kazimoto et al. (2015b)
	1827 ± 10	U-Th-Pb monazite, microprobe	Metapelite	Kazimoto et al. (2015b)
	1879 ± 9	U-Pb zircon, LA ICP MS	MS-Bt granitic gneiss	Kazimoto et al. (2014)
	1900 ± 14	U-Pb zircon, SHRIMP	Bt gneiss	Boniface (2009)
	1977 ± 40	U-Pb zircon, SHRIMP	Mafic granulite	Boniface (2011)
Lupa	1871 ± 12, 1873 ± 5, 1876 ± 10, 1885 ± 9, 1886 ± 6, 1894 ± 45	Re-Os sulfides (pyrite etc.), N-TIMS	Au quartz veins	Lawley et al. (2013b)
	1953 ± 6, 1937 ± 4, 1953 ± 37	Re-Os sulfides (pyrite etc.), N-TIMS	Au quartz veins	Lawley et al. (2013b)
	1930 ± 3Ma, 1921 ± 7Ma	U-Pb titanite, ID-TIMS	Au quartz veins	Lawley et al. (2014)
Mbozi	1814 ± 7	U-Th-Pb monazite, microprobe	Metapelite	Boniface (2009)
Nyika	1969 ± 0.4, 1988 ± 0.6	$^{207}Pb/^{206}Pb$ zircon	Cordierite gneiss, anatectic granite	Ring et al. (1997)
	2002 ± 0.3	$^{207}Pb/^{206}Pb$ zircon	Enderbite	Ring et al. (1997)
Ubende	1886 ± 16, 1866 ± 14	U-Pb zircon, SHRIMP	Eclogite	Boniface et al. (2012)
	1831 ± 11, 1817 ± 26	U-Pb zircon, SHRIMP, microprobe	Metapelite	Boniface et al. (2012)
	1828 ± 8, 1839 ± 7, 1848 ± 6, 1854 ± 4	Ar-Ar barroisite	Mafic tectonites	Boven et al. (1999)
Ufipa	1949 ± 16, 1901 ± 37, 1919 ± 12, 1835 ± 11	U-Pb zircon, SHRIMP	Metapelite	Boniface and Appel (2018)
	1901 ± 37	U-Pb zircon, SHRIMP	Metapelite	Boniface (2009)
	1924 ± 77	U-Pb zircon, LA-MS	Eclogite	This study
Upangwa	1820	U-Pb zircon, LA-SC/MC-ICP-MS	Bt orthogneiss	Thomas et al. (2016)
	1808 ± 9	U-Th-Pb monazite, microprobe	Metapelite	Boniface and Appel (2017)
Mesoproterozoic ages				
Upangwa	991 ± 32, 1083 ± 16	U-Pb zircon, LA-SC/MC-ICP-MS	Opx-Cpx granulite, Grt-Bt orthogneiss	Thomas et al. (2016)
	944 ± 4	U-Th-Pb monazite, microprobe	Metapelite	Boniface and Appel (2017)
Lupa	975 ± 6 - 1057 ± 56	Re-Os sulfides (pyrite etc.), N-TIMS	Au quartz veins	Lawley et al. (2013b)
Wakole	1170 ± 10, 1022 ± 5, 1016 ± 10	U-Th-Pb monazite, microprobe	Metapelite	Boniface et al. (2014)
	1166 ± 14, 1007 ± 6	U-Pb zircon, SHRIMP	Metapelite	Boniface et al. (2014)
Katuma	1171 ± 17	U-Th-Pb monazite, microprobe	Metapelite (hydrothermal fluids)	Kazimoto et al. (2015b)
	719 ± 38	Pb isotopic data on galena	Hydrothermal sulfides	Stendal et al. (2004)
Ubende	1091 ± 9	U-Pb zircon, SHRIMP	Metapelite	Boniface et al. (2012)
Neoproterozoic ages				
Upangwa	565 ± 4, 559 ± 8	U-Th-Pb monazite, microprobe	Metapelite	Boniface and Appel (2017)
Nyika	872 ± 51	U-Pb zircon, LA-SC/MC-ICP-MS	Granitic orthogneiss	Thomas et al. (2016)
	533 ± 5, 500	$^{207}Pb/^{206}Pb$ zircon, SHRIMP	Eclogite	Ring et al. (2002)
Ubende	596 ± 41	U-Pb zircon, SHRIMP	Eclogite	Boniface et al. (2012)
	601 ± 7	U-Th-Pb monazite, microprobe	Metapelite	Boniface et al. (2012)
Ufipa	524 ± 12, 548 ± 39, 593 ± 20	U-Pb zircon, SHRIMP	Eclogite	Boniface and Schenk (2012)

Note: ID-TIMS—isotope dilution-thermal ionization mass spectrometry; N-TIMS—negative TIMS; LA-ICP-MS—laser ablation–inductively coupled plasma–mass spectrometry; SC/MC—single collector/multicollector; SHRIMP—sensitive high-resolution ion microprobe; MS—magnetic susceptibility. Mineral abbreviations are according to Kretz (1983) and Whitney and Evans (2010).

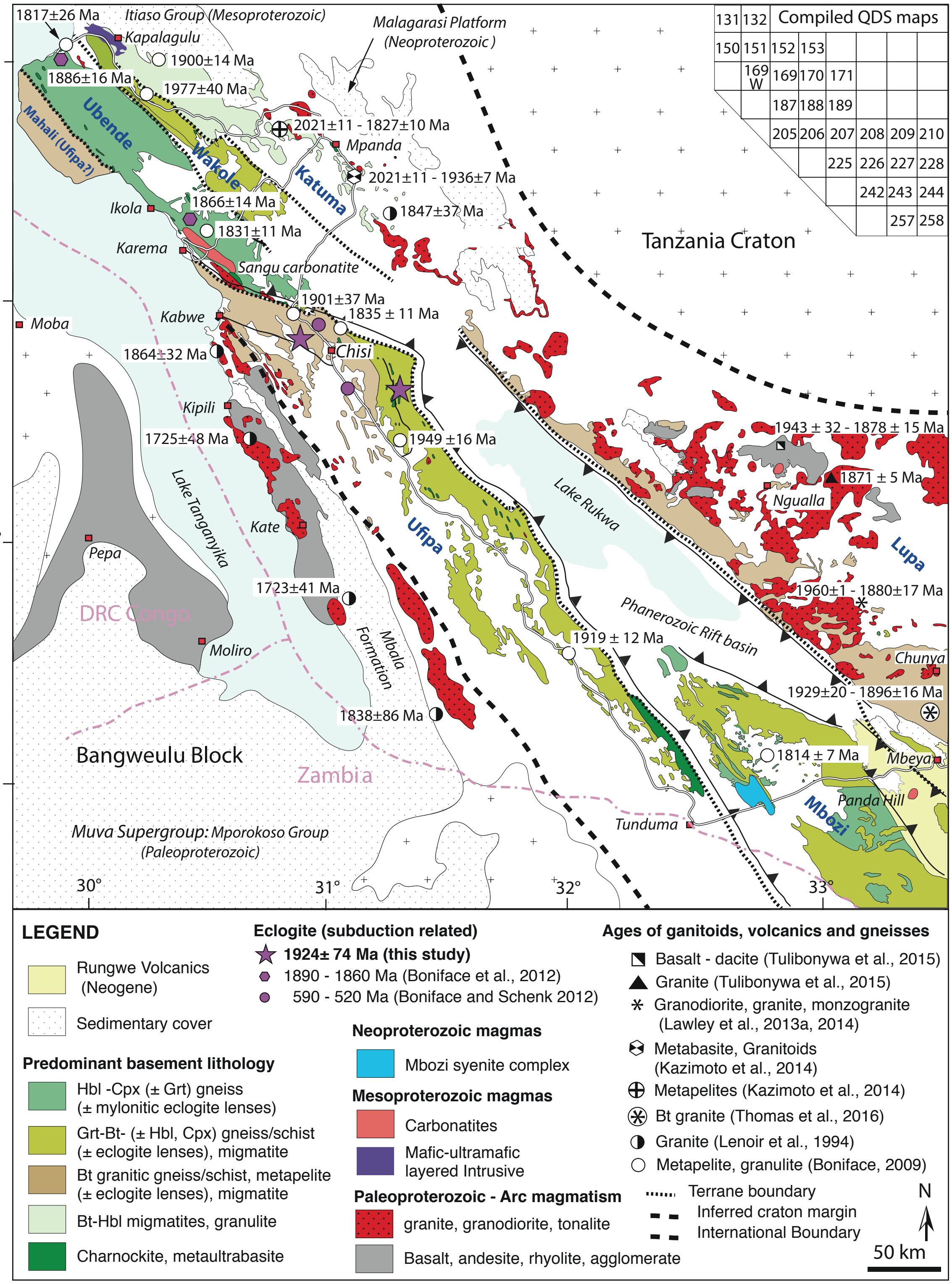

Figure 8. Geological map of the northern Ubendian Belt showing the main lithologies and their ages in different terranes. The map was compiled by combining and modifying 28 quarter degree sheet (QDS) maps published by the Geological Survey of Tanzania (Teale et al., 1958; Halligan and Birch, 1961a, 1961a; Kennerley, 1962; van Loenen and Kennerley, 1962b, 1962a; van Loenen and Kabengele, 1962; Mudd, 1962; Orridge, 1962; Macfarlane et al., 1962; Macfarlane et al., 1964; Macfarlane, 1963, 1965, 1966; Iskahakov et al., 1970; Miyashev et al., 1970; Smirnov et al., 1970; Semyanov et al., 1970; Smirnov et al., 1971b, 1971a; Biyashev et al., 1971; Iskhakov et al., 1971; Trifan et al., 1972; Tolochko et al., 1972; Semyanov et al., 1972a, 1972b, 1972c; Smirnov et al., 1973; Harkin and Harpum, 1978). Bt—biotite; Cpx—clinopyroxene; Grt—garnet; Hbl—hornblende.

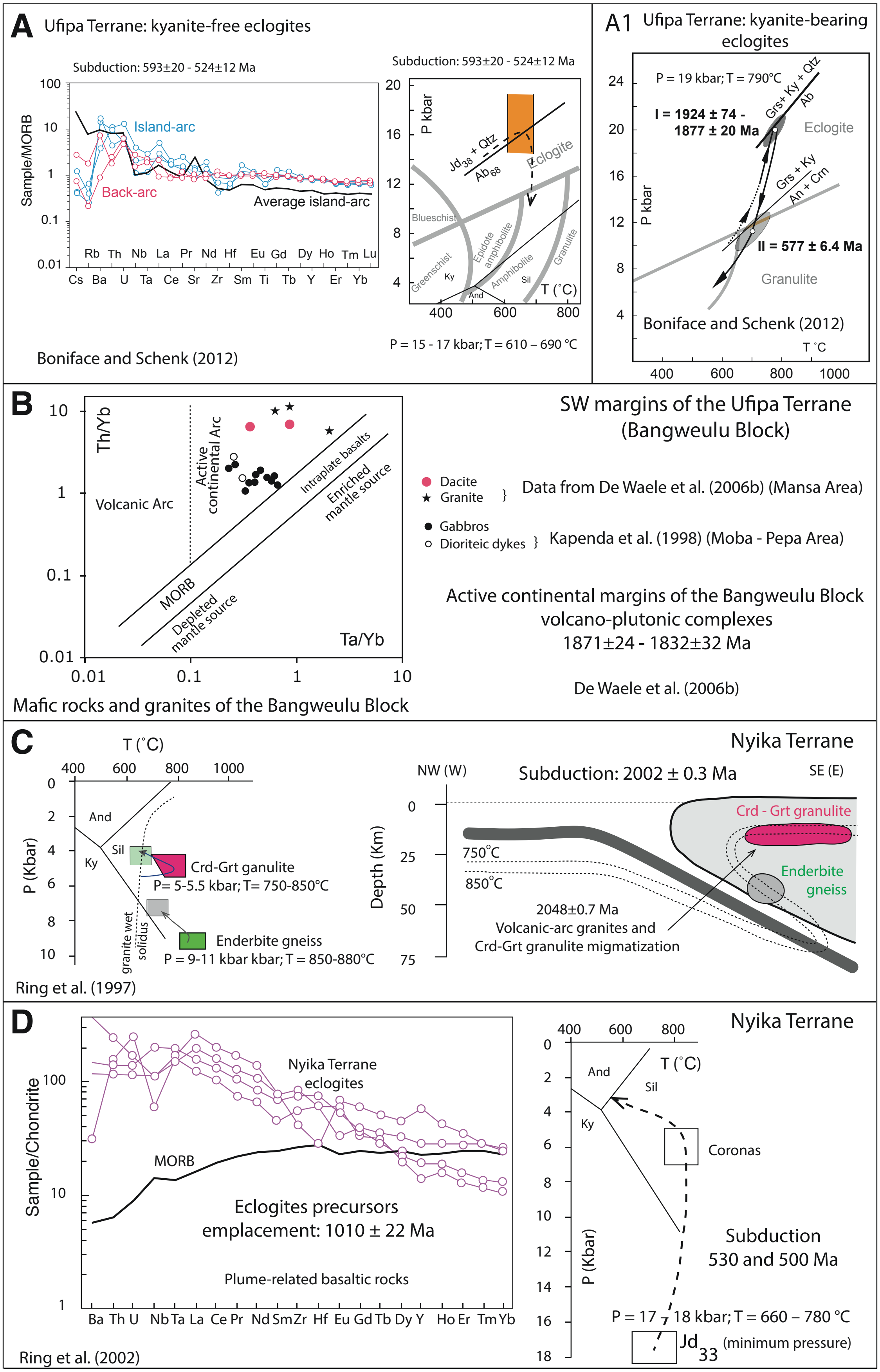
A
Ufipa Terrane: kyanite-free eclogites
Subduction: 593±20 - 524±12 Ma
Sample/MORB
Island-arc
Back-arc
Average island-arc
Rb Th Nb La Pr Nd Hf Eu Gd Dy Ho Tm Lu
Cs Ba U Ta Ce Sr Zr Sm Ti Tb Y Er Yb
P kbar
Eclogite
Blueschist
Greenschist
Epidote amphibolite
Amphibolite
Granulite
T (°C)
P = 15 - 17 kbar; T = 610 – 690 °C
Boniface and Schenk (2012)
A1 Ufipa Terrane: kyanite-bearing eclogites
P = 19 kbar; T = 790°C
I = 1924 ± 74 - 1877 ± 20 Ma
II = 577 ± 6.4 Ma
Eclogite
Granulite
Grs + Ky + Qtz
Ab
Grs + Ky
An + Crn
Boniface and Schenk (2012)
T °C
B
Th/Yb
Ta/Yb
Volcanic Arc
Active continental Arc
MORB
Intraplate basalts
Enriched mantle source
Depleted mantle source
Mafic rocks and granites of the Bangweulu Block
SW margins of the Ufipa Terrane (Bangweulu Block)
Dacite
Granite
Data from De Waele et al. (2006b) (Mansa Area)
Gabbros
Dioriteic dykes
Kapenda et al. (1998) (Moba - Pepa Area)
Active continental margins of the Bangweulu Block volcano-plutonic complexes
1871±24 - 1832±32 Ma
De Waele et al. (2006b)
C
T (°C)
P (Kbar)
And
Sil
Ky
Crd-Grt ganulite
P= 5-5.5 kbar; T= 750-850°C
Enderbite gneiss
P = 9-11 kbar kbar; T = 850-880°C
granite wet solidus
Ring et al. (1997)
Nyika Terrane
Subduction: 2002 ± 0.3 Ma
NW (W)
SE (E)
Depth (Km)
750°C
850°C
Crd - Grt granulite
Enderbite gneiss
2048±0.7 Ma
Volcanic-arc granites and
Crd-Grt granulite migmatization
D
Sample/Chondrite
Nyika Terrane eclogites
MORB
Eclogites precursors emplacement: 1010 ± 22 Ma
Plume-related basaltic rocks
Ba Th U Nb Ta La Ce Pr Nd Sm Zr Hf Eu Gd Tb Dy Y Ho Er Tm Yb
Ring et al. (2002)
Nyika Terrane
T (°C)
And
Sil
Ky
Coronas
Subduction
530 and 500 Ma
P (Kbar)
P = 17 – 18 kbar; T = 660 – 780 °C
Jd33 (minimum pressure)

Figure 9.

Figure 9. Geochronology and tectonic settings of eclogites, volcanics, and granitoids of the Western Ubendian Corridor. (A) Neoproterozoic kyanite-free eclogites of the Ufipa Terrane, adapted from Boniface and Schenk (2012). (A1) Paleoproterozoic kyanite-bearing eclogites of the Ufipa Terrane with Neoproterozoic granulite facies overprint. (B) Gabbros, diorites, tuff, basalts, and granites of the margins of the Bangweulu Block, geochemical and geochronological data from Kapenda et al. (1998) and De Waele and Fitzsimons (2007). (C) Paleoproterozoic Crd-Grt gneisses and enderbite gneisses of the Nyika Terrane, data from Ring et al. (1997). (D) Paleoproterozoic eclogites of the Nyika Terrane (Ring et al., 2002).

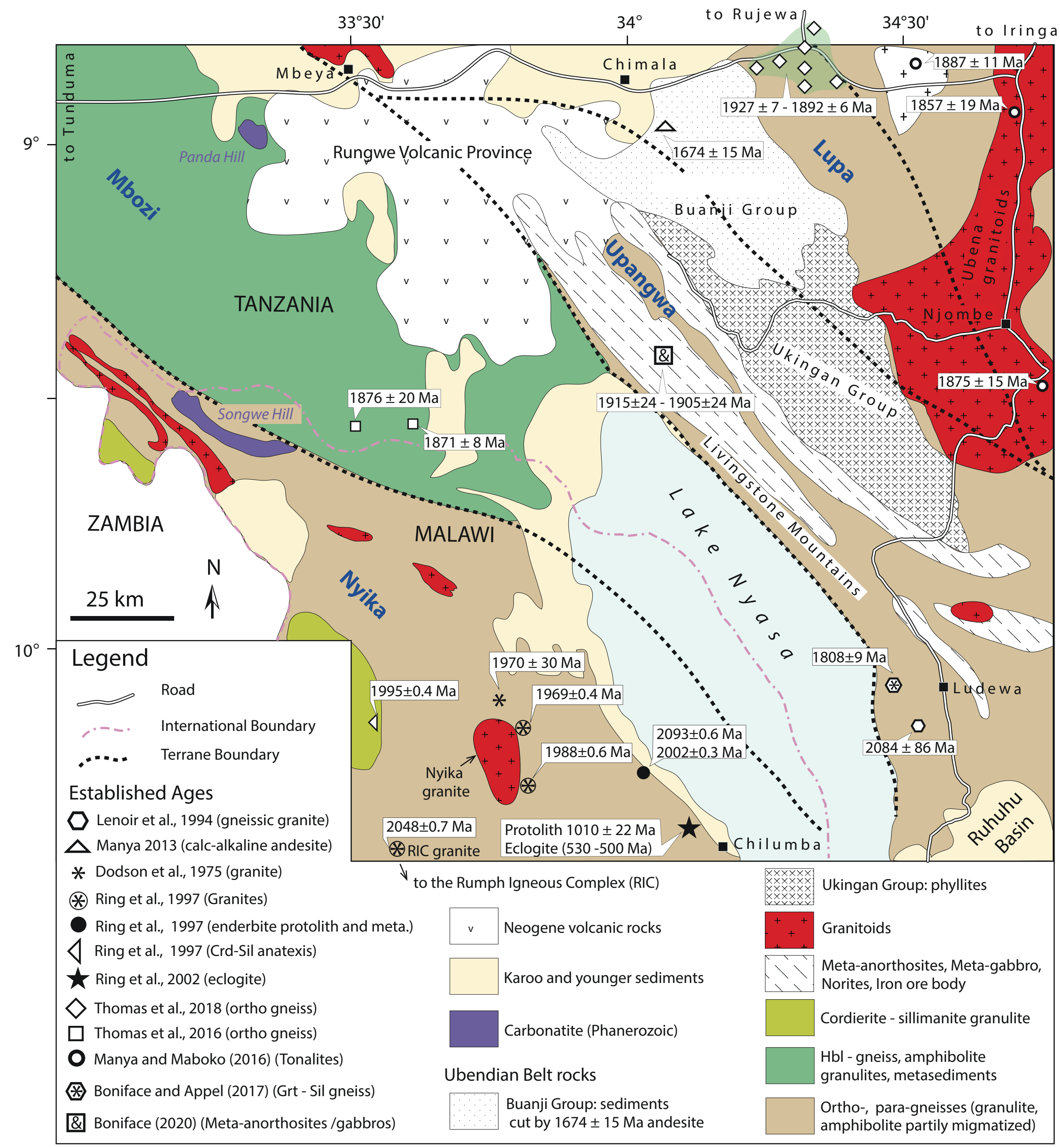

Figure 10. Geological map of the southern Ubendian Belt showing the main lithologies and their ages in different terranes. The map was compiled from several quarter degree sheet maps and other published information (Haldemann, 1953; Harpum and Brown, 1958; Harpum, 1958; Thatcher, 1974; Pinna et al., 2004).

Crd-Grt-Sil felsic granulites of the Nyika Terranes were metamorphosed at relatively low pressure (P = 0.50–0.55 GPa and T = 750–850 °C) coeval to the high-pressure granulite and were metamorphosed in the upper plate of a subduction zone between 1995 ± 0.6 and 1988 ± 0.6 Ma Pb-Pb zircon (Fig. 9C; Ring et al., 1997). The Nyika granite, and other Bt granites are interpreted as collisional-type granites that intruded between 1970 ± 30 and 1969 ± 0.4 (U-Pb and Pb-Pb zircon) after the peak of granulite facies metamorphism (Fig. 10; Dodson et al., 1975; Ring et al., 1997). Granites with volcanic-arc magmas affinity are dated at 2048 ± 0.7 Ma (Pb-Pb zircon) from the Rumphi Igneous Complex (RIC) (Fig. 10), and are therefore related to the onset of subduction and generation of enderbitic gneiss precursors (Ring et al., 1997).

4.1.3. Magmatism and Other Events in the Western Ubendian Corridor

The Ufipa and Nyika Terranes have common boundaries with the Paleoproterozoic Bangweulu and Irumide Belt, respectively (Fig. 3A). The boundary between the Ufipa Terrane and the Bangweulu Block is covered by the Paleoproterozoic sedimentary rocks (Mbala Formation: sandstone, siltstone, mudstone, conglomerate), which overlie the Paleoproterozoic Kate-Kipili volcanic rocks (dacite, rhyolites, agglomerate) and the Paleoproterozoic granitoid (granite, Bt-granite, granodiorite, syenogranite) (Table 1 and Fig. 8). The Mbala Formation (part of the Muva Supergroup that is entirely intruded by a 1145 ± 20 Ma (Rb-Sr whole-rock isochron) syenite (e.g., Brewer et al., 1979) and the Paleoproterozoic volcanic and plutonic rocks extend to the Democratic Republic of Congo, in the Bangweulu Block where they are well characterized petrologically, geochemically, and geochronologically (Unrug, 1984; Kabengele et al., 1991; Kapenda et al., 1998; De Waele et al., 2006a; Debruyne et al., 2014).

The volcanic and plutonic rocks (quartz diorites and andesitic/dacitic rocks) of the Moba-Pepa area (Figs. 2 and 8: Democratic Republic of Congo) have calc-alkaline magmas affinity and have trace-element compositions with high Th/Ta and La/Ta values; low Sr/Ce ratios indicating the involvement of a subduction component at the magma source (Fig. 9B; Kabengele et al., 1991; Kapenda et al., 1998). The granitoids associated with volcanic rocks in the Moba-Pepa area yield a whole-rock Rb-Sr emplacement age of 1861 ± 28 Ma (Kabengele et al., 1991). Similarly, to the southern end of the Bangweulu Block, granites and volcanic tuffs that form the basement to the Muva Supergroup have U-Pb zircon crystallization ages that range between 1868 ± 7 and 1860 ± 13 Ma (De Waele and Fitzsimons, 2007). In Tanzania, similar results have been constrained from the granitoids in the Kate-Kipili area (Fig. 8), where Kate and Ufipa granites yield U-Pb zircon and Rb-Sr whole-rock ages at 1864 ± 32 and 1838 ± 86 Ma (Schandelmeier, 1983; Lenoir et al., 1994); however, younger granitoids in the same area have U-Pb zircon ages between 1725 ± 48 and 1723 ± 41 Ma (Lenoir et al., 1994). The Kate granites have a strong calc-alkaline magma affinity and are classified as I-type granites (Nanyaro et al., 1983).

4.2. Ubende, Mbozi, and Upangwa Terranes

The Ubende, Mbozi, and Upangwa Terranes have common geochronological and geological patterns (Fig. 3A). We hereby group the Ubende, Mbozi, and Upangwa Terranes as the Central Ubendian Corridor. The common geological feature to all these terranes is the predominance of metamorphosed igneous rocks with mafic compositions interlayered with lenses of metamorphosed ultramafic intrusions locally (Harpum, 1952; Morris, 1952; Haldemann, 1953; Sutton et al., 1954; Halligan and Birch, 1961b; Macfarlane, 1966; Smirnov et al., 1971b; Tolochko et al., 1972; Nanyaro et al., 1981; Boniface, 2014).

4.2.1. Paleoproterozoic Eclogites in the Central Ubendian Corridor

The Ubende Terrane is the only unit in the Central Ubendian Corridor that hosts mafic rocks metamorphosed to eclogite facies conditions. The Ubende Terrane is mainly composed of foliated metabasites that include Hbl-gneisses, amphibolites, Grt-Hbl gneiss, mafic granulites, and Grt-Cpx gneisses. The foliated metabasites enclose layers of foliated eclogite, serpentinized ultramafic bodies, metapelites, and quartzites, which is considered to be an ophiolite suite (Table 1; Sutton et al., 1954; Halligan and Birch, 1961b; Macfarlane, 1966; Smirnov et al., 1971b; Tolochko et al., 1972; Nanyaro et al., 1981; Sklyarov et al., 1998). However, according to the definition proposed during the 1972 Penrose Conference (ophiolite sequence consists, from bottom to top, of upper mantle peridotites, layered ultramafic-mafic rocks, layered to isotropic gabbros, sheeted dikes, extrusive rocks, and a sedimentary cover [see Dilek and Furnes, 2014, and reference therein]), there are no clear sequences of ophiolite mapped in the Ubendian-Usagaran Belt, but deformed and metamorphosed assemblages of ultramafic, mafic and sedimentary rocks that former authors loosely defined as ophiolites. Deformed metabasites of Ubendian-Usagaran origin have been geochemically characterized and interpreted as relics of former oceanic crusts (see Boniface et al., 2012; Evans et al., 2012; Boniface and Tsujimori, 2019).

The P-T conditions of the foliated high-pressure granulites (interpreted as retrogressed eclogites) are estimated at P = 1.22–1.37 GPa and T = 840–900 °C (Muhongo et al., 2002). The foliated high-pressure granulites (retrogressed eclogites) are composed of garnet porphyroclasts with inclusions of omphacite (Jd_{17}). The garnet core and omphacite inclusions yield a maximum pressure of 1.5 GPa indicating prograde eclogite facies conditions (Boniface et al., 2012). Additionally, Sklyarov et al. (1998) described a pod of slightly foliated kyanite-bearing eclogite from the Ubende Terrane and estimated P-T conditions at P = 1.71 (±0.07)–1.97 (±0.15 GPa and T = 609 (±66)–724 (±13) °C. However, subsequent studies by Boniface et al. (2012) and our current research group were unable to locate the kyanite-bearing eclogite pods in the Ubende described by Sklyarov et al. (1998). The foliated eclogites of the Ubende Terrane have MORB and E-MORB affinities and trace-element ratios ranging from 0.2

to 1.4 for Nb/La and from 0.9 to 1.5 for $(La/Sm)_N$, which are interpreted to be relics of subducted basalts that erupted at mid-oceanic ridge or back-arc settings (Boniface et al., 2012). Prior to mylonitization, the Ubende Terrane eclogites formed in a warm subduction zone (geothermal gradient 13 °C/km) with metamorphic conditions of P = 1.5 GPa and T = 700 °C. The subduction of an oceanic lithosphere occurred between 1886 ± 16 and 1866 ± 14 Ma (U-Pb zircon) (Fig. 11A; Boniface et al., 2012).

4.2.2. Other Tectonic Events in the Central Ubendian Corridor

The subduction in the Ubende Terrane was followed by a regional metamorphic event between 1817 ± 26 and 1831 ± 11 Ma (U-Pb zircon and U-Th-Pb monazite) recorded in Grt-Ky metapelites. Finally, regional Mesoproterozoic (1091 ± 9 Ma: U-Pb zircon,) and Neoproterozoic (596 ± 41 Ma: U-Pb zircon) metamorphic events reworked the eclogite and metapelites of the Ubende Terrane (Boniface et al., 2012).

The niobium-iron bearing Sangu carbonatite complex intrudes in the Ubende Terrane basement between the Ikola and Karema villages (Fig. 8). The carbonatite complex consists of several foliated lens-shaped bodies aligned NW-SE and assumed to have intruded the Ubendian basement in Mesoproterozoic time, coeval to the 1040 ± 40 Ma (K-Ar phlogopite) Ngualla carbonatite in the Lupa Terrane (Coetzee, 1963; Smirnov et al., 1971a; Cahen et al., 1984).

The Ubende Terrane gneisses are also intruded by a complex suite of lenticular bodies (mafic, ultramafic, gabbro-norite

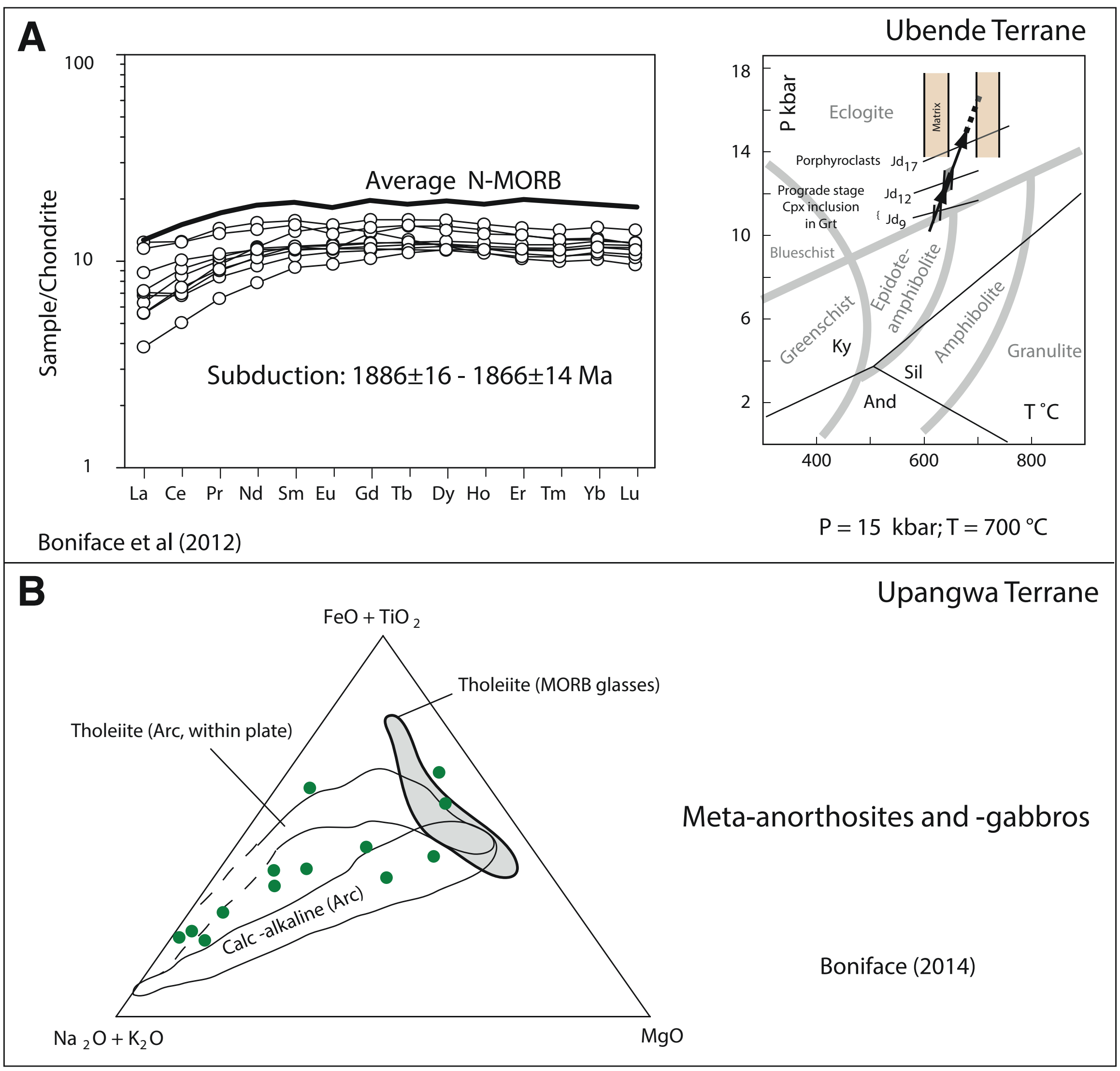

Figure 11. Metamorphic conditions, geochronology, and tectonic settings of rocks from the Central Ubendian Corridor. (A) Paleoproterozoic eclogites from the Ubende Terrane, adapted from Boniface et al. (2012). N-MORB—normal–mid-ocean ridge basalt. (B) Meta-anorthosites and metagabbros from the Upangwa Terrane, adapted from Boniface (2014).

association), which are correlated to the Mesoproterozoic Kapalagulu mafic-ultramafic (1392 ± 26 Ma: U-Pb zircon) layered intrusive complex in the Wakole Terrane (Fig. 8; Smirnov et al., 1971a; Maier et al., 2007). Cu-Ni–bearing quartz veins with paragenesis of pentlandite-pyrrhotite-chalcopyrite occur in metabasite and gabbro-norite intrusions (Coetzee, 1963; Smirnov et al., 1971a; Tamaini et al., 1988). The Cu-Ni occurrence in the mafic-ultramafic young intrusions of the Ubende Terrane is probably another feature for correlating these intrusions to the Mesoproterozoic Kapalagulu igneous complex (see Maier et al., 2008; Wilhelmij and Cabri, 2016).

The Mbozi Terrane is composed of a granulites-amphibolites suite (Grt-Opx-Cpx granulites, Grt-Cpx-Hbl granulites, amphibolites) occurring together with amphibolite- to granulite-facies metasedimentary rocks (Bt gneiss, Grt-Bt gneiss, Sil-Grt-Bt gneiss, and quartzites), quartzo-feldspathic gneisses and minor granites and meta-anorthosites (Fig. 8; Teale et al., 1958; Kennerley, 1962; Macfarlane, 1966; Ramadhani and Kamihanda, 2014b; Ramadhani et al., 2015). Major- and trace-element composition of mafic granulites, Hbl gneisses, and meta-anorthosites suggest basaltic and andesitic precursor magmas with strong calc-alkaline and tholeiite MORB glass affinity, which points to their formation in a back-arc and island-arc tectonic settings (Boniface, 2015). Biotite-bearing granitic orthogneisses associated with granulites-amphibolites suite give U-Pb zircon crystallization ages of 1876 ± 20 and 1871 ± 8 Ma (Fig. 10; Thomas et al., 2016). However, the age of granulite facies metamorphism in the Mbozi Terrane remains speculative. Grt-Bt-Sil metapelitic gneisses from the northern Mbozi Terrane have been dated at 1814 ± 7 Ma (U-Th-Pb monazite: metamorphic ages) (Boniface, 2009).

The characteristic rocks of the Upangwa Terrane are meta-anorthosite and meta-gabbro bodies that are associated with meta-iron ore bodies, and they enclose lenses of platinum-palladium gold-bearing ultramafic rock association (serpentinites, dunites, wehrlites, and pyroxenites) (Stockley, 1948; Morris, 1952; Harpum, 1958, 1970; Daly, 1988; Evans et al., 2012; Ramadhani and Kamihanda, 2014a). The Upangwa Terrane meta-anorthosites and meta-gabbros belong to the MORB tholeiite and calc-alkaline magma series (Fig. 11B). Their REE patterns display two distinct spidergrams: a pattern with gentle REE negative slope with positive Ce and Eu anomaly; and a pattern with light (L)REE enrichments and heavy (H)REE depletions with no negative Eu anomaly (Evans et al., 2012; Boniface, 2015). The geochemical composition of the anorthosite rocks is interpreted to point to the formation of their precursor magma at the subduction zone settings with significant addition of a subduction component as reflected in the high Ba/La ratio, and the positive Ce anomaly points to the addition of subduction component by partial melting of marine sediments rich in manganese deposits (Boniface, 2015). The crystallization ages of the Upangwa Terrane meta-anorthosites and meta-gabbros range between 1915 ± 24 and 1905 ± 24 Ma (U-Pb zircon: Boniface, 2020), which is most likely the timing of the Upangwa iron-ore bodies and the associated mafic-ultramafic bodies in the area.

The Upangwa Terrane is also composed of high-grade orthogneisses (tonalitic, dioritic, and granodioritic intrusives) and paragneisses, schists, and migmatites derived from both metasediments and meta-igneous rocks, and the foliated granitoid shield that is locally known as the Ubena granitoids (Fig. 10). The crystallization ages of the Upangwa Terrane orthogneisses range between 1927 ± 7 and 1892 ± 6 Ma (U-Pb zircon: Thomas et al., 2018). This age range is slightly older than the crystallization age of the Ubena granitoids that intruded the areas between 1887 ± 11 and 1857 ± 19 Ma (U-Pb zircon) as described below (Manya and Maboko, 2016).

The Ubena granitoids crop out in Iringa and extend to the eastern margins of the Upangwa Terrane (Fig. 3A and Fig. 10). The Ubena granitoids are mainly composed of groups of tonalites, aplitic granites, and high-K granitic gneisses (Stockley, 1948; Haldemann, 1953; Harpum, 1958). At the eastern margins of the Upangwa Terrane, the tonalites and high-K granites were emplaced between 1887 ± 11 and 1857 ± 19 Ma (U-Pb zircon) as derivatives of underplated mafic rocks (Manya and Maboko, 2016). In the Iringa area (Fig. 4), the granitoids (1871 ± 30 Ma: U-Pb zircon) are associated with the calc-alkaline trachyandesites-dacites-trachytes-rhyolites Ndembera metavolcanics (1896 ± 29 Ma: U-Pb zircon) and are believed to form a single suite of volcano-plutonic rocks derived from crustal anatexis of basic meta-igneous rocks mixed with a minor metasedimentary component in an intracontinental setting (Bahame et al., 2016).

Younger sedimentary basins (the Buanji and Ukingan Groups) straddle the boundary between the Upangwa Terrane and the Lupa Terrane and overlie uncomformably to the Ubendian basement rocks (Fig. 10; Stockley, 1948; Harpum, 1958). The Buanji Group (shales, siltstones, ferruginous sandstone, current-bedded quartzitic sandstone, and in-place greywacke, and conglomerate) overlies the Ukingan Group (intensely folded, over-folded, low-grade rocks: slates, phyllites, schists, quartzites, and cataclasite). The Buanji Group is intruded and capped by effusive high-K calc-alkaline subduction related basaltic andesitic lavas dated at 1674 ± 15 Ma (U-Pb zircon) (Manya, 2013).

The Upangwa Terrane marks a triple junction between the Paleoproterozoic Ubendian Belt, the Mesoproterozoic Irumide Belt, and the Neoproterozoic Mozambique Belt (Fig. 3). Thomas et al. (2016) and Boniface and Appel (2017) have described the metamorphic reworking of the Ubendian crust (1808 ± 9 Ma detrital monazite) in the Upangwa Terrane at 1045 ± 25 to 944 ± 4 Ma and between 565 ± 4 and 559 ± 8 Ma during the Irumide and Mozambique orogenesis, respectively. Lenoir et al. (1994) reported magmatic bodies with an age of 724 ± 6 Ma in the Upangwa Terrane. The oldest protolith age of a tonalitic orthogneiss in the Upangwa Terrane has been dated at 2084 ± 86 Ma by (Theunissen et al., 1992). In addition to those younger ages, Thomas et al. (2018) estimate the age of potassic granite from around Chimala area at 1408 ± 6 Ma (U-Pb Zircon). The emplacement age of the alkali intrusion in southern Ubendian Belt points to extensional tectonics in Mesoproterozoic Era.

4.3. Katuma and Lupa Terranes

The Katuma and Lupa Terranes are hereby referred to as the Eastern Ubendian Corridor. The Katuma and Lupa Terranes mark the contacts between the Archean Tanzania Craton and the Ubendian-Usagaran Belt; they are affected by voluminous Paleoproterozoic magmatism and reworked Archean granitoids, and they host abundant gold and base metal quartz ± carbonate vein deposits (Fig. 8; Van Straaten, 1984; Mnali, 2002; Stendal et al., 2004; Manya, 2011; Lawley et al., 2013a; Kazimoto et al., 2014, 2015a).

The Lupa Terrane is composed of Archean reworked rocks that include migmatized quartzo-feldspathic and granitic orthogneisses and foliated granites, which are intruded by Ngualla metavolcanics (meta-rhyolite, meta-dacite, meta-andesite, and meta-agglomerate), metabasites (diorite, appinite, and gabbro), and Bt ± Hbl granites, Hbl granodiorite, syenogranite, and Bt-Ms granite (Fig. 8; Gallagher, 1939; Teale et al., 1958; Mudd, 1962; Orridge, 1962; Macfarlane et al., 1962; Macfarlane, 1965).

The foliated Archean granites in the Lupa Terrane have U-Pb zircon ages that range between 2758 ± 9 and 2723 ± 10 Ma, reflecting the reworked margins of the Neoarchean Tanzania Craton (Manya, 2011; Kabete et al., 2012; Lawley et al., 2013a; Tulibonywa et al., 2015; Thomas et al., 2016). The foliated Archean granites in the Lupa Terrane were reworked by the emplacement of felsic to intermediate composition granitoids (syenogranite, granite, Bt granite, monzogranite, and granodiorite), which is coeval with the explosive Ngualla basaltic andesite metavolcanics emplaced between 1959.6 ± 1.1 and 1919 ± 37 Ma (U-Pb zircon) (Table 2: Lawley et al., 2013a, 2014; Tulibonywa et al., 2015; Thomas et al., 2016). The pluto-volcanic rocks in the Lupa Terranes have strong calc-alkaline magmas affinity and have REE elements with features like magmas that erupt at the continental arc setting (consistent depletion of Nb and Ta, trace-element ratios: Th/Yb vs. Ta/Yb, Nb/La vs. La/Sm, Zr/Y vs. Zr) (Figs. 12A and 12B: Lawley et al., 2013a; Tulibonywa et al., 2017).

The second magmatic reworking of the older rocks in the Lupa Terrane occurred between 1896 ± 16 and 1871 ± 5 Ma (U-Pb zircon) and was accompanied by the emplacement of gabbroic plutons (gabbro, diorite, appanite), gabbroic dykes, felsic granitoids (granite and Bt granite), and Ngualla porphyritic dacites to rhyodacites volcanics (Table 2: Lawley et al., 2013a; Tulibonywa et al., 2015; Thomas et al., 2016). The second episode of pluto-volcanic magmatism in the Lupa Terrane as in the first episode occurred also at a continental arc margins (Table 2: Lawley et al., 2013a; Tulibonywa et al., 2017).

Lawley et al. (2013a) described how the plutons of the Lupa Terrane are all hydrothermally altered except for the 1880 ± 17 Ma (U-Pb zircon) gabbroic dykes cutting a suite of Archean-Paleoproterozoic granitic-gabbroic intrusions in the area. The structurally controlled hydrothermal veins in the Lupa Terrane are associated with gold-rich deposits (e.g., Gallagher, 1939, 1941; Van Straaten, 1984). The deformation events associated with precipitation of gold-rich quartz-sulfide veins occurred between 1953 ± 6 and 1871 ± 12 Ma (U-Pb titanite and zircon) (Lawley et al., 2013a, 2014). Lawley et al. (2014) concluded that the existing geochronological data point to a protracted, but episodic 1960–1880 Ma magmatic history that overlaps with main phases of deformation and deposition of gold in the Lupa Terrane at ca. 1950 Ma, 1940 Ma, and 1880 Ma. However, a Mesoproterozoic deformation event associated with pyrite-gold-quartz veins has been reported to occur between 1057 ± 56 and 975 ± 6 Ma (Re-Os sulfides) (Lawley et al., 2013b).

The Ngualla carbonatite plug (hosts REE) is the youngest known magmatic body in the Lupa Terrane dated at 1040 ± 40 Ma (K-Ar phlogopite) (Mudd, 1962; Cahen and Snelling, 1966). The carbonatite crystallization age coincides with the last period of pyrite-gold-quartz veins emplacement in Mesoproterozoic time (Lawley et al., 2013b).

The Katuma Terrane in the NE Ubendian Belt like the Lupa Terrane is composed of Archean metabasites (Grt-Cpx granulites, gabbro-norite) and granitoids dated between 2713 ± 11 and 2553 ± 10 Ma (U-Pb zircon) that are intruded and affected by Proterozoic plutonism and metamorphic events (Kazimoto et al., 2015a). The Proterozoic rock units of the Katuma Terrane include meta-igneous rocks (Grt amphibolites, granitic to granodioritic Hb-Bt gneisses that are migmatized and granitized), metasedimentary rocks (pelitic schists and gneisses/migmatitic, calc-silicates, marble, interlayers of quartzites), and intrusions of undeformed Bt granite and granodiorite (Smirnov et al., 1970; Semyanov et al., 1970; Biyashev et al., 1977; Kazimoto et al., 2015a).

The reworking of the Archean crust (margins of the Tanzania Craton) in the Katuma Terrane started by the emplacement of amphibolites with a protolith U-Pb zircon age of 2021 ± 11 Ma and migmatization and granitization of Archean metabasites between 2045 ± 12 and 2025 ± 8 Ma (U-Pb zircon), which was followed by the emplacement of Bt granites and granodiorites between 1993 ± 6 and 1936 ± 20 Ma (U-Pb zircon) and metamorphism of sedimentary rocks that were probably overlaid between 2060 and 2300 Ma (Kazimoto et al., 2015a). The time window for emplacement of granitoids in the Katuma Terrane overlaps with the granulite facies metamorphism recorded in gneisses and migmatites (mafic-granulites, metapelites, calc-silicate, metapelite, B gneisses) to have occurred between 1977 ± 40 and 1900 ± 14 Ma (U-Pb zircon) (Table 3: Lenoir et al., 1994; Boniface, 2009, 2011; Kazimoto et al., 2014, 2015a, 2015b).

The Katuma Terrane granitoids have strong continental arc affinity; thus, it was concluded by Kazimoto et al. (2015a) that in the Paleoproterozoic, the Katuma Terrane was an active continental margin, below which a Paleoproterozoic oceanic lithosphere was subducting (Fig. 12C). The geochemistry of a ca. 1970 Ma mafic granulite in the Katuma Terrane resembles that of tholeiite basalts that erupt at lower continental crustal settings with typical Nb-Ta and Hf-Zr negative anomalies of arc volcanics (Fig. 12D: Boniface, 2011).

The Katuma Terrane records a recurrence metamorphism and reworking of older crusts between 1879 ± 9 and 1827 ± 10 Ma

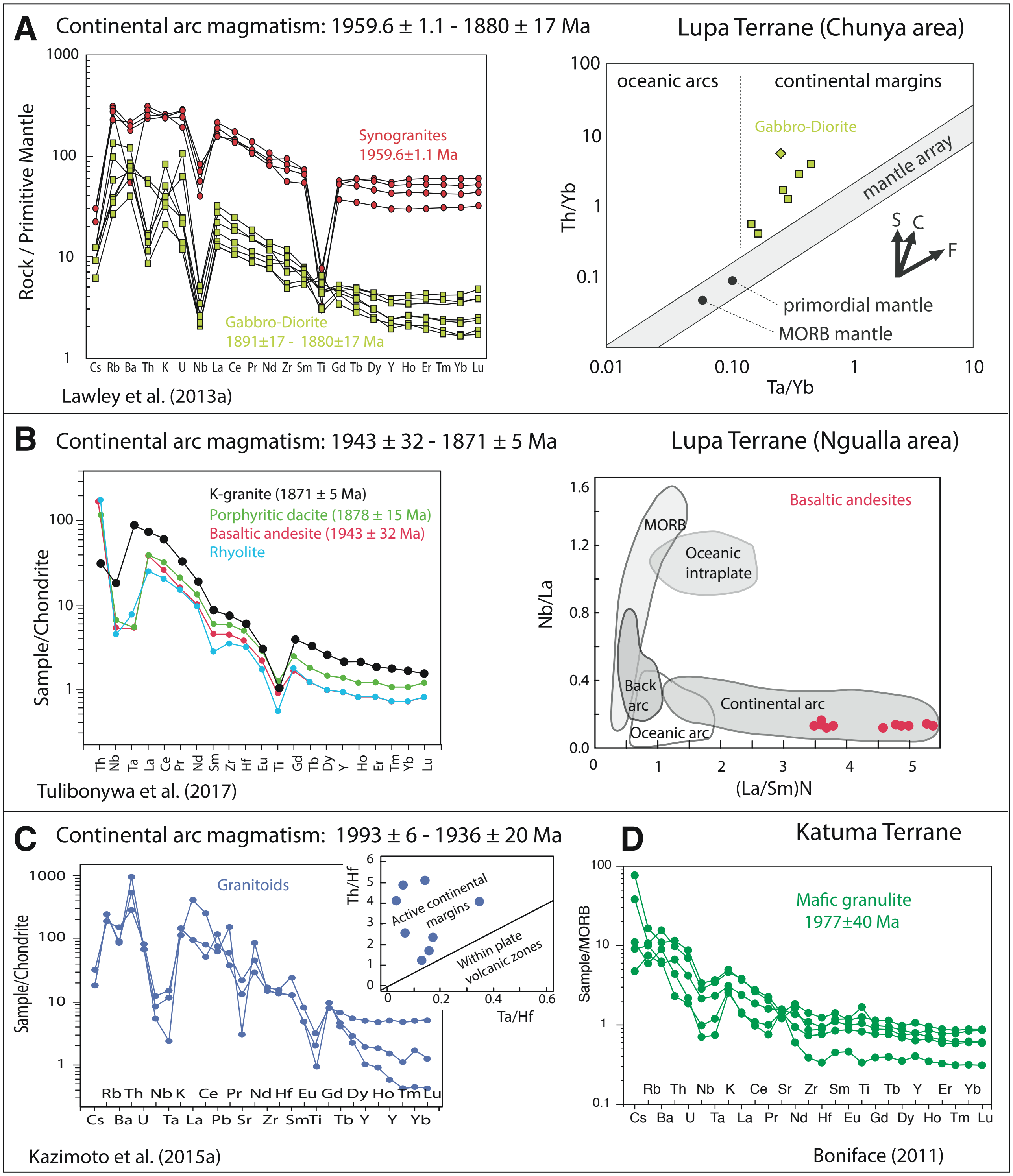

Figure 12. Geochronology and tectonic settings of rocks from the Eastern Ubendian Corridor. (A) Gabbro-diorite and granitoids from the Lupa Terrane (Chunya area), adapted from Lawley et al. (2013a). MORB—mid-ocean ridge basalt. (B) volcanic rocks and granitoids from the Lupa Terrane (Ngualla area), adapted from Tulibonywa et al. (2017). (C) Granitoids and ortho-gneisses from the Katuma Terrane, adapted from Kazimoto et al. (2015a).

(U-Pb zircon; U-Th-Pb monazite) (Kazimoto et al., 2014, 2015a, 2015b). The last recorded period of deformation in the Katuma Terrane that was characterized by the injection of hydrothermal fluids associated with deposition of carbonate-quartz veins and gold and base-metals occurred in the Stenian–Tonian Periods, which is demonstrated by dating of hydrothermally altered monazite at 1171 ± 17 Ma (U-Th-Pb monazite) by Kazimoto et al. (2014) and a vein-type galena at 719 ± 38 Ma (Pb galena) by Stendal et al. (2004).

4.4. Wakole Terrane

The Wakole Terrane is predominantly composed of pelitic metasedimentary rocks (Bt-Grt-Ky schists) interlayered with quartzites and garnetiferous hornblende-gneisses (McConnell 1950; Smirnov et al., 1970; Iskahakov et al., 1970; Smirnov et al., 1971b). The high-grade metasedimentary rocks of the Wakole Terrane were metamorphosed at T = 670–680 °C, P = 0.85–0.89 GPa between 1170 ± 10 and 1001 ± 7 Ma (U-Pb zircon and U-Th-Pb monazite) and have no record of pre-Mesoproterozoic ages (Boniface et al., 2014). The Wakole Terrane rock assemblages, the grade of metamorphism, and the timing of peak metamorphism resemble the neighboring Karagwe-Ankolean Belt in the north (Fig. 13), which comprises (1) the western domain (WD) or the Akanyaru Supergroup mainly consisting of deformed, greenschist- to amphibolite-facies metasedimentary rocks, and (2) the eastern domain (ED) or the Kagera Supergroup characterized by an eastward decrease of deformation and metamorphism (Tack et al., 1994; Fernandez-Alonso et al., 2012; Boniface et al., 2014). The Wakole Terrane is therefore excluded from the Paleoproterozoic Ubendian Terranes that form the western, central, and eastern Paleoproterozoic Ubendian corridors (Fig. 8 and Fig. 10).

The metasediments of the Wakole Terrane have been interpreted to relate to the Mesoproterozoic Supergroup rocks of the Kibaran Belt and Karagwe-Ankolean Belt, which formed in failed rift basins dated with a minimum rifting age of 1403 ± 14 Ma (U-Pb zircon age of the Kabanga mafic-ultramafic layered intrusion) (see Fig. 11; Maier et al., 2007; Fernandez-Alonso et al., 2012; Boniface et al., 2014).

The Mesoproterozoic rift basins in the Kibaran Belt and Karagwe-Ankolean Belt align NE-SW, parallel to the Musongati-Kabanga trends (Fig. 13; Fernandez-Alonso and Theunissen, 1998; Tack et al., 2010; Fernandez-Alonso et al., 2012). The Itiaso Group quartzites and the metapelitic sediments of

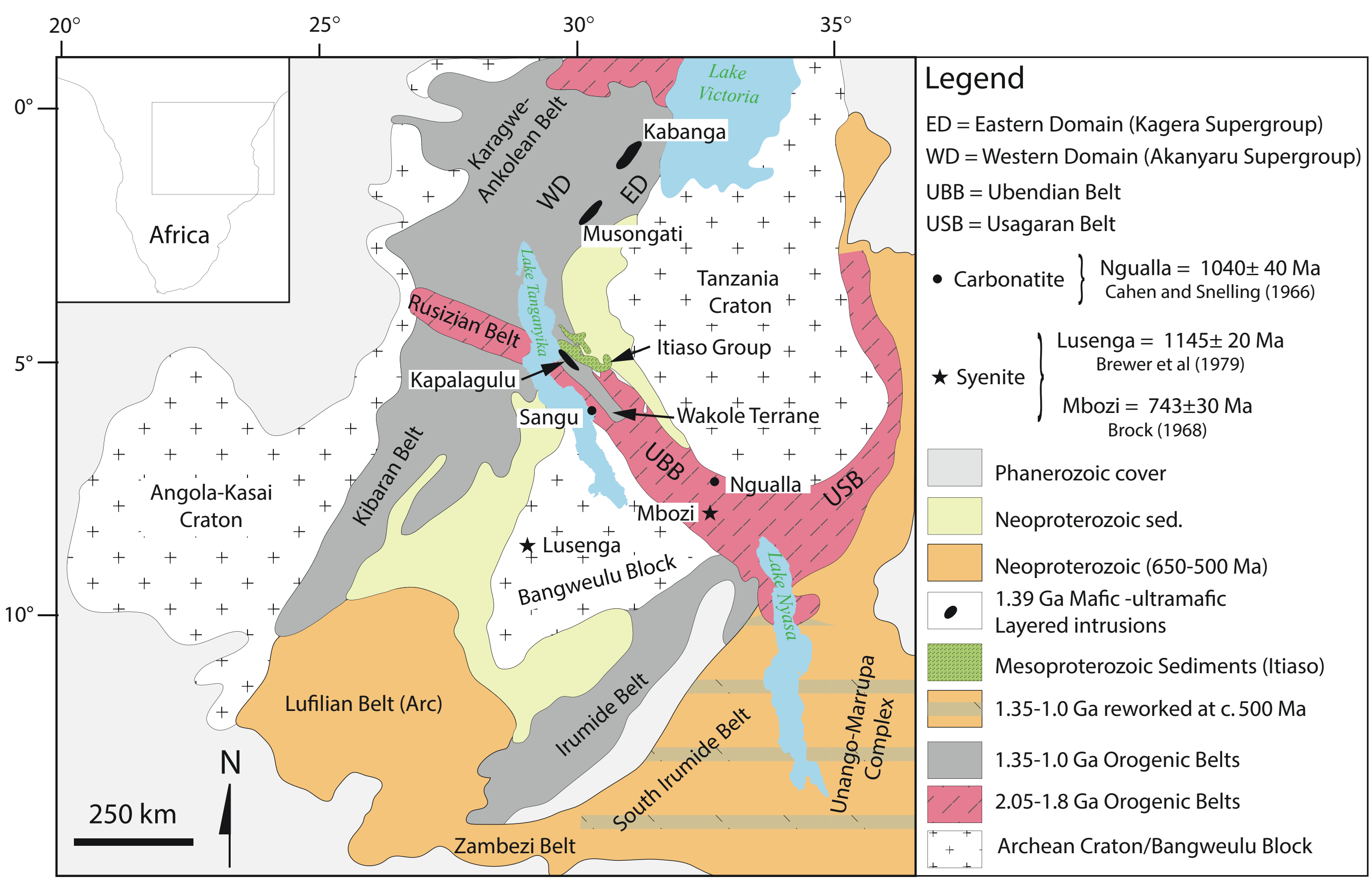

Figure 13. Relationship between the Mesoproterozoic Wakole Terrane/Itiaso Group and Mesoproterozoic Kibaran-Karagwe-Ankolean Belt and the Kapalagulu-Musongati-Kabanga layered mafic-ultramafic complex.

the Wakole Terrane (Fig. 13) were probably formed in the same continental rift basins aligned parallel to the NW-SE–trending Ubendian Belt, therefore making a triple junction with NE-SW Musongati-Kabanga alignment and the Kibaran-Karagwe-Ankolean Belt trend. Kapalagulu mafic ultramafic-layered complex with an emplacement age of 1392 ± 26 Ma intrudes the Itiaso Group, hence marking the minimum age of the Itiaso quartzite (Fig. 13; Wadsworth et al., 1982; Maier et al., 2007).

During the climax of the Mesoproterozoic tectonomagmatic events ca. 1000 Ma, the Ubendian Belt and Bangweulu Block experienced an episode of alkali magmatism between the Stenian and Tonian Periods. Plugs of carbonatites and syenites were emplaced that include the Ngualla carbonatite, Sangu carbonatite and Mbozi syenite, which were emplaced between 1040 ± 40 and 685 ± 62 Ma, and the Lusenya syenite in the Bangweulu Block (in Zambia) dated at 1145 ± 20 Ma (Cahen and Snelling, 1966; Brock, 1968; Ray, 1974; Brewer et al., 1979). This geologic event may be related to the extensional tectonics that probably opened the Neoproterozoic ocean basins in the Ubendian Belt (Boniface and Schenk, 2012).

5. SUBDUCTION AND TECTONICS IN THE USAGARAN BELT

The Usagaran Belt of Cahen et al. (1984) is a Paleoproterozoic orogen sandwiched between the Archean Tanzania Craton and the Neoproterozoic Mozambique Belt (Fig. 14). The Usagaran Belt is located at the southeastern margin of the Tanzania Craton and is regarded as the foreland of the polymetamorphic Mozambique Belt that thrusted westward onto the Tanzania Craton (see Fritz et al., 2005; Sommer et al., 2005, and references therein). The internal structural fabrics (foliation, shear zones, and gneissic bands) are oriented NE-SW to E-W in its southern part (Mruma, 1989; Reddy et al., 2003; Fritz et al., 2005). The Usagaran Belt is divided into three main lithologically distinct tectonic units, namely the Isimani Group, Konse Group, and Ndembera Group (Meinhold, 1970; Mruma, 1989, 1995; Sommer et al., 2005; Fritz et al., 2005; Legler et al., 2015), for which geology, geochronology, and geochemical data will be described below in turn.

5.1. The Isimani Group: Paleoproterozoic Eclogites

The Isimani Group is composed of highly deformed high-grade metamorphic rocks forming two major groups of mafic amphibolites and leucocratic orthogneisses (Meinhold, 1970; Mruma, 1989). The mafic amphibolites are compositionally banded and garnet-rich, and they include layers of high-pressure mafic granulites, eclogites, and kyanite-metapelites. The leucocratic orthogneiss is the most abundant association and occurs as a coarse-grained rock with in situ melting layers and inclusions of amphibolite boudins interpreted as deformed mafic dykes (Mruma, 1989; Reddy et al., 2003).

Mineral assemblages from the Isimani Group rocks point to high-grade metamorphic *P-T* conditions at amphibolite, granulite and eclogite facies, which are overprinted by low-grade metamorphic *P-T* conditions at greenschist facies localized on shear corridors and thrust zones (Mruma, 1989; Reddy et al., 2003; Collins et al., 2004; Mori et al., 2018). High-pressure granulite and retrograde eclogites with a strong MORB affinity crop out at the Yalumba Hill within the mafic amphibolites units and have been dated at 2000 Ma (see Fig. 15A, Table 4; Möller et al., 1995; Collins et al., 2004). The eclogite facies metamorphism reached a peak metamorphic condition at P = ~1.8 GPa and T = 750 °C (Möller et al., 1995). The Yalumba Hill eclogite with trace- and rare earth element geochemistry like mid-ocean ridge basalt was interpreted as to have formed during subduction of oceanic lithosphere followed by collision in the northern Usagaran Belt (see Fig. 15A; Möller et al., 1995; Collins et al., 2004; Fritz et al., 2005).

5.2. The Konse Group

The Konse Group is composed of metamorphosed (greenschist facies) pillow lava basalts along with volcano-sedimentary assemblage (quartzite, mica-schist, meta-tuff and meta-dolomite) forming ~350 m thick successions and laterally defining a narrow strip trending NE-SW, sandwiched between the Tanzania Craton and the high-grade gneisses of Isimani Group (Figs. 14 and 16). The volcanic and sedimentary rocks of the Konse Group have well-preserved primary structures that include magmatic structures (pillow lavas) and sedimentary structures (cross-bedding, ripple marks, and flute marks) that point to their formation in a submarine environment (Whittingham, 1959; Mruma, 1989, 1995).

Boniface and Tsujimori (2019) have presented data that indicate that the Konse pillow lavas have tholeiitic compositions with REE patterns similar to the composition of N-MORB and transitional MORB (T-MORB) and they display elevated Ba, Th, U, and Sr contents, typical of modern back-arc oceanic crust. The Konse pillow basalts make analogue the Tethyan-type (Jurassic–Cretaceous) suprasubduction-zone ophiolite evolution and emplacement in the Precambrian (see Boniface and Tsujimori, 2019; Dilek and Furnes, 2019). Some of the most extensively studied Tethyan ophiolites appear to have developed in arc-forearc settings through subduction of the ocean floor combined with slab rollback, crustal extension, and hydration of refractory peridotite processes (Dilek and Polat, 2008). Tethyan ophiolites and other Phanerozoic ophiolites commonly show a progression from MORB geochemical affinities (pillow lava, sheeted dikes, and gabbros) to island-arc tholeiite (basaltic andesites, andesites, dacites, and rhyolites) and boninitic geochemical affinities, thus indicating a complex pattern of igneous accretion that involved multiple stages and sources of melt evolution and life cycles in suprasubduction zone (Ishikawa et al., 2002; Dilek and Polat, 2008; Dilek and Furnes, 2011). The classification of Phanerozoic ophiolites has facilitated the identification of a specific tectonic setting for ophiolite generation even in Precambrian time. For example, Dilek and Furnes (2011) inferred a suprasubduction-zone fore-arc basin subtype ophiolites for the 3.8 Ga Isua supracrustal belt in Greenland, among other tectonic settings from different belts. The occurrence of suprasubduction-zone ophiolites in the 3.8 Ga crust suggests that the Phanerozoic-type seafloor spreading and subduction zone processes were operating at this time. However, the Precambrian ophiolites differ from their Phanerozoic counterparts by the rare occurrence of or the lack of sheeted dikes that can be explained by much higher spreading rates and higher mantle temperatures in the Archean than at present or in the Phanerozoic. Other unique features of the Precambrian ophiolites include the presence of high-Mg andesites, komatiitic-picritic lavas, and dunitic to wehrlitic sills (Dilek and Polat, 2008; Dilek and Furnes, 2011). Furthermore, higher potential mantle temperatures are likely to have caused higher degrees of partial melting, resulting in the formation of thicker oceanic crust (>20 km) in the Archean than at present (~5–10 km) (Dilek and Polat, 2008).

New geochronological data indicate that the Konse pillow basalts have a crystallization age of ca. 2050 Ma (Boniface et al.,

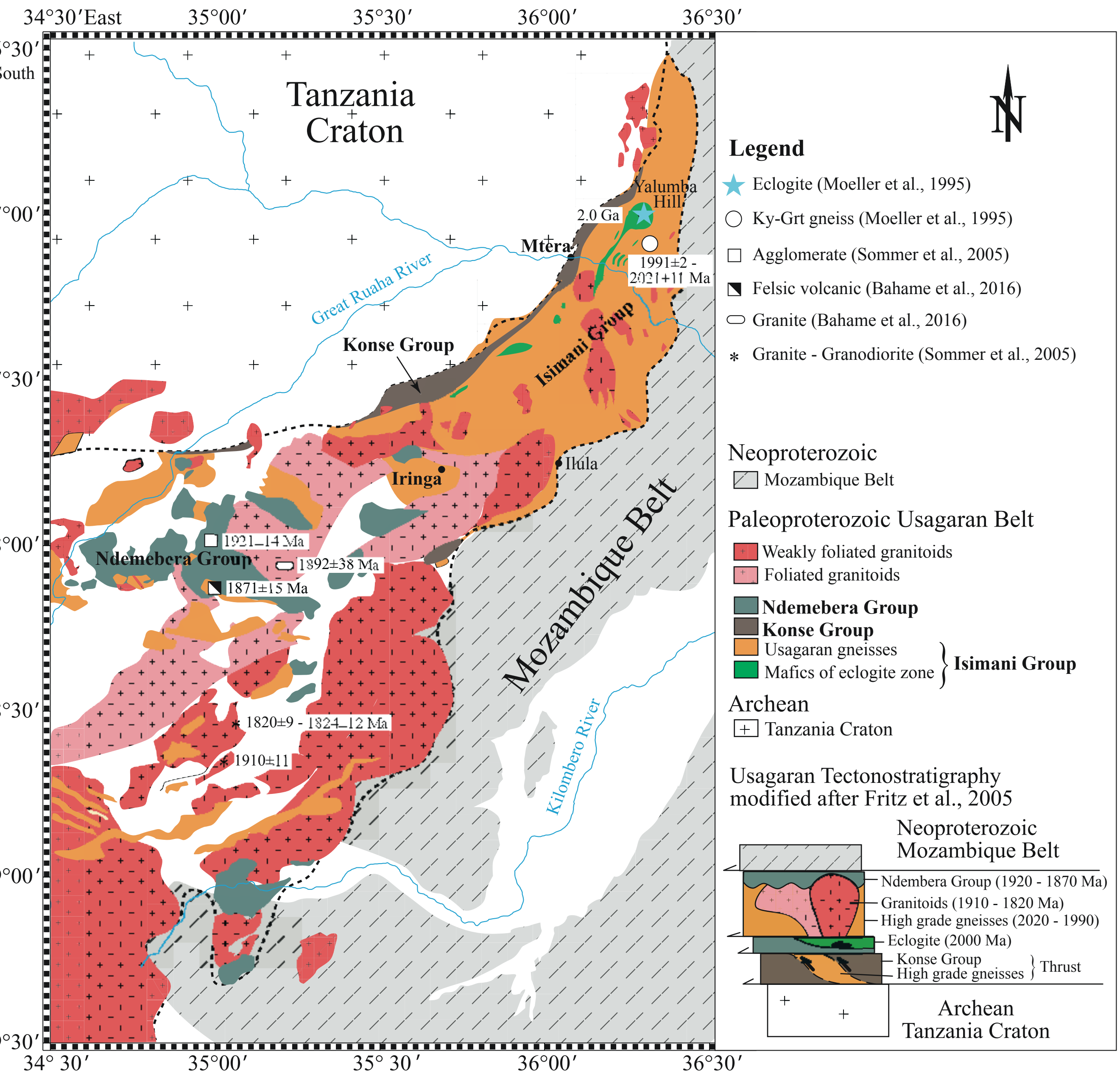

Figure 14. Geological map of the Usagaran Belt showing location of the main tectonic units: Isimani Group, Konse Group, and Ndembera Group, the map is modified after the compilation of 56 available quarter degree sheets (QDS) by Fritz et al. (2005).

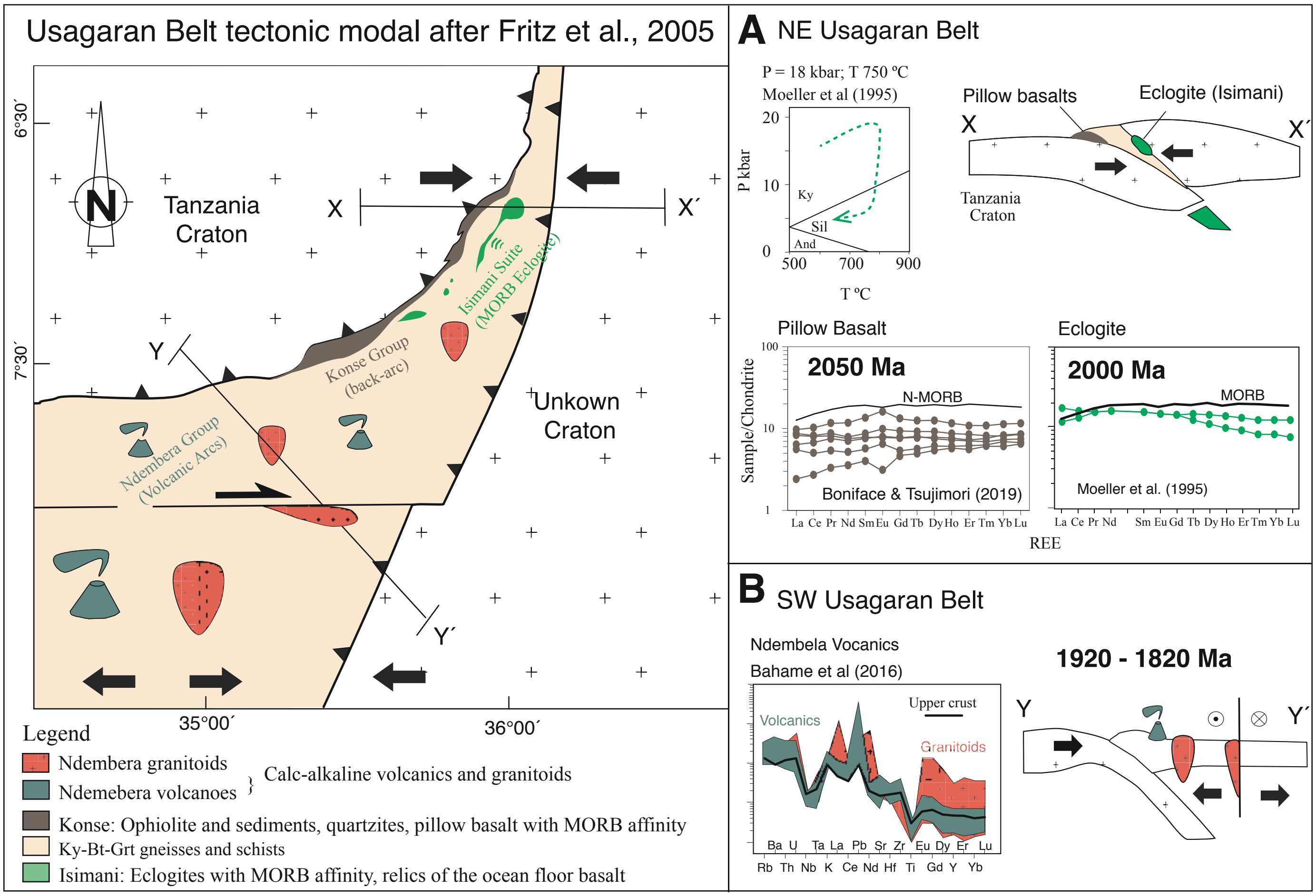

Figure 15. Paleoproterozoic collision and arc magmatism geotectonic model of the Usagaran orogen after Fritz et al. (2005), supported by geochemical data from volcanic and plutonic rocks by Bahame et al. (2016) and Manya and Maboko (2016). MORB—mid-ocean ridge basalt.

2019), which is a coeval age with the formation of the Yalumba eclogites with MORB affinity ca. 2000 Ma (see Table 4). Based on the proximity and age relations of the Yalumba eclogite and the Konse rock assemblages, Boniface and Tsujimori (2019) interpreted that the two units were derived from the same ocean basin. Therefore, we conclude that, while the Yalumba eclogites represent relics of subducted ocean floor basalts, the Konse pillow basalts and the associated submarine sediments represent a dismembered ocean plate stratigraphy (an ophiolitic section). The Konse Group rock sequence was deformed during a thrusting event in the Neoproterozoic Era (Boniface, 2019).

The Konse Group shares tectonic contacts with the Tanzania Craton and the Isimani Group high-grade gneisses defined by easterly dipping thrusts (Whittingham, 1959; Mruma, 1989). The Tanzania Craton forms a base upon which the Konse Group tectonically sits, and the high-grade gneisses of the Isimani Group were thrown on top of the Konse Group (Fig. 16). The westward thrusts are considered to have occurred between 596 and 550 Ma, concomitant with the westward transport of the Eastern Granulite of the Mozambique Belt (meta-anorthosites) onto the Western Granulites of Tanzania and the Mesoproterozoic Unango-Marrupa Complexes of Mozambique (Sommer et al., 2005; Vogt et al., 2006; Rossetti et al., 2008; Viola et al., 2008; Fritz et al., 2009, 2013).

5.3. The Ndembera Group

The Ndembera Group is composed of explosive metavolcanics (basal agglomerates, andesitic tuffs and lavas, and dacitic to rhyolitic lavas and tuffs) capped with metasedimentary rocks (quartzites, quartzo-feldspathic schists, and phyllites). The volcano-sedimentary sequence rests uncomformably over the high-grade gneisses of the Usagaran Belt (Kursten, 1963; Mruma, 1989). The explosive meta-volcanic rocks are accompanied by voluminous granitoids (microcline biotite rich granite), which extend to the south to form a large granitoid shield locally known as the Ubena granitoids (see Figs. 2 and 4). The Ndembera metavolcanics and granitoids yield crystallization ages between

TABLE 4. MAGMATIC AND METAMORPHIC AGES FROM THE USAGARAN BELT

Group/ Geological Eon	Magmatic ages (Ma)	Analytical technique	Lithology	Authors
Archean				
Isimani	2427 ± 15, 3022 ± 10	U-Pb zircon, SIMS	Para-gneisses (detrital ages)	Collins et al. (2004)
	2705 ± 11	U-Pb zircon, SHRIMP	Granite	Reddy et al. (2003)
Ndembera	2519 ± 9			
Paleoproterozoic				
Konse	2048.6 ± 3.8	In situ zircon U-Pb dating, ICP-MS	Pillow-basalts	Boniface et al., 2019
Isimani	1877 ± 7	U-Pb zircon, SHRIMP	Granite	Reddy et al. (2003)
Ndembera	1910 ± 11	U-Pb zircon, SHRIMP	Granodiorite	Sommer et al. (2005)
	1820 ± 9, 1824 ± 12	U-Pb zircon, SHRIMP	Granite, granodiorite	Sommer et al. (2005)
	1921 ± 14	U-Pb zircon, SHRIMP	Rhyolitic agglomerate	Sommer et al. (2005)
	1871 ± 15	U-Pb zircon, SHRIMP	Felsic volcanic	Bahame et al. (2016)
	1892 ± 38	U-Pb zircon, SHRIMP	Granite	Bahame et al. (2016)
	1900, 1700	K-Ar muscovite	Granitoids	Gabert and Wendt (1974)
	1771 ± 145	Rb-Sr whole-rock	Granite	Priem et al. (1979)
Paleoproterozoic				
Isimani	1991 ± 2, 1997 ± 2, 2021 ± 11	U-Pb zircon, SIMS	Ky-Grt gneiss, Bt leucogranitic gneiss	Collins et al. (2004)
	1999.1 ± 1.1	U-Pb zircon, SIMS	Eclogite	Collins et al. (2004)
	2000 ± 2	^{207}Pb-^{206}Pb monazite	Eclogite	Möller et al. (1995)
Neoproterozoic				
Isimani	535.4 ± 2.3	K-Ar muscovite	Bt granitic gneiss (orthogneiss)	Reddy et al. (2003)

Note: SHRIMP—sensitive high-resolution ion microprobe; SIMS—secondary ion mass spectrometry, ICP-MS—inductively coupled plasma–mass spectrometry.

1921 ± 14 and 1871 ± 15 Ma (K-Ar muscovite and U-Pb zircon) (Gabert and Wendt, 1974; Sommer et al., 2005; Bahame et al., 2016). The Ubena Hbl tonalites and Bt high-K granites have been dated between 1887 ± 11 and 1820 ± 9 Ma (U-Pb zircon) (Sommer et al., 2005; Manya and Maboko, 2016).

Geochemical and isotopic data indicate that the Ndembera and Ubena volcano-plutonic rocks have strong calc-alkaline volcanic arc magma affinity (Bahame et al., 2016; Manya and Maboko, 2016). The granites and meta-volcanic rocks (Ndembera and Ubena) share similar geochemical features, including very coherent REE patterns characterized by enrichment of the LREE relative to the HREE, depletion of high field strength elements (Nb-Ta and Ti), which is a typical signature of arc magmas (Fig. 15B; Bahame et al., 2016; Manya and Maboko, 2016). Therefore, a geotectonic evolution model of the Usagaran Belt proposes a continental collision with eclogite occurrences in the north and arc accretion with island arc magmatism in the south occurring between 2000 and 1820 Ma (Fig. 15; Fritz et al., 2005).

6. DISCUSSION

In the modern tectonic regime, belts of strongly deformed oceanic plate stratigraphy with internal H*P*-L*T* metamorphism form an accretionary prism between the trench and the magmatic arc that has H*P*-L*T* metamorphism (Brown and Johnson, 2018; Brown, 2006). This association forms exclusively at island and Andean arcs and is recognized as one of the hallmark signatures of plate tectonics (Kusky et al. 2018). Therefore, the record of H*P*-L*T* metamorphism and associated tectonic events in the Ubendian-Usagaran Belt implies that Proterozoic tectonic regimes in the Ubendian-Usagaran Belt make analogue the operation of Phanerozoic mobile-lid tectonics in the Precambrian and manifest a complete record of Wilson Cycle at the margins of the Tanzania Craton in Precambrian, i.e., rifting, subduction, arc and back-arc magmatism, and collision. The eclogites of the Ubendian-Usagaran Belt and the associated lithological assemblages (e.g., metapelites, quartzites, meta-dolomites) are probably relics of ocean plate stratigraphy that represent an accretionary complex that formed at a plate boundary trench through off-scraping of the upper crustal portion of subducted rigid oceanic lithosphere (e.g., see Komiya et al., 1999). Original rock assemblages of the oceanic plate stratigraphy include: MORB, pelagic sequence (chert, banded iron formations, Mn nodules, and dolomites), hemipelagic sequence (shale and mudstone), and turbidite sequence (conglomerate, continental blocks).

The arc signature of some Ubendian Belt eclogites associated with metasediments (metapelites and quartzites) implies that their mafic protoliths formed above a subduction zone. The eclogite protolith were probably part of a turbidite sequence

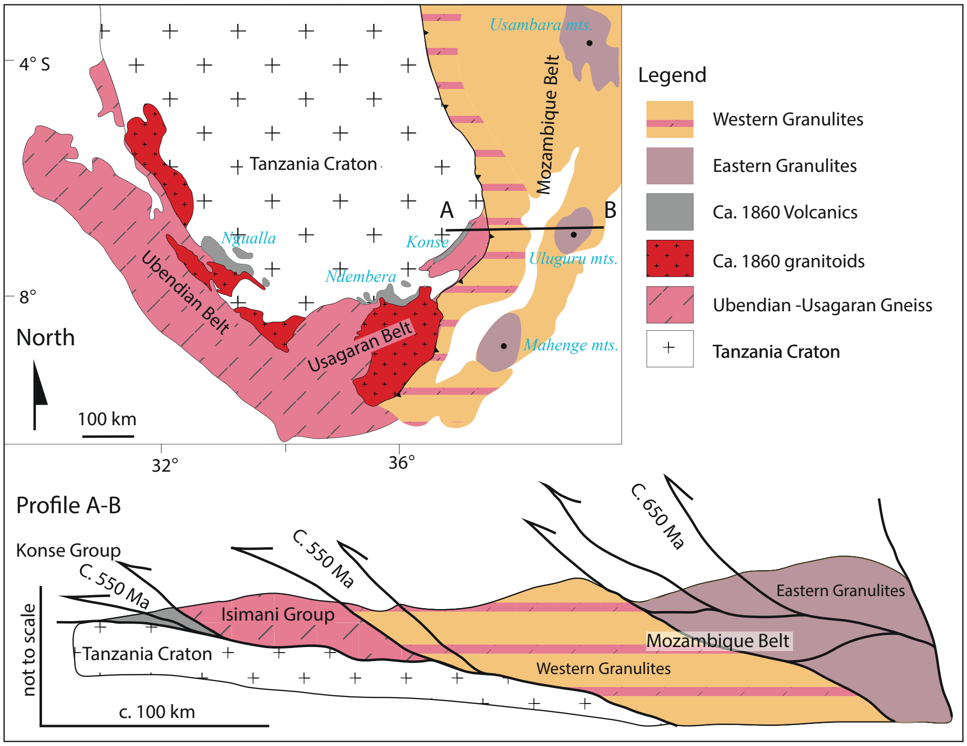

Figure 16. Neoproterozoic fold and thrust tectonics of the Mozambique Belt: Westward thrusting model of the Mozambique Belt onto the Usagaran Belt and Tanzania Craton, modified after Fritz et al. (2005; 2013).

eroded from nearby or far-distant arc basalt blocks that were channeled into a subduction zone as mélanges that recrystallized and deformed to eclogites and metasediments (metapelites and quartzites). Spatial and temporal distribution of eclogites (*HP*-*LT* events) and the subsequent tectonic events in the Ubendian Usagaran Belt have resulted to the rethinking of a new tectonic subdivision of the Ubendian Belt and development of a new tectonic model that describes the evolution of the Ubendian-Usagaran Belt in Proterozoic (Paleoproterozoic to Neoproterozoic). The Ubendian-Usagaran Belt is a site of global interest where rare Precambrian tectonic events are fully recorded and preserved.

6.1. New Tectonic Subdivisions: Key Features

The accumulation of structural, geochronological, petrological, and geochemical data from the Ubendian-Usagaran Belt over decades, along with our new data, allow the review and proposition of a new evolution model of the Ubendian-Usagaran

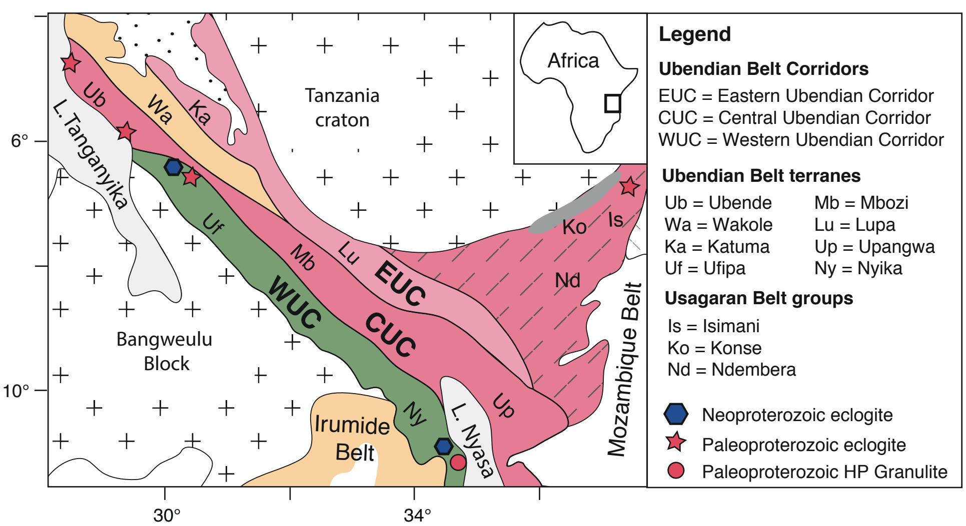

Figure 17. The geological map of the Ubendian-Usagaran Belt illustrating the distribution of the new subdivision of the Ubendian Corridors. The terrane boundaries are adopted from Daly (1988).

orogeny. Therefore, we divide the Ubendian Belt into three domains (the Western Ubendian Corridor, Central Ubendian Corridor, and Eastern Ubendian Corridor) (Fig. 17). The new subdivision is based on spatial distribution of H*P*-L*T* metamorphic data (eclogites and high pressure granulites) and on temporal clusters of tectonothermal events related with subduction (e.g., arc-magmatism, collision, and rifting events). The key features of the new tectonic subdivisions are described below.

6.1.1. Western Ubendian Corridor

The Western Ubendian Corridor is composed of the Ufipa and Nyika Terrane. The defining features of the Western Ubendian Corridor are the presence of two Proterozoic suture zones: (1) the Orosirian subduction related metamorphism at 2000 Ma and 1920–1890 Ma, which was coupled with arc magmatism and regional metamorphism; and (2) the Ediacaran to Cambrian (590–500 Ma) subduction related metamorphism characterized by the collisional metamorphism but lacking Neoproterozoic arc-related magmatism (Fig. 18).

The identification of H*P*-L*T* metamorphic events (eclogites and high-pressure granulites) dated at 2002 ± 0.3 Ma (high-pressure granulites enderbites in the Nyika Terrain) and at 1924 ± 74 to 1877 ± 20 Ma (kyanite-bearing eclogites in the Ufipa Terrane) explain the origin of arc-related magmatism and regional metamorphism that peaked between 1950 and 1900 Ma in the Western Ubendian Corridor and in the neighboring

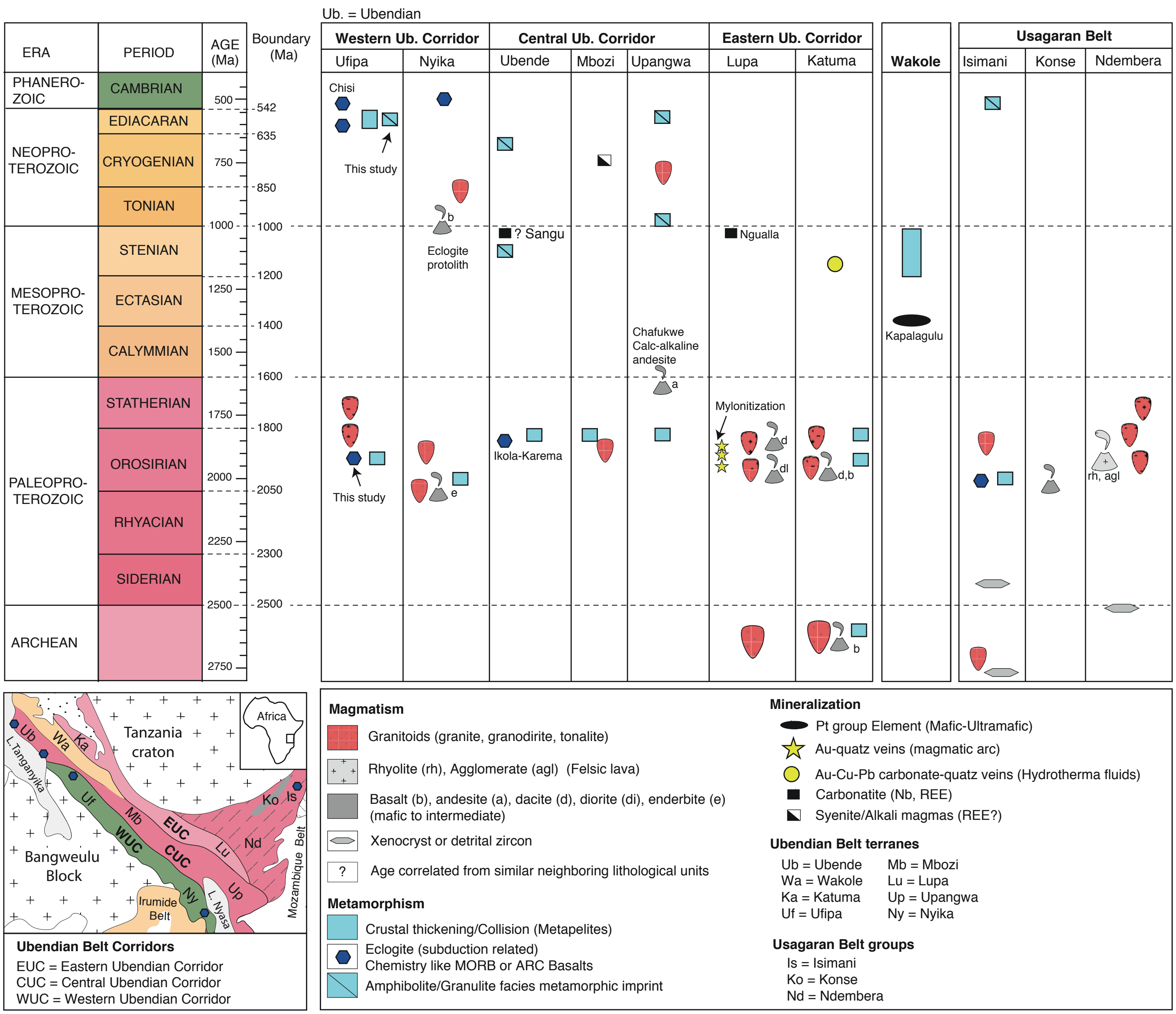

Figure 18. A chart depicting Orosirian to Cambrian metamorphic and magmatic events of the Ubendian-Usagaran Belt. MORB—mid-ocean ridge basalt; REE—rare earth elements.

terranes. The new geochronological data indicate that the kyanite-bearing eclogites of the Ufipa Terrane was formed due to a subducting slab at 1924 ± 74 to 1877 ± 20 Ma, which was a driving force of the regional crustal thickening metamorphism, granitization, arc magmatism, and deformation and precipitation of gold that occurred between 1950 and 1900 Ma (Tables 5 and 6; Dodson et al., 1975; Ring et al., 1997; Lawley et al., 2013a, 2013b; Tulibonywa et al., 2015; Lawley et al., 2014; Thomas et al., 2016; Boniface and Appel, 2018).

Eclogites of the Ufipa Terrane are enclosed in metasediments (Bt gneiss, Bt-Grt-Ky/Sil gneiss/schist, migmatites, quartzite) with metamorphic ages at 1949 ± 16 and 1901 ± 37 Ma overlapping with the subduction component. This eclogite-metasedimentary lithological assemblage could represent deformed and metamorphosed ocean plate stratigraphy. The younger suture zone reflects similar lithological assemblages in which Neoproterozoic metapelitic rocks occur together with 590–560 Ma eclogites.

The contact between the Ufipa Terranes and the Bangweulu Block and the entire boundary of the Bangweulu Block are characterized by plutons and volcanic rocks with strong volcanic arc magmatic affinity that erupted between 1871 ± 24 and 1832 ± 32 Ma (Schandelmeier, 1983; Kabengele et al., 1991; Lenoir et al., 1994; Kapenda et al., 1998; De Waele et al., 2006a). The existence of a ca. 1890–1800 Ma subduction-related magmatism around the margins of the Bangweulu Block was interpreted as melting in a subducted passive margin (metacratonic environment) (De Waele et al., 2006b; Liégeois et al., 2013), which indicates that probably the Bangweulu Block existed as an isolated block until ca. 1800 Ma when it was fused with the Ufipa Terrane, which records another collisional metamorphism at 1835 ± 11 Ma (Boniface and Appel, 2018). The Ufipa Terrane and Bangweulu Block contact also records a post-orogenic magmatic event dated between 1725 ± 48 and 1723 ± 41 Ma (Lenoir et al., 1994), which is probably a result of tectonic relaxation. In the contrary, De Waele et al. (2006b) do not consider that the magmas in the Bangweulu Block were emplaced in an arc but in a subducted metacratonitized passive margin following a subduction and collision between 2050 and 1950 Ma. The model of De Waele et al. (2006b) cannot explain the existence of 1890–1860 Ma eclogite with MORB affinity between the Tanzania Craton and Bangweulu Block. Therefore, we propose the ca. 1890–1800 Ma arc

TABLE 5. MAGMATIC AND METAMORPHIC AGES OF THE WESTERN UBENDIAN CORRIDOR

Terrane	Ages (Ma)	Error	Analytical technique	Lithology	Authors	Interpretation
Nyika	2093	0.6	$^{207}Pb/^{206}Pb$ zircon	Enderbite (protolith)	Ring et al. (1997)	Arc magmatism
Nyika	2048	0.7	$^{207}Pb/^{206}Pb$ zircon	Granite,	Ring et al. (1997)	Arc magmatism
Nyika	2002	0.3	$^{207}Pb/^{206}Pb$ zircon	Enderbite	Ring et al. (1997)	Subduction
Nyika	1988	0.6	$^{207}Pb/^{206}Pb$ zircon	Cordierite gneiss	Ring et al. (1997)	Collision
Nyika	1970	30	U-Pb zircon	Granite	Dodson et al. (1975)	Arc magmatism
Nyika	1969	0.4	$^{207}Pb/^{206}Pb$ zircon	Anatectic granite	Ring et al. (1997)	Arc magmatism
Nyika	1969	0.4	$^{207}Pb/^{206}Pb$ zircon	Granite	Ring et al. (1997)	Arc magmatism
Ufipa	1949	16	U-Pb zircon, SHRIMP	Metapelite	Boniface and Appel (2018)	Accretion/collision
Ufipa	1924	74	U-Pb zircon, LA-MS	Eclogite	This study	Subduction
Ufipa	1919	12	U-Pb zircon, SHRIMP	Metapelite	Boniface and Appel (2018)	Accretion/collision
Ufipa	1901	37	U-Th-Pb monazite, microprobe	Metapelite	Boniface and Appel (2018)	Accretion/collision
Bangweulu Block	1871	24	U-Pb SHRIMP zircon	Basalt	De Waele et al. (2006b)	Arc magmatism
Bangweulu Block	1868	7	U-Pb SHRIMP zircon	Basalt	De Waele et al. (2006b)	Arc magmatism
Bangweulu Block	1866	9	U-Pb SHRIMP zircon	Granite	De Waele et al. (2006b)	Arc magmatism
Ufipa	1864	32	U-Pb zircon, TIMS	Granite	Lenoir et al. (1994)	Arc magmatism
Bangweulu Block	1862	8	U-Pb SHRIMP zircon	Granite	De Waele et al. (2006b)	Arc magmatism
Bangweulu Block	1862	19	U-Pb SHRIMP zircon	Basalt	De Waele et al. (2006b)	Arc magmatism
Bangweulu Block	1860	13	U-Pb SHRIMP zircon	Granite	De Waele et al. (2006b)	Arc magmatism
Bangweulu Block	1856	4	U-Pb SHRIMP zircon	Rhyolitic tuff	De Waele et al. (2006b)	Arc magmatism
Ufipa	1838	86	Rb-Sr	Granite	Schandelmeier (1983)	Arc magmatism
Ufipa	1835	11	U-Th-Pb monazite, microprobe	Metapelite	Boniface and Appel (2018)	Accretion/collision
Bangweulu Block	1832	32	U-Pb SHRIMP zircon	Granite	De Waele et al. (2006b)	Arc magmatism
Ufipa	1725	48	U-Pb zircon, TIMS	Granite	Lenoir et al. (1994)	Arc magmatism
Ufipa	1723	41	U-Pb zircon, TIMS	Granite	Lenoir et al. (1994)	Arc magmatism

Note: LA-MS—laser ablation–mass spectrometry; SHRIMP—sensitive high-resolution ion microprobe; TIMS—thermal ionization mass spectrometry.

TABLE 6. MAGMATIC AND METAMORPHIC AGES OF THE EASTERN UBENDIAN CORRIDOR

Terrane	Ages (Ma)	Error	Analytical technique	Lithology	Authors	Interpretation
Lupa	2758	9	U-Pb zircon, LA-MC-ICP-MS	Granite	Lawley et al. (2013a)	Arc magmatism
Lupa	2739	10	U-Pb zircon, LA-MC-ICP-MS	Granite	Lawley et al. (2013a)	Arc magmatism
Lupa	2731	29	U-Pb zircon, LA-SC/MC-ICP-MS	Granite	Thomas et al. (2016)	Arc magmatism
Lupa	2723	10	U-Pb zircon, LA-MC-ICP-MS	Granite	Lawley et al. (2013a)	Arc magmatism
Lupa	2688		Nd ages	Granite	Manya (2011)	Arc magmatism
Lupa	2682	10	U-Pb zircon, SHRIMP	Granite	Tulibonywa et al. (2015)	Arc magmatism
Lupa	1959.6	1.1	U-Pb zircon,ID-TIMS, LA-MC-ICP-MS	Granite	Lawley et al. (2013a)	Arc magmatism
Lupa	1958.5	1.3	U-Pb zircon,ID-TIMS, LA-MC-ICP-MS	Syenogranite	Lawley et al. (2013a)	Arc magmatism
Lupa	1953	6	Re-Os sulfides (pyrite, etc.), N-TIMS	Au quartz veins	Lawley et al. (2013b)	Hydrothermal fluids
Lupa	1953	37	Re-Os sulfides (pyrite, etc.), N-TIMS	Au quartz veins	Lawley et al. (2013b)	Hydrothermal fluids
Lupa	1943	32	U-Pb zircon, SHRIMP	basaltic andesite	Tulibonywa et al. (2015)	Arc magmatism
Lupa	1942	14	U-Pb zircon,ID-TIMS, LA-MC-ICP-MS	monzogranite	Lawley et al. (2013a)	Arc magmatism
Lupa	1937	4	Re-Os sulfides (pyrite, etc.), N-TIMS	Au quartz veins	Lawley et al. (2013b)	Hydrothermal fluids
Lupa	1934.5	1	U-Pb zircon,ID-TIMS, LA-MC-ICP-MS	Granodiorite	Lawley et al. (2013a)	Arc magmatism
Lupa	1930	3	U-Pb titanite, ID-TIMS	Au quartz veins	Lawley et al. (2014)	Hydrothermal fluids
Lupa	1930	3	U-Pb Titanite, ID-TIMS	granite	Lawley et al. (2014)	Arc magmatism
Lupa	1929	20	U-Pb zircon, LA-SC/MC-ICP-MS	Bt Granites	Thomas et al. (2016)	Arc magmatism
Lupa	1921	7	U-Pb titanite, ID-TIMS	Au quartz veins	Lawley et al. (2014)	Hydrothermal fluids
Lupa	1921	7	U-Pb Titanite, ID-TIMS	Granodiorite,	Lawley et al. (2014)	Arc magmatism
Lupa	1919	37	U-Pb zircon, LA-SC/MC-ICP-MS	Bt Granites	Thomas et al. (2016)	Arc magmatism
Lupa	1896	16	U-Pb zircon, LA-SC/MC-ICP-MS	Bt Granites	Thomas et al. (2016)	Arc magmatism
Lupa	1894	45	Re-Os sulfides (pyrite etc.), N-TIMS	Au quartz veins	Lawley et al. (2013b)	Hydrothermal fluids
Lupa	1891	17	U-Pb zircon, LA-MC-ICP-MS	Quartz diorite	Lawley et al. (2013a)	Arc magmatism
Lupa	1886	6	Re-Os sulfides (pyrite etc.), N-TIMS	Au quartz veins	Lawley et al. (2013b)	Hydrothermal fluids
Lupa	1885	9	Re-Os sulfides (pyrite etc.), N-TIMS	Au quartz veins	Lawley et al. (2013b)	Hydrothermal fluids
Lupa	1880	17	U-Pb zircon, LA-MC-ICP-MS	Gabbroic dyke	Lawley et al. (2013a)	Arc magmatism
Lupa	1878	15	U-Pb zircon, SHRIMP	Porphyritic dacites to rhyodacites	Tulibonywa et al. (2015)	Arc magmatism
Lupa	1876	10	Re-Os sulfides (pyrite etc.), N-TIMS	Au quartz veins	Lawley et al. (2013b)	Hydrothermal fluids
Lupa	1873	5	Re-Os sulfides (pyrite etc.), N-TIMS	Au quartz veins	Lawley et al. (2013b)	Hydrothermal fluids
Lupa	1871	12	Re-Os sulfides (pyrite etc.), N-TIMS	Au quartz veins	Lawley et al. (2013b)	Hydrothermal fluids
Lupa	1871	5	U-Pb zircon, SHRIMP	Granite	Tulibonywa et al. (2015)	Arc magmatism
Katuma	2713	11	U-Pb zircon, LA-ICP-MS	Granodiorite	Kazimoto et al. (2014)	Arc magmatism
Katuma	2677	29	U-Pb zircon, LA-ICP-MS	Granite	Kazimoto et al. (2014)	Arc magmatism
Katuma	2651	5	U-Pb zircon, LA-ICP-MS	Metabasite	Kazimoto et al. (2014)	Arc magmatism
Katuma	2650	8	U-Pb zircon, LA-ICP-MS	Metabasites	Kazimoto et al. (2014)	Accretion/collision
Katuma	2645	34	U-Pb zircon, LA-ICP-MS	Mafic granulite	Kazimoto et al. (2014)	Arc magmatism
Katuma	2643	4	U-Pb zircon, LA-ICP-MS	Gabbronorite	Kazimoto et al. (2014)	Arc magmatism
Katuma	2638	5	U-Pb zircon, LA-ICP-MS	Orthogneiss	Kazimoto et al. (2014)	Arc magmatism
Katuma	2553	10	U-Pb zircon, LA-ICP-MS	Granitoids	Kazimoto et al. (2014)	Arc magmatism
Katuma	2046	11	U-Pb zircon, LA-ICP-MS	Leucosome of orthogneiss	Kazimoto et al. (2014)	Accretion/collision
Katuma	2025	7	U-Pb zircon, LA-ICP-MS	Paleosome of orthogneiss	Kazimoto et al. (2014)	Accretion/collision
Katuma	2021	11	U-Pb zircon, LA-ICP-MS	Amphibolite	Kazimoto et al. (2014)	Arc magmatism
Katuma	1993	6	U-Pb zircon, LA-ICP-MS	Bt-granite	Kazimoto et al. (2014)	Arc magmatism
Katuma	1977	40	U-Pb zircon, SHRIMP	Mafic granulite (high pressure)	Boniface (2011)	Subduction
Katuma	1967	16	U-Th-Pb monazite, microprobe	Metapelite	Kazimoto et al. (2015a)	Accretion/collision
Katuma	1963	14	U-Pb zircon, LA-ICP-MS	Calc-silicate rock	Kazimoto et al. (2014)	Accretion/collision
Katuma	1958	8	U-Pb zircon, LA-ICP-MS	Metapelite	Kazimoto et al. (2014)	Accretion/collision
Katuma	1957	10	U-Th-Pb monazite, microprobe	Metapelite	Kazimoto et al. (2015a)	Accretion/collision
Katuma	1952	7	U-Pb zircon, LA-ICP-MS	Hbl-Bt granite	Kazimoto et al. (2014)	Arc magmatism
Katuma	1941	8	U-Pb zircon, LA-ICP-MS	Metapelite	Kazimoto et al. (2014)	Accretion/collision
Katuma	1938	11	U-Th-Pb monazite, microprobe	Metapelite	Kazimoto et al. (2015b)	Accretion/collision
Katuma	1936	20	U-Pb zircon, LA-ICP-MS	Hbl-Bt granite	Kazimoto et al. (2014)	Arc magmatism
Katuma	1902	73	Rb-Sr whole rock, TIMS	Bt Gneiss	Lenoir et al. (1994)	Accretion/collision
Katuma	1900	14	U-Pb zircon, SHRIMP	Bt Gneiss	Boniface (2009)	Accretion/collision
Katuma	1879	9	U-Pb zircon, LA-ICP-MS	MS-Bt Granitic gneiss	Kazimoto et al. (2014)	Accretion/collision
Katuma	1848	16	U-Th-Pb monazite, microprobe	Metapelite	Kazimoto et al. (2015a)	Accretion/collision
Katuma	1847	37	Rb-Sr whole rock, TIMS	Granite	Lenoir et al. (1994)	Arc magmatism
Katuma	1837	6	U-Th-Pb monazite, microprobe	Metapelite	Kazimoto et al. (2015a)	Accretion/collision
Katuma	1827	10	U-Th-Pb monazite, microprobe	Metapelite	Kazimoto et al. (2015b)	Accretion/collision

Note: ID-TIMS—isotope dilution-thermal ionization mass spectrometry; N-TIMS—negative TIMS: LA-ICP-MS—laser ablation–inductively coupled plasma–mass spectrometry; SC/MC—single collector/multicollector; SHRIMP—sensitive high-resolution ion microprobe.

magmas in the Bangweulu Block as the results of 1890–1860 Ma subduction and the subsequent collision ca. 1830 Ma (Boniface and Schenk, 2012; Boniface and Appel, 2018).

6.1.2. Central Ubendian Corridor

The characteristic features of the Central Ubendian Corridor are the predominance of metamorphosed mafic-ultramafic rocks, i.e., amphibolites, Hbl gneisses, mafic granulites, high-pressure granulites, lenses of eclogites, and serpentinites in the Ubende Terrane, Mbozi Terrane, and Upangwa Terrane. Metamorphosed mafic-ultramafic units of the Central Ubendian Corridor also occur with quartzites and pelitic gneisses (Stockley, 1948; Harpum, 1952, 1958, 1970; Morris, 1952; Haldemann, 1953; Sutton et al., 1954; Teale et al., 1958; Halligan and Birch, 1961b; Kennerley, 1962; Macfarlane, 1966; Smirnov et al., 1971b; Tolochko et al., 1972; Nanyaro et al., 1981; Boniface, 2015). The association of mafic-ultramafic rocks and metasediments (quartzites and pelitic gneisses) in the Ubende and Upangwa Terranes is considered as the possible remains of completely distorted oceanic plate stratigraphy (ophiolitic rocks) (e.g., Nanyaro et al., 1981; Evans et al., 2012).

The accumulation of geochronological data indicates that magmatism and metamorphism in the Central Ubendian Corridor occurred between 1887 ± 11 and 1808 ± 9 Ma (See Table 7; Boven et al., 1999; Sommer et al., 2005; Boniface, 2009; Boniface et al., 2012; Manya and Maboko, 2016; Thomas et al., 2016; Boniface and Appel, 2017). Foliated eclogites with MORB like geochemistry formed in a subduction zone that existed between 1886 ± 16 and 1866 ± 14 Ma in the Ubende Terrane (Boniface et al., 2012). The subduction of an oceanic lithosphere was concomitant with arc magmatism in the Mbozi and Upangwa Terranes which host magmatic rocks with crystallization ages between 1927 ± 7 and 1857 ± 19 Ma (Manya and Maboko, 2016; Thomas et al., 2016, 2018).

Dextral lateral shear deformation at amphibolite facies metamorphic conditions is recorded in the tectonites of the Ubende Terrane to have occurred between 1854 ± 4 and 1828 ± 8 Ma (Boven et al., 1999), which points to the dextral lateral shear deformation to coinciding with regional metamorphism of pelitic gneisses that occurred between 1831 ± 11 and 1808 ± 9 Ma throughout the Central Ubendian Corridor (Boniface, 2009; Boniface et al., 2012; Boniface and Appel, 2017). Therefore, the metamorphism of pelitic gneisses and the accompanying dextral lateral shear deformation in the Central Ubendian Corridor probably mark the second collision event in the Ubendian Belt that followed the subduction event and the accompanying arc-magmatism events dated between 1890 and 1860 Ma.

The Upangwa Terrane records a Statherian calc-alkaline andesite volcanism at 1674 ± 14 Ma (Manya, 2013), which has volcanic arc affinity. The regional significance of this single arc volcanic event is enigmatic. However, it could be a result of a post-orogenic extensional tectonics similar to the post-orogenic calc-alkaline extension volcanism of the northern Da-Hinggan Mountains, in northeastern China, and the 1.66–1.61 Ga

TABLE 7. MAGMATIC AND METAMORPHIC AGES OF THE CENTRAL UBENDIAN CORRIDOR

Terrane	Age (Ma)	Error	Analytical Technique	Lithology	Author	Interpretation
Ubena granitoids	1887	11	U-Pb zircon, LA-MC-ICP-MS	Hbl tonalites	Manya and Maboko (2016)	Arc magmatism
Ubende	1886	16	U-Pb zircon, SHRIMP	Eclogite	Boniface et al. (2012)	Subduction
Ubena granitoids	1877	15	U-Pb zircon, LA-MC-ICP-MS	Bt high-K granites	Manya and Maboko (2016)	Arc magmatism
Mbozi	1876	20	U-Pb zircon, LA-SC/MC-ICP-MS	Bt granitic orthogneiss	Thomas et al. (2016)	Arc magmatism
Mbozi	1871	8	U-Pb zircon, LA-SC/MC-ICP-MS	Bt granitic orthogneiss	Thomas et al. (2016)	Arc magmatism
Ubende	1866	14	U-Pb zircon, SHRIMP	Eclogite	Boniface et al. (2012)	Subduction
Ubena granitoids	1857	19	U-Pb zircon, LA-MC-ICP-MS	Bt high K granites	Manya and Maboko (2016)	Arc magmatism
Ubende	1854	4	Ar-Ar barroisite	Mafic tectonites	Boven et al. (1999)	Dextral lateral shear deformation
Ubende	1848	6	Ar-Ar barroisite	Mafic tectonites	Boven et al. (1999)	Dextral lateral shear deformation
Ubende	1839	7	Ar-Ar barroisite	Mafic tectonites	Boven et al. (1999)	Dextral lateral shear deformation
Ubende	1831	11	U-Pb zircon, SHRIMP, microprobe	Metapelite	Boniface et al. (2012)	Collision metamorphism
Ubende	1828	8	Ar-Ar barroisite	Mafic tectonites	Boven et al. (1999)	Dextral lateral shear deformation
Ubena granitoids	1824	12	U-Pb zircon, SHRIMP	Faintly foliated granite	Sommer et al. (2005)	Arc magmatism
Upangwa	1820		U-Pb zircon, LA-SC/MC-ICP-MS	Bt orthogneiss	Thomas et al. (2016)	Collision metamorphism
Ubena granitoids	1820	9	U-Pb zircon, SHRIMP	Faintly foliated granite	Sommer et al. (2005)	Arc magmatism
Ubende	1817	26	U-Pb zircon, SHRIMP, microprobe	Metapelite	Boniface et al. (2012)	Collision metamorphism
Mbozi	1814	7	U-Th-Pb monazite, microprobe	Metapelite	Boniface (2009)	Collision metamorphism
Upangwa	1808	9	U-Th-Pb monazite, microprobe	Metapelite	Boniface and Appel (2017)	Collision metamorphism
Upangwa	1674	15	U-Pb zircon, SHRIMP	Andesite	Manya (2013)	Arc magmatism

Note: LA-ICP-MS—laser ablation–inductively coupled plasma–mass spectrometry; SC/MC—single collector/multicollector; SHRIMP—sensitive high-resolution ion microprobe.

alkaline magmatism in the Irumide (e.g., Fan et al., 2003; De Waele et al. 2006b).

6.1.3. Eastern Ubendian Corridor

The characteristic feature of the Eastern Ubendian Corridor (the Katuma and Lupa Terranes) is the predominance of highly deformed reworked Archean crust (orthogneisses and metabasites) with crystallization ages between 2758 ± 9 and 2553 ± 10 Ma (Manya, 2011; Lawley et al., 2013a; Thomas et al., 2016; Kazimoto et al., 2015a; Tulibonywa et al., 2015). Metasedimentary rocks (quartzite layers, migmatitic Bt gneiss layers, Bt-Ms-Sil gneiss/schist layers) are also present (Table 2).

The Archean crust of the Katuma Terrane were migmatized and granitized between 2045 ± 12 and 2025 ± 8 Ma and followed by the emplacement of amphibolites with arc geochemical affinity and with a protolith age of 2021 ± 11 Ma (Kazimoto et al., 2015a), which points to the reworking of the Archean crust on a magmatic arc settings. The high-pressure granulites (1.02 GPa) with metamorphic age of 1977 ± 40 Ma (Boniface, 2011), have a maximum age of 2017 Ma by considering the upper error limit, which is coeval with the arc magmatism. The high-pressure granulites were probably formed in a subduction zone that was coupled with arc magmatism.

The Katuma arc system was characterized by the emplacement of granitoids (Bt granites and granodiorites), which occurred in a protracted period dated between 1993 ± 6 and 1936 ± 20 Ma that overlaps with deformation and metamorphism at amphibolite to granulite facies conditions that ended ca. 1900 ± 14 Ma. The deformation and metamorphism probably were due to collision or accretion to the Tanzania Craton that followed a ca. 1920 Ma subduction metamorphism event recorded in the Western Ubendian Corridor (Table 5; Table 6; Lenoir et al., 1994; Boniface, 2009, 2011; Kazimoto et al., 2014, 2015a, 2015b).

The last Paleoproterozoic period of arc magmatism, metamorphism, and deformation of pelitic gneisses and orthogneisses in the Katuma Terrane occurred between 1879 ± 9 and 1827 ± 10 Ma (Lenoir et al., 1994; Kazimoto et al., 2014, 2015a, 2015b), which overlaps with a ca. 1890–1860 Ma subduction metamorphism event recorded in the Ubende Terrane (Boniface et al., 2012).

Like the Katuma Terrane, the Lupa Terrane comprises Archean arc granitoids dated between 2758 ± 9 and 2682 ± 10 Ma (Lawley et al., 2013a; Thomas et al., 2016; Manya, 2011; Tulibonywa et al., 2015). The initial volcanic arc-related emplacement of granitoids in the Lupa Terrane is recorded to be between 1959.6 ± 1.1 and 1958.5 ± 1.3 Ma (Lawley et al., 2013a). The arc magmatism was followed by a deformation event at 1953 ± 6 Ma, which was accompanied by hydrothermal fluid migration along shear zones and precipitation of gold in quartz-sulfide veins (Table 6; Lawley et al., 2013b).

Between 1940 and 1920 Ma, the Lupa Terrane recorded another period of deformation and precipitation of gold in quartz-sulfide veins, explosive volcanism (pyroclastic and basaltic andesite volcanism), and emplacement plutons in a volcanic arc setting (Table 6; Lawley et al., 2013a, 2013b, 2014; Tulibonywa et al., 2015; Thomas et al., 2016). Deformation, metamorphism, and arc magmatism in the time window between 1950 and 1900 are recorded in other terranes of the Ubendian Belt and might be related to collisional or accretion tectonics of the arcs to the Craton, which followed a ca. 1920–1890 Ma subduction metamorphism event recorded in the Western Ubendian Corridor (Table 6; Lenoir et al., 1994; Boniface, 2009, 2011; Kazimoto et al., 2014, 2015a, 2015b).

The last Paleoproterozoic period of deformation, hydrothermal alteration and magmatism in the Lupa Terranes occurred between 1896 ± 16 and 1871 ± 5 Ma, when plutons (Bt granites, quartz diorite, gabbroic dyke) and volcanics (porphyritic dacites to rhyodacites) with arc magma affinity were emplaced in the Lupa Terranes accompanied by formation, hydrothermal fluids circulation in shear zones and precipitation of gold in quartz-sulfide veins (Table 6; Lawley et al., 2013a, 2013b; Tulibonywa et al., 2015; Thomas et al., 2016). This time window of arc magmatism in the Lupa Terrane overlaps with the subduction zone metamorphism and arc magmatism in the Central Ubendian Corridor as well as voluminous arc magmatism in the Bangweulu Block and in the Usagaran Belt (Fig. 19).

6.2. New Tectonic Model: Evolution from Orosirian to Cambrian

6.2.1. Paleoproterozoic (Orosirian) geodynamics

The tectono-magmatic evolution of the Ubendian Belt in the Paleoproterozoic occurred between 2100 and 1800 Ma, spanning a period of ~300 m.y. The driving force for the deformation and metamorphism of the Ubendian Belt rocks was multiple episodes of subduction of oceanic lithosphere, which resulted in arc magmatism and accretion or collision of terranes (Fig. 19). The subduction of the oceanic lithosphere was accompanied by the formation of high-pressure granulites and eclogites at ca. 2000 Ma, 1920–1890 Ma, and 1890–1860 Ma (Fig. 19; Ring et al., 1997; Boniface, 2011; Boniface et al., 2012).

Based on the available geochemical, geochronological, and structural data, at ca. 2100 Ma we envisage the southwestern and southeastern margins of the Tanzania Craton to have been active margins with a series of isolated island arcs separated by subducting oceanic and continental lithospheres. The isolated blocks include: the Bangweulu Block, Ufipa Terrane, Nyika Terrane, and the aggregate of the Katuma-Lupa Terrane. The Central Ubendian Corridor (Ubende-Mbozi-Katuma Terranes) probably nucleated as an oceanic island between the Western Ubendian Corridor and Eastern Ubendian Corridor (Fig. 19). At ca. 2050 Ma, the Konse pillow basalts and the associated submarine sediments had formed at the southeastern side of the Tanzania Craton, not shown in Figure 19, and at ca. 1999 Ma during the collision event in the Usagaran Belt, the Konse Group was dismembered from a subducting oceanic plate and was emplaced onto the Tanzania Craton.

At ca. 2000 Ma, at the southwestern side of the Tanzania Craton, the Ufipa Terrane fused with the Nyika Terrane, and in

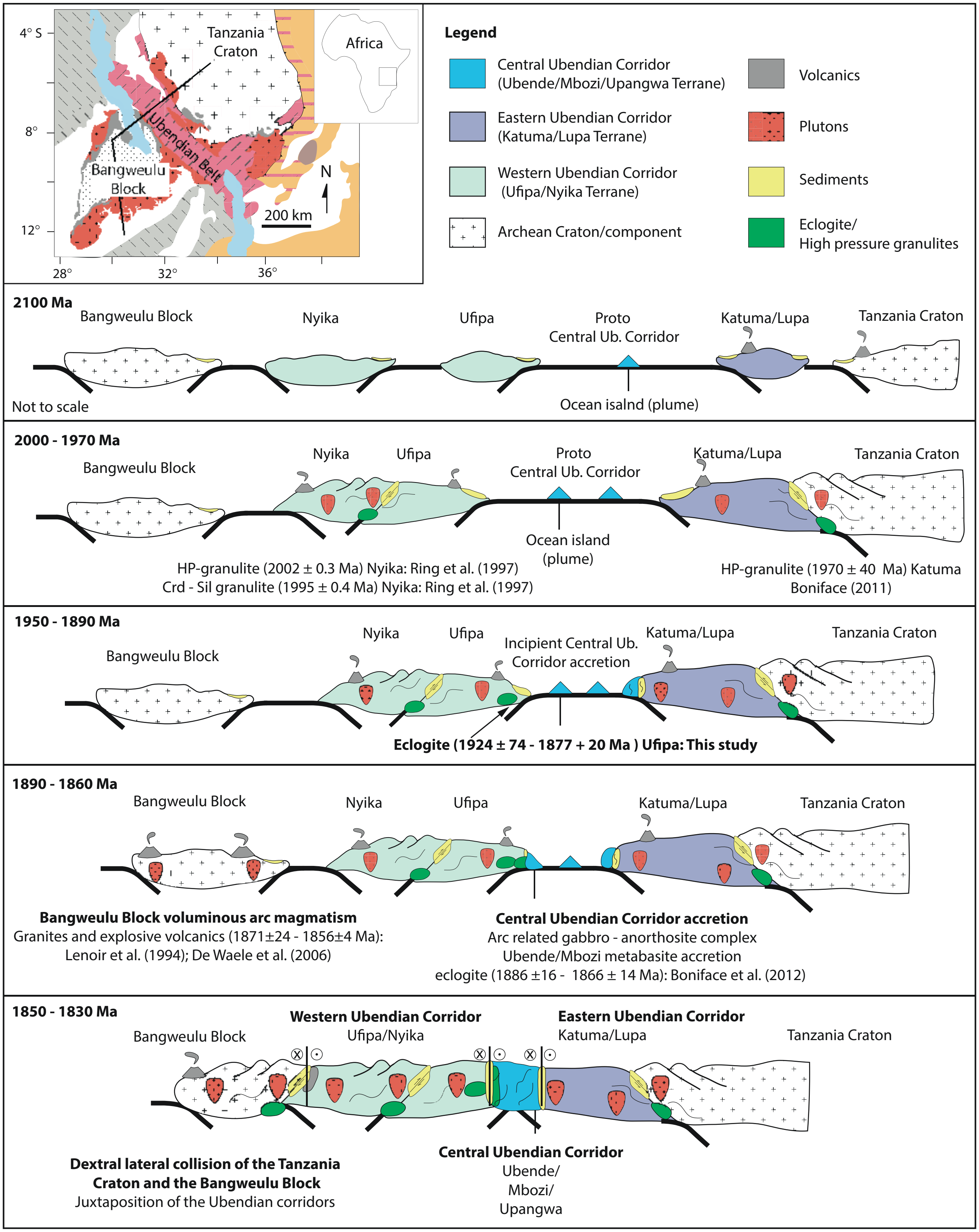

Figure 19. Paleoproterozoic tectonic evolution model of the Ubendian Belt.

the meanwhile the Katuma-Lupa Terrane accreted to the Tanzania Craton. Eclogite-facies high-pressure granulites formed in the Nyika and Katuma Terranes and in the Usagaran Belt as a product of subduction. The subduction event in the Usagaran Belt at 2000 Ma concluded the closing of an ocean at the southeastern margins of the Tanzania Craton. The ocean existed ca. 2050 Ma when the Konse pillow basalts crystallized and later got dismembered from a subducting plate at the back-arc tectonic setting along with submarine sediments (quartzite, meta-chert, meta-dolomite, and metapelites). The 2000 Ma subduction zone metamorphism was coupled with arc magmatism and crustal thickening metamorphism that continued to ca. 1970 Ma (Fig. 19).

Between 1950 and 1900 Ma was another active period in the Ubendian Belt that was characterized by volcanic arc magmatism, crustal thickening metamorphism and arc accretions, deformation and precipitation of gold from hydrothermal fluids, which are concomitant with the ca. 1920 Ma subduction zone metamorphism in the Western Ubendian Corridor (Fig. 19). Between 1890 and 1860 Ma the margins of the Bangweulu Block and the Tanzania Craton were again active. During this time, the oceanic lithosphere between the Ufipa-Nyika Terrane and the Bangweulu Block, and that between Ufipa-Nyika and Katuma-Lupa continued to be subducted (Fig. 19). The subduction process resulted in the formation of eclogites and high-pressure granulites of the Central Ubendian Corridor and also triggered regional voluminous plutonism and explosive volcanism at the margins of the Tanzania Craton and Bangweulu Block (Fig. 19).

The oceans that existed between the Tanzania Craton and Bangweulu Block closed between 1850 and 1830 Ma. The mafic Central Ubendian Corridor was consequently juxtaposed between the Western and Central Ubendian Corridors by a dextral lateral shear collision, which resulted in the formation of barroisite tectonites along deep-sited NW-SE–trending shear boundaries of the Ubende Terrane. The crustal thickening metamorphism that followed a ca. 1890–1860 Ma subduction metamorphism event ended ca. 1800 Ma, concluding the Ubendian Belt orogenic cycle in Orosirian Period.

6.2.2. Mesoproterozoic Geodynamics

After the final collision at ca. 1800 Ma, the Ubendian Belt stayed quiet until the Calymmian–Ectasian Period (1408 ± 6 to 1392 ± 26 Ma) when the region experienced extensional tectonics (rifting), which resulted in the Kapalagulu mafic-ultramafic–layered igneous complex and the Chimala potassic granite to intrude the Ubendian Belt along the NW-SE–trending rift structure (Fig. 20; Maier et al., 2007; Thomas et al., 2018). Similarly, a rifting event resulted in the magmatism and intrusion of the Musongati-Kabanga mafic-ultramafic–layered igneous complex at 1403 ± 14 Ma, along the NE-SW–trending structure in the Kibaran Belt (Karagwe-Ankolean Belt) (Fig. 20; Maier et al., 2007).

Metasedimentary rocks of the Karagwe-Ankolean Belt (known as the Eastern Domain and Western Domain) are interpreted as to have been deposited in the NE-SW basins of a failed rift that started to form during the Musongati-Kabanga magmatism at ca. 1400 Ma and that existed until 1200 Ma when it started to close (Meert et al., 1994; Maier et al., 2007; Tack et al., 2010). The Wakole-Itiaso metasedimentary rocks were deposited at the same time but in the NW-SE–trending basins that opened along the Ubendian Belt (Wadsworth et al., 1982; Maier et al., 2007; Boniface et al., 2014), therefore making a triple junction with the NE-SW Musongati-Kabanga alignment (Fig. 20). We therefore propose that the NW-SE orientation of the Kapalagulu intrusion aligns with a Mesoproterozoic rifting event that formed the ocean basins along the Ubendian Belt. The Mesoproterozoic rifting and probably the formation of ocean basins along the Ubendian Belt is manifested by the Mesoproterozoic-Neoproterozoic alkaline magmatism (Sangu and Ngualla carbonatites, Lusenga and Mbozi syenite complexes, plume-related alkali basalt of the Nyika Terrane) and the Neoproterozoic small ocean basins "Ufipa Ocean" that existed between the Tanzania Craton and the Bangweulu Block (Cahen and Snelling, 1966; Brock, 1968; Brewer et al., 1979; Ring et al., 1997; Boniface and Schenk, 2012).

The structural relations between the NE-SW Musongati-Kabanga alignment (failed rift) and the NW-SE Kapalagulu orientation (successful rifting) are probably similar to the modern structural relations between the East African Rift system and the Red Sea. The latter has opened whereas the East African Rift system has not extended sufficiently to form ocean basins (see Daly et al., 1989; Ring, 2014). The "Ufipa Ocean" probably opened to connect with the Mozambique Ocean that separated East and West Gondwana in the Neoproterozoic (e.g., Meert, 2003; Collins and Pisarevsky, 2005).

6.2.3. Neoproterozoic Geodynamics

The presence of 596 ± 41 Ma eclogites with back-arc and island-arc basalt affinity in the Ufipa Terrane points to subduction zone metamorphism and closing of the "Ufipa Ocean" (Fig. 20; Boniface and Schenk, 2012). However, the closing of the 1400 Ma rift basins started in the north, in the Karagwe-Ankolean Belt and in the Wakole Terrane, which experienced crustal thickening metamorphism and granitization between 1170 and 1000 Ma (Cahen et al., 1984; Ikingura et al., 1992; Kokonyangi et al., 2006; Tack et al., 2010; Dewaele et al., 2011; Boniface et al., 2014). The northern Ubendian Belt (Ubende and Katuma Terranes) was also reworked between 1170 ± 10 and 1091 ± 9 Ma during the closing along the Wakole-Itiaso basins (Boniface et al., 2012; Kazimoto et al., 2014).

Collisional metamorphism and reworking of the Ubendian Belt between 570 and 550 Ma followed the subduction metamorphic event that started ca. 590 Ma (Boniface et al., 2012; Boniface and Appel, 2017; 2018). Due to the lack of arc-related magmatism that preceded the Neoproterozoic subduction, the Ubendian Belt was part of a continental crust that was metacratonitized (Boniface and Appel 2018). The subduction and closing of the oceans between the Tanzania Craton and the Bangweulu Block were concluded in Cambrian Period ca. 500 Ma, when the southern Ubendian Belt recorded another subduction zone metamorphic event in the Nyika Terrane (Fig. 20; Ring et al., 1997).

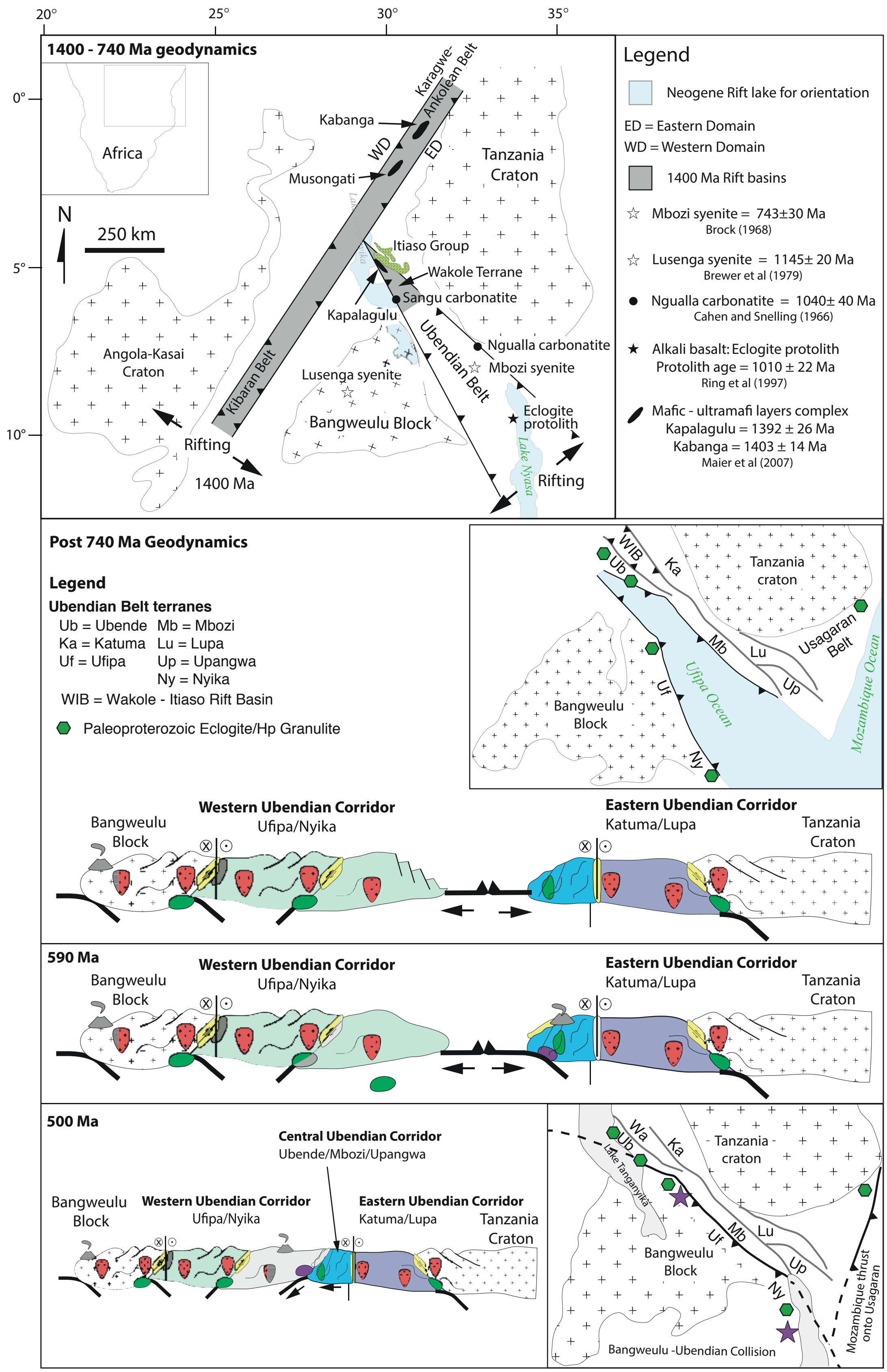

Figure 20. Mesoproterozoic–Neoproterozoic geodynamics of the Ubendian Belt.

The NW to WNW Neoproterozoic sinistral transpressional strike-slip ductile-brittle deformation regime along the Ubendian Belt (Theunissen et al., 1996) was probably the result of collision between the Tanzania Craton and the Bangweulu Block, which was concomitant with the final stage of the Gondwana amalgamation event termed the Kuungan Orogeny (600–500 Ma) (e.g., Meert, 2003). During the same time window (596–550 Ma) the Mozambique Ocean was completely closed as the Mozambique Belt thrusted onto the Usagaran Belt and Tanzania Craton (Fritz et al., 2013).

7. SUMMARY AND CONCLUSIONS

(*i*) The records of rare Precambrian H*P*-L*T* metamorphic interface (eclogite with MORB affinity) in the 2000–1860 Ma Ubendian-Usagaran Belt along with lithological assemblages of pillow lavas with affinity to suprasubduction-zone ophiolites, metapelites, meta-dolomites, and quartzites possibly attest to the relics of disrupted ocean plate stratigraphy and or ophiolites implying the operation of Phanerozoic mobile-lid tectonics in the Precambrian.

(*ii*) Our new data (U-Pb in situ dating of zircon) and the interpretations of the existing data reveal a new age of a H*P*-L*T* metamorphic event in Ubendian Belt dated between 1920 and 1890 Ma from kyanite-bearing eclogites. The data add to the already established H*P*-L*T* metamorphic events at 1890–1860 Ma and 590–520 Ma in the Ubendian Belt and at 2000 Ma in the Usagaran Belt.

(*iii*) Arc–back-arc signatures from some eclogites and the associated metasediments (metapelites and quartzites) imply that the eclogite's mafic protoliths formed above a subduction zone. The protoliths were probably part of a turbidite sequence eroded from nearby or far-distant arc basalt blocks that were channeled into a subduction zone as mélanges that recrystallized and deformed to eclogites and metasediments (metapelites and quartzites).

(*iv*) Petrology and geochemical data of distinct H*P*-L*T* metamorphic events in the Ubendian-Usagaran reveal subduction events of oceanic lithosphere in relatively warm subduction zones in the Proterozoic.

(*v*) The Ubendian-Usagaran events also record rifting, arc and back-arc magmatism, and collisional tectonic events that preceded or followed a H*P*-L*T* tectonic event. These tectonic events manifest a complete record of the Wilson Cycle at the margins of the Tanzania Craton in Precambrian.

(*vi*) Spatial and temporal distribution of H*P*-L*T* events results in a new tectonic subdivision of the Ubendian Belt and development of a new tectonic model that describes the evolution of the Ubendian-Usagaran Belt in the Proterozoic.

(*vii*) The new tectonic subdivision of the Ubendian Belt is described as: (1) Western Ubendian Corridor mainly composed of two Proterozoic suture zones (subduction at 1920–1890 Ma and 590–500 Ma) in the Ufipa and Nyika Terranes; (2) Central Ubendian Corridor predominated by metamorphosed mafic-ultramafic rocks in the Ubende, Mbozi, and Upangwa Terranes that include the 1890–1860 Ma eclogites with MORB affinity in the Ubende Terrane; and (3) Eastern Ubendian Corridor (the Katuma and Lupa Terranes) characterized by reworked Archean crust (with crystallization ages between 2758 ± 9 and 2553 ± 10 Ma). The Archean crust was reworked in the Paleoproterozoic.

(*viii*) Proterozoic suture zones found in the Western Ubendian Corridor (2000, 1920–1890, and 590–520 Ma) are centerpieces of the Ubendian-Usagaran new tectonic model along with sutures in the Central Ubendian Corridors (1890–1860 Ma) and in the Usagaran Belt (2000 Ma).

(*ix*) The new tectonic model describes the evolution of the Ubendian-Usagaran Belt from the Orosirian (2050–1800 Ma) to the Cambrian (500 Ma). The model explains that the Ubendian-Usagaran Belt attained its current fabrics and configuration through rifting, subduction, volcanic-arc and back-arc magmatism, collisional, and reworking events.

8. ACKNOWLEDGMENTS

This research was partly supported by the Center for Northeast Asian Studies, Tohoku University, and partly supported by the grants from the MEXT/JSPS KAKENHI (JP24403010, JP15H05212, and JP18H01299) to T. Tsujimori, and for a visiting professorship at Tohoku University to N. Boniface. We acknowledge Yildirim Dilek (volume editor) and anonymous reviewers whose constructive review comments significantly improved the article. We thank GSA Books Science Editor Christian Koeberl for handling our manuscript. We appreciate the constructive comments from Jean-Paul Liégeois who at some point in time contributed to shape our manuscript. We are also grateful to the University of Dar es Salaam for the support in various forms throughout our field visits in 2012, 2013, 2015, and 2016. We thank Mr. R. Kinyaiya for driving us safely in a Toyota Land Cruiser 70 in difficult but beautiful field conditions.

REFERENCES CITED

Andersen, L., and Unrug, R., 1984, Geodynamic evolution of the Bangweulu block, northern Zambia: Precambrian Research, v. 25, p. 187–212, https://doi.org/10.1016/0301-9268(84)90032-9.

Bahame, G., Manya, S., and Maboko, M.A., 2016, Age and geochemistry of coeval felsic volcanism and plutonism in the Palaeoproterozoic Ndembera Group of southwestern Tanzania: Constraints from SHRIMP U-Pb zircon and Sm–Nd data: Precambrian Research, v. 272, p. 115–132, https://doi.org/10.1016/j.precamres.2015.10.017.

Bingen, B., Jacobs, J., Viola, G., Henderson, I.H.C., Skar, O., Boyd, R., Thomas, R.J., Solli, A., Key, R.M., and Daudi, E.X.F., 2009, Geochronology of the Precambrian crust in the Mozambique belt in NE Mozambique, and implications for Gondwana assembly: Precambrian Research, v. 170, p. 231–255, https://doi.org/10.1016/j.precamres.2009.01.005.

Biyashev, M., Pentelkov, V., Emelyanov, S., Chuklanov, B., Stepnov, E. Matrenitzky, T., and Novikov, A., 1977, Geological map of Sitalike: Dodoma, Geology and Mines Division, Geological Survey of Tanzania, Geological map quarter degree sheet, 170, 1:125,000.

Boniface, N., 2009, Eburnian, Kibaran and Panafrican metamorphic events in the Ubendian belt (Tanzania): Petrology and zircon geochronology [Ph.D. thesis]: University of Kiel, Germany.

Boniface, N., 2011, Petrography and geochemistry of mafic granulites of the Ubendian Belt: Contribution to insights into the lower continental crust of the Paleoproterozoic: Tanzania Journal of Science, v. 37, p. 129–143.

Boniface, N., 2015, Geochemistry: Grouping of rocks to co-genetic magma suites and data interpretation in terms of possible geo-tectonomagmatic setting: Geological Survey of Tanzania, Technical report, ISBN 978-9987-765-00-3.

Boniface, N., 2019, An overview of the Ediacaran-Cambrian orogenic events at the southern margins of the Tanzania Craton: Implication for final assembly of Gondwana: Journal of African Earth Sciences, v. 150, p. 123–130, https://doi.org/10.1016/j.jafrearsci.2018.10.015.

Boniface, N., 2020, Geochronology of massif-type anorthosites - gabbros from the Ubendian Belt, Tanzania: Tanzania Journal of Sciences, v. 46, no. 1, p. 61–75, https://www.ajol.info/index.php/tjs/article/view/196283.

Boniface, N., and Appel, P., 2017, Stenian-Tonian and Ediacaran metamorphic imprints in the southern Paleoproterozoic Ubendian Belt, Tanzania: Constraints from in situ monazite ages: Journal of African Earth Sciences, v. 133, p. 25–35, https://doi.org/10.1016/j.jafrearsci.2017.05.005.

Boniface, N., and Appel, P., 2018, Neoproterozoic reworking of the Ubendian Belt crust: Implication for an orogenic cycle between the Tanzania Craton and Bangweulu Block during the assembly of Gondwana: Precambrian Research, v. 305, p. 358–385, https://doi.org/10.1016/j.precamres.2017.12.011.

Boniface, N., and Schenk, V., 2007, Polymetamorphism in the Paleoproterozoic Ubendian Belt, Tanzania: Geochimica et Cosmochimica Acta, v. 71, no. 15, Suppl. S, p. A107.

Boniface, N., and Schenk, V., 2012, Neoproterozoic eclogites in the Paleoproterozoic Ubendian Belt of Tanzania: Evidence for a Pan-African suture between the Bangweulu Block and the Tanzania Craton: Precambrian Research, v. 208–211, p. 72–89, https://doi.org/10.1016/j.precamres.2012.03.014.

Boniface, N., and Tsujimori, T., 2014, Dating of Proterozoic orogenic events around the Tanzania Craton: new insights from in-situ zircon and monazite geochronology, *in* Ima2014, 1–5 September 2014, Johannesburg, South Africa [abs.]: International Mineralogical Association, 21st General Meeting, p. 204.

Boniface, N., and Tsujimori, T., 2016, 1.96 Ga kyanite-epidote eclogites with 605 Ma granulite facies overgrowth in the Ubendian Belt, Tanzania, *in* Goldschmidt2016, 26 June–6 July 2016, Yokohama, Japan [abs]: no. 263, https://goldschmidt.info/2016/abstracts/abstractView?id=2016002607.

Boniface, N., and Tsujimori, T., 2019, Pillow lava basalts with back-arc MORB affinity from the Usagaran Belt, Tanzania: relics of Orosirian ophiolites: Journal of the Geological Society, v. 176, p. 1007–1021, https://doi.org/10.1144/jgs2018-205.

Boniface, N., Schenk, V., and Appel, P., 2012, Paleoproterozoic eclogites of MORB-type chemistry and three Proterozoic orogenic cycles in the Ubendian belt (Tanzania): Evidence from monazite and zircon geochronology, and geochemistry: Precambrian Research, v. 192–195, p. 16–33, https://doi.org/10.1016/j.precamres.2011.10.007.

Boniface, N., Schenk, V., and Appel, P., 2014, Mesoproterozoic high-grade metamorphism in pelitic rocks of the northwestern Ubendian Belt: Implication for the extension of the Kibaran intra-continental basins to Tanzania: Precambrian Research, v. 249, p. 215–228, https://doi.org/10.1016/j.precamres.2014.05.010.

Boniface, N., Tsujimori, T., Mruma, A., 2019, Geochronology and geochemistry of the Konse Pillow basalts, Tanzania: Implication for a new stratigraphic sequence of the Usagaran Belt: Tanzania Geological Society, 2019 Annual General Meeting, Books of Abstracts, p. 6-7, https://www.tgs.or.tz/publication/attachments/4/Book_of_Abstracts_-_TGS_Workshop_2019.pdf.

Boven, A., Theunissen, K., Sklyarov, E., Klerkx, J., Melnikov, A., Mruma, A., and Punzalan, L., 1999, Timing of exhumation of a high-pressure mafic granulite terrane of the Paleoproterozoic Ubende Belt (West Tanzania): Precambrian Research, v. 93, p. 119–137, https://doi.org/10.1016/S0301-9268(98)00101-6.

Boyd, R., Nordgulen, O., Thomas, R.J., Bingen, B., Bjerkgard, T., Grenne, T., Henderson, I., Melezhik, V.A., Often, M., Sandstad, J.S., Solli, A., Tveten, E., Viola, G., Key, R.M., Smith, R.A., Gonzalez, E., Hollick, L.J., Jacobs, J., Jamal, D., Motuza, G., Bauer, W., Daudi, E., Feitio, P., Manhica, V., Moniz, A., and Rossea, D., 2010, The geology and geochemistry of the East African Orogen in Northeastern Mozambique: South African Journal of Geology, v. 113, no. 1, p. 87–129, https://doi.org/10.2113/gssajg.113.1.87.

Brewer, M., Haslam, H., Darbyshire, P., and Davis, A., 1979, Rb-Sr Age Determinations in the Bangweulu Block, Luapula Province, Zambia: London, Institute of Geological Sciences, Report 79/5.

Brock, P.W.G., 1968, Metasomatic and Intrusive nepheline-bearing rocks from the Mbozi syenite-gabbro complex, southwestern Tanzania: Canadian Journal of Earth Sciences, v. 5, no. 3, p. 387–419, https://doi.org/10.1139/e68-039.

Brown, M., 2006, Duality of thermal regimes is the distinctive characteristic of plate tectonics since the Neoarchean: Geology, v. 34, no. 11, p. 961–964, https://doi.org/10.1130/G22853A.1.

Brown, M., and Johnson, T., 2018, Secular change in metamorphism and the onset of global plate tectonics: The American Mineralogist, v. 103, no. 2, p. 181–196, https://doi.org/10.2138/am-2018-6166.

Cahen, K., and Snelling, N.J., 1966, The Geochronology of Equatorial Africa: Amsterdam, North-Holland Publishing Co., Ltd., 195 p.

Cahen, L., Snelling, N.J., Delhal, J., and Vail, J., 1984, The Geochronology and Evolution of Africa: Oxford, Clarendon Press, 512 p.

Cawood, P.A., Kröner, A., and Pisarevsky, S., 2006, Precambrian plate tectonics: criteria and evidence: GSA Today, v. 16, p. 4–11, https://doi.org/10.1130/GSAT01607.1.

Cawood, P.A., Hawkesworth, C.J., Pisarevsky, S.A., Dhuime, B., Capitanio, F.A., and Nebel, O., 2018, Geological archive of the onset of plate tectonics: Philosophical Transactions, Royal Society. Mathematical, Physical, and Engineering Sciences, v. 376, 20170405, https://doi.org/10.1098/rsta.2017.0405.

Coetzee, G., 1963, Datierungen von granitischen Gesteinen im Dodoman und Usagaran System und in der Ndembera Serie (Tanzania): Carbonatites of the Karema Depression, west Tanganyika: South African Journal of Geology, v. 66, p. 283–340 https://hdl.handle.net/10520/AJA10120750_1546.

Collins, A.S., and Pisarevsky, S.A., 2005, Amalgamating eastern Gondwana: the evolution of the circum-Indian orogens: Earth-Science Reviews, v. 71, p. 229–270, https://doi.org/10.1016/j.earscirev.2005.02.004.

Collins, A.S., Reddy, S.M., Buchan, C., and Mruma, A., 2004, Temporal constraints on Palaeoproterozoic eclogite formation and exhumation (Usagaran Orogen, Tanzania): Earth and Planetary Science Letters, v. 224, no. 1–2, p. 175–192, https://doi.org/10.1016/j.epsl.2004.04.027.

Corfu, F., Hanchar, J.M., Hoskin, P.W.O., and Kinny, P.D., 2003, Atlas of zircon textures, *in* Hanchar, J.M., and Hoskin, P.W.O., eds., Zircon: Mineralogical Society of America and Geochemical Society Reviews in Mineralogy and Geochemistry, v. 53, p. 469–500, https://doi.org/10.1515/9781501509322-019.

Cutten, H., Johnson, S.P., and De Waele, B., 2006, Protolith ages and timing of metasomatism related to the formation of whiteschists at Mautia Hill Tanzania: implications for the assembly of Gondwana: The Journal of Geology, v. 114, p. 683–698, https://doi.org/10.1086/507614.

Daly, M., and Unrug, R., 1982, The Muva Supergroup, northern Zambia: Geological Society of South Africa Transactions, v. 85, p. 155–165.

Daly, M.C., 1988, Crustal shear zones in Central Africa: a kinematic approach to Proterozoic tectonics: Episodes, v. 11, no. 1, p. 5–11, https://doi.org/10.18814/epiiugs/1988/v11i1/003.

Daly, M.C., Klerkx, J., and Nanyaro, J.T., 1985, Early Proterozoic terranes and strike-slip accretion in the Ubendian belt of southwest Tanzania [abs.]: Terra Cognita, v. 5, p. 257.

Daly, M.C., Chorowicz, J., and Fairhead, J.D., 1989, Rift basin evolution in Africa: the influence of reactivated steep basement shear zones: Geological Society of London Special Publication 44, no. 1, p. 309–334, https://doi.org/10.1144/GSL.SP.1989.044.01.17.

De Waele, B., and Fitzsimons, I.C.W., 2007, The nature and timing of Palaeoproterozoic sedimentation at the southeastern margin of the Congo Craton; zircon U-Pb geochronology of plutonic, volcanic and clastic units in northern Zambia: Precambrian Research, v. 159, p. 95–116, https://doi.org/10.1016/j.precamres.2007.06.004.

De Waele, B., Kampunzu, A.B., Mapani, B.S.E., and Tembo, F., 2006a, The Mesoproterozoic Irumide Belt of Zambia: Journal of African Earth Sciences, v. 46, no. 1–2, p. 36–70, https://doi.org/10.1016/j.jafrearsci.2006.01.018.

De Waele, B., Liégois, J.P., Nemchin, A.A., and Tembo, F., 2006b, Isotopic and geochemical evidence of Proterozoic episodic crustal reworking within the Irumide belt of south-central Africa, the southern metacratonic boundary of an Archaean Bangweulu Craton: Precambrian Research, v. 148, no. 3–4, p. 225–256, https://doi.org/10.1016/j.precamres.2006.05.006.

De Waele, B.F., Wingate, M.T.D., Tembo, F., Mapani, B.S.E., and Belousova, E.A., 2009, The geochronological framework of the Irumide Belt: a prolonged crustal history along the margin of the Bangweulu Craton: American Journal of Science, v. 309, p. 132–187, https://doi.org/10.2475/02.2009.03.

Debruyne, D., Wilderode, J.V., Balcaen, L., Vanhaecke, F., and Muchez, P., 2014, Geochemistry and isotopic evolution of the central African Domes, Bangweulu and Irumide regions: Evidence for cryptic Archean sources and a Paleoproterozoic continental arc: Journal of African Earth Sciences, v. 100, p. 145–163, https://doi.org/10.1016/j.jafrearsci.2014.06.013.

Dewaele, S., Henjes-Kunst, F., Melcher, F., Sitnikova, M., Burgess, R., Gerdes, A., Fernandez, M.A., Clercq, F.D., Muchez, P., and Lehmann, B., 2011, Late Neoproterozoic overprinting of the cassiterite and columbite-tantalite bearing pegmatites of the Gatumba area, Rwanda (Central Africa): Journal of African Earth Sciences, v. 61, no. 1, p. 10–26, https://doi.org/10.1016/j.jafrearsci.2011.04.004.

Dilek, Y., and Furnes, H., 2011, Ophiolite genesis and global tectonics: Geochemical and tectonic fingerprinting of ancient oceanic lithosphere: Geological Society of America Bulletin, v. 123, no. 3-4, p. 387–411, https://doi.org/10.1130/B30446.1.

Dilek, Y., and Furnes, Y., 2014, Origins of ophiolites: Elements, v. 10, p. 93–100, https://doi.org/10.2113/gselements.10.2.93.

Dilek, Y., and Furnes, H., 2019, Tethyan ophiolites and Tethyan seaways: Journal of the Geological Society, v. 176, p. 899–912, https://doi.org/10.1144/jgs2019-129.

Dilek, Y., and Polat, A., 2008, Suprasubduction zone ophiolites and Archean tectonics: Geology, v. 36, no. 5, p. 431–432, https://doi.org/10.1130/Focus052008.1.

Dodson, M.H., Cavanagh, B.J., Thatcher, E.C., and Aftalion, M., 1975, Age limits for the Ubendian metamorphic episode in northern Malawi: Geological Magazine, v. 112, no. 4, p. 403–410, https://doi.org/10.1017/S0016756800046793.

Duchesne, J.C., Liégeois, J.P., Deblond, A., and Tack, L., 2004, Petrogenesis of the Kabanga–Musongati layered mafic–ultramafic intrusions in Burundi (Kibaran Belt): geochemical, Sr–Nd isotopic constraints and Cr–Ni behavior: Journal of African Earth Sciences, v. 39, p. 133–145, https://doi.org/10.1016/j.jafrearsci.2004.07.055.

Eckert, J.O., Newton, R.C., and Kleppa, O.J., 1991, The DH of reaction and recalibration of garnet-pyroxene-plagioclase-quartz geobarometer in the CMAS system by solution calorimetry: American Mineralogist, v. 76, p. 148–160.

Ellis, D.J., Green, D.H., 1985. Garnet-forming Reactions in Mafic Granulites from Enderby Land, Antarctica—Implications for Geothermometry and Geobarometry, Journal of Petrology, v. 26, no. 3, p. 633–662, https://doi.org/10.1093/petrology/26.3.633.

Evans, D.M., Barrett, F.M., and Prichard, H.M., 2012, Platinum-palladium-gold mineralization in the Nkenja mafic-ultramafic body, Ubendian metamorphic belt, Tanzania: Mineralium Deposita, v. 47, p. 175–196, https://doi.org/10.1007/s00126-011-0353-8.

Fan, W.M., Guo, F., Wang, Y.J., and Lin, G., 2003, Late Mesozoic calc-alkaline volcanism of post-orogenic extension in the northern Da Hinggan Mountains, northeastern China: Journal of Volcanology and Geothermal Research, v. 121, p. 115–135, https://doi.org/10.1016/S0377-0273(02)00415-8.

Fernandez-Alonso, M., and Theunissen, K., 1998, Airborne geophysics and geochemistry provide new insights in the intracontinental evolution of the Mesoproterozoic Kibaran Belt (Central Africa): Geological Magazine, v. 135, p. 203–216, https://doi.org/10.1017/S0016756898008310.

Fernandez-Alonso, M., Cutten, H., Waele, B.D., Tack, L., Tahon, A., Baudet, D., and Barritt, S., 2012, The Mesoproterozoic Karagwe-Ankole Belt (formerly the NE Kibara Belt): The result of prolonged extensional intracratonic basin development punctuated by two short-lived far-field compressional events: Precambrian Research, v. 216–219, p. 63–86, https://doi.org/10.1016/j.precamres.2012.06.007.

Ferry, J.M., and Watson, E.B., 2007, New thermodynamic models and revised calibrations for the Ti-in-zircon and Zr-in-rutile thermometers: Contributions to Mineralogy and Petrology, v. 154, p. 429–437, https://doi.org/10.1007/s00410-007-0201-0.

François, C., Debaille, V., Paquette, J.-L., Baudet, D., and Javaux, E.J., 2018, The earliest evidence for modern-style plate tectonics recorded by H*P*-L*T* metamorphism in the Paleoproterozoic of the Democratic Republic of the Congo: Scientific Reports, v. 8, article no. 15452, https://doi.org/10.1038/s41598-018-33823-y.

Fritz, H., Tenczer, V., Hauzenberger, C.A., Wallbrecher, E., Hoinkes, G., Muhongo, S., and Mogessie, A., 2005, Central Tanzanian tectonic map: A step forward to decipher Proterozoic structural events in the East African Orogen: Tectonics, v. 24, no. 6, TC6013.

Fritz, H., Tenczer, V., Hauzenberger, C., Wallbrecher, E., and Muhongo, S., 2009, Hot granulite nappes—Tectonic styles and thermal evolution of the Proterozoic granulite belts in East Africa: Tectonophysics, v. 477, no. 3–4, p. 160–173.

Fritz, H., Abdelsalam, M., Ali, K., Bingen, B., Collins, A., Fowler, A., Ghebreab, W., Hauzenberger, C., Johnson, P., Kusky, T., Macey, P., Muhongo, S., Stern, R., and Viola, G., 2013, Orogen styles in the East African Orogen: A review of the Neoproterozoic to Cambrian tectonic evolution: Journal of African Earth Sciences, v. 86, p. 65–106, https://doi.org/10.1016/j.jafrearsci.2013.06.004.

Gabert, G., and Wendt, I., 1974, Datierungen von granitischen Gesteinen im Dodoman und Usagaran System und in der Ndembera Serie (Tanzania): Geologisches Jahrbuch, v. 11, p. 3–55.

Gallagher, D., 1939, A preliminary account of the geology of a portion of the Lupa gold field (Tanganyika): Economic Geology and the Bulletin of the Society of Economic Geologists, v. 34, no. 3, p. 243–267, https://doi.org/10.2113/gsecongeo.34.3.243.

Gallagher, D., 1941, A microscopic study of some ores of the Lupa gold field, Tanganyika Territory, East Africa: Economic Geology and the Bulletin of the Society of Economic Geologists, v. 36, no. 3, p. 306–323, https://doi.org/10.2113/gsecongeo.36.3.306.

Haldemann, E.G., 1953, Additional Notes on the Geology of Upangwa, Njombe District: The Basic Rocks and their Economic Aspects: Geological Survey of Tanganyika unpublished report.

Halligan, R., and Birch, R., 1961a, Geological map of Kakungu: Dodoma, Tanzania Mineral Resources Division, Geological Survey of Tanzania, Quarter-degree geological map sheet series of Tanzania, 132, 1:125,000.

Halligan, R., and Birch, R., 1961b, Geological map of Mgambo: Dodoma, Tanzania Mineral Resources Division, Geological Survey of Tanzania, Quarter-degree geological map sheet series of Tanzania, 131, 1:125,000.

Hanson, R.E., 2003, Proterozoic geochronology and tectonic evolution of southern Africa, *in* Yoshida, M., et al., eds., Proterozoic East Gondwana: Supercontinent Assembly and Breakup: Geological Society of London Special Publication 206, p. 427–463, https://doi.org/10.1144/GSL.SP.2003.206.01.20.

Harkin, D.A., and Harpum, J.R., 1978, Geological map of Tukuyu: Dodoma, Tanzania Mineral Resources Division, Geological Survey of Tanzania, Quarter-degree geological map sheet series of Tanzania, 259, 1:125,000:

Harley, S.L., 1984, An experimental study of the partitioning of Fe and Mg between garnet and orthopyroxene: Contributions to Mineralogy and Petrology, v. 86, p. 359–373, https://doi.org/10.1007/BF01187140.

Harpum, J.R., 1952, The Titanium-bearing Iron Occurrence of the Njombe District, South-west of Tanganyika: Geological Survey of Tanganyika internal report.

Harpum, J.R., 1958, Geological map of Kipengere: Dodoma, Tanzania Mineral Resources Division, Geological Survey of Tanzania, Quarter-degree geological map sheet series of Tanzania, 260, 1:125,000.

Harpum, J.R., 1970, Summary of the geology of Tanzania, part V: Structure and geotectonics of the Precambrian: Tanzania, Ministry of Commerce and Industries Mineral Resources Division, Memoir 1, 58 p., 2 maps.

Harpum, J.R., and Brown, P.E., 1958, Geological map of Chimala: Dodoma, Tanzania Mineral Resources Division, Geological Survey of Tanzania, Quarter-degree geological map sheet series of Tanzania, 246, 1:125,000.

Hauzenberger, C.A., Sommer, S., Fritz, H., Bauernhofer, A., Kröner, A., Hoinkes, G., Wallbrecher, E., and Thoeni, M., 2007, SHRIMP U-Pb zircon and Sm–Nd garnet ages from granulite facies basement of SE-Kenya: evidence for Neoproterozoic polycyclic assembly of the Mozambique belt: Journal of the Geological Society, v. 164, p. 189–201, https://doi.org/10.1144/0016-76492005-081.

Holland, T.J.B., 1979, Experimental determination of the reaction paragonite = jadeite + kyanite + H_2O, and internally consistent thermodynamic data for part of the system Na_2O-Al_2O_3-SiO_2-H_2O, with applications to eclogites and blueschists: Contributions to Mineralogy and Petrology, v. 68, p. 293–301, https://doi.org/10.1007/BF00371551.

Holland, T.J.B., 1980, The reaction albite = jadeite + quartz determined experimentally in the range 600–1200 °C: The American Mineralogist, v. 65, p. 129–134.

Ikingura, J.R., Reynolds, P.H., Watkinson, D.H., and Bell, K., 1992, $^{40}Ar/^{39}Ar$ dating of micas from granites of NE Kibaran Belt (Karagwe-Ankolean), NW Tanzania [and the Middle East]: Journal of African Earth Sciences, v. 15, no. 3–4, p. 501–511, https://doi.org/10.1016/0899-5362(92)90031-7.

Ishikawa, T., Nagaishi, K., and Umino, S., 2002, Boninitic volcanism in the Oman ophiolite: Implications for thermal conditions during transition from spreading ridge to arc: Geology, v. 30, p. 899–902, https://doi.org/10.1130/0091-7613(2002)030<0899:BVITOO>2.0.CO;2.

Iskahakov, B.L., Shuvalov, S.Y., Stefanovsky, W.W., Kostunin, E., and Mahanga, W.L., 1970, Geological map of Nkamba: Quarter Degree Sheet 169. Map reproduced in 1997 by F.N.P. Makyao, E.G. Kanza, B. Troöng, B. Eriksson, and E.B. Temu, Map, Geological Survey of Tanzania.

Iskhakov, B., Shuvalov, S., Kireev, A., Pentelov, V., Trifan, M., and Gavrilov, G., 1971, Geological map of Mlala Hills: Geological Survey of Tanzania, Geological map of Tanzania Quarter Degree Sheet 171 (compiled and edited by B. Troöng and E.B. Temu in 1998).

Johnson, S.P., Cutten, H., Muhongo, S.M., and De Waele, B., 2003, Neoarchaean magmatism and metamorphism of the western granulites in the central domain of the Mozambique belt, Tanzania: U-Pb shrimp geochronology and P-T estimates: Tectonophysics, v. 375, p. 125–145, https://doi.org/10.1016/j.tecto.2003.06.003.

Johnson, S.P., De Waele, B., and Liyungu, K.A., 2006, U-Pb sensitive high-resolution ion microprobe (SHRIMP) zircon geochronology of granitoid rocks in eastern Zambia: Terrane subdivision of the Mesoproterozoic Southern Irumide Belt: Tectonics, v. 25, no. TC6004, p. 1–29, https://doi.org/10.1029/2006TC001977.

Kabengele, M., Lubala, R., and Cabanis, B., 1991, Caracterisation pétrologique et géochimique du magmatisme ubendien du secteur de Pepa-Lubumba, sur le plateau des Marungu (Nord-Est du Shaba, Zaire): Signification géodynamique dans l'évolution de la chaíene ubendienne: Journal of African Earth Sciences, v. 13, no. 2, p. 243–265, https://doi.org/10.1016/0899-5362(91)90009-N.

Kabete, J., McNaughton, N., Groves, D., and Mruma, A., 2012, Reconnaissance SHRIMP U-Pb zircon geochronology of the Tanzania Craton: Evidence for Neoarchean granitoid-greenstone belts in the Central Tanzania Region and the Southern East African Orogen: Precambrian Research, v. 216, p. 232–266, https://doi.org/10.1016/j.precamres.2012.06.020.

Kapenda, D., Kampunzu, A., Cabanis, B., Namegabe, M., and Tshimanga, K., 1998, Petrology and geochemistry of post-kinematic mafic rocks from the Paleoproterozoic Ubendian belt, NE Katanga (Democratic Republic of Congo): Geologische Rundschau or International Journal of Earth Sciences, v. 87, no. 3, p. 345–362, https://doi.org/10.1007/s005310050214.

Kazimoto, E.O., Schenk, V., and Berndt, J., 2014, Neoarchean and Paleoproterozoic crust formation in the Ubendian Belt of Tanzania: Insights from zircon geochronology and geochemistry: Precambrian Research, v. 252, p. 119–144, https://doi.org/10.1016/j.precamres.2014.06.020.

Kazimoto, E.O., Schenk, V., and Appel, P., 2015a, The age of Au–CU-Pb bearing veins in the poly-orogenic Ubendian Belt (Tanzania): U–Th–total Pb dating of hydrothermally altered monazite: Contributions to Mineralogy and Petrology, v. 169, no. 1, 1088, https://doi.org/10.1007/s00410-014-1088-1.

Kazimoto, E.O., Schenk, V., and Appel, P., 2015b, Granulite-facies metamorphic events in the northwestern Ubendian Belt of Tanzania: Implications for the Neoarchean to Paleoproterozoic crustal evolution: Precambrian Research, v. 256, p. 31–47, https://doi.org/10.1016/j.precamres.2014.10.016.

Kennerley, J., 1962, Geological map of Itaka: Dodoma, Geological Survey of Tanzania, Geological map of Tanzania, Quarter degree sheet 243, 1:125 000.

Kokonyangi, J.W., Kampunzu, A.B., Armstrong, R., Yoshida, M., Okudaira, T., Arima, M., and Ngulube, D.A., 2006, The Mesoproterozoic Kibaride belt (Katanga, SE D.R. Congo): Journal of African Earth Sciences, v. 46, no. 1–2, p. 1–35, https://doi.org/10.1016/j.jafrearsci.2006.01.017.

Komiya, T., Maruyama, S., Masuda, T., Nohda, S., Hayashi, M., and Okamoto, K., 1999, Plate Tectonics at 3.8–3.7 Ga: Field Evidence from the Isua Accretionary Complex, Southern West Greenland: Journal of Geology, v. 107, p. 515–554, https://doi.org/10.1086/314371.

Koziol, A.M., 1989, Recalibration of the garnet–plagioclase–Al_2SiO_5–quartz (GASP) geobarometer and applications to natural parageneses: Eos (Transactions, American Geophysical Union), v. 70, p. 493.

Kretz, R., 1983, Symbols for rock-forming minerals: The American Mineralogist, v. 68, no. 1–2, p. 277–279.

Krogh, E.J., 1988, The garnet-clinopyroxene Fe-Mg geothermometer—A reinterpretation of existing experimental data: Contributions to Mineralogy and Petrology, v. 99, p. 44–48, https://doi.org/10.1007/BF00399364.

Kursten, M., 1963, Geological Map of Sao Hill: Dodoma, Tanzania Mineral Resources Division, Geological Survey of Tanzania, Quarter-degree geological map sheet series of Tanzania, 232, 1:125,000.

Kusky, T.M., Windley, B.F., and Polat, A., 2018, Geological evidence for the operation of plate tectonics throughout the Archean: Records from Archean paleo-plate boundaries: Journal of Earth Science, v. 29, no. 6, p. 1291–1303, https://doi.org/10.1007/s12583-018-0999-6.

Lawley, C.J., Selby, D., Condon, D.J., Horstwood, M., Millar, I., Crowley, Q., and Imber, J., 2013a, Lithogeochemistry, geochronology and geodynamic setting of the Lupa Terrane, Tanzania: Implications for the extent of the Archean Tanzanian Craton: Precambrian Research, v. 231, p. 174–193, https://doi.org/10.1016/j.precamres.2013.02.012.

Lawley, C.J., Selby, D., and Imber, J., 2013b, Re-Os molybdenite, pyrite, and chalcopyrite geochronology, Lupa Goldfield, southwestern Tanzania: Tracing metallogenic time scales at midcrustal shear zones hosting orogenic Au deposits: Economic Geology and the Bulletin of the Society of Economic Geologists, v. 108, p. 1591–1613, https://doi.org/10.2113/econgeo.108.7.1591.

Lawley, C., Selby, D., Condon, D., and Imber, J., 2014, Palaeoproterozoic orogenic gold style mineralization at the southwestern Archaean Tanzanian cratonic margin, Lupa Goldfield, SW Tanzania: Implications from U-Pb titanite geochronology: Gondwana Research, v. 26, no. 3–4, p. 1141–1158, https://doi.org/10.1016/j.gr.2013.08.025.

Legler, C., Barth, A., Knobloch, A., Mruma, A.H., Myumbilwa, Y., Magigita, M., Msechu, M., Ngole, T., Stanek, K.P., Boniface, N., Kagya, M., Manya, S., Berndt, T., Stahl, M., Gebremichael, M., Dickmayer, E., Repper, C., Falk, D., and Stephan, T., 2015, Minerogenic Map of Tanzania and Explanatory Notes for the Minerogenic Map of Tanzania, 1:1.5 M: Geological Survey of Tanzania.

Lenoir, J.L., Liégois, J.P., Theunissen, K., and Klerkx, J., 1994, The Palaeoproterozoic Ubendian shear belt in Tanzania: geochronology and structure: Journal of African Earth Sciences, v. 19, no. 3, p. 169–184, https://doi.org/10.1016/0899-5362(94)90059-0.

Liégeois, J.P., Abdelsalam, M.G., Ennih, N., and Ouabadi, A., 2013, Metacraton: Nature, genesis and behavior: Gondwana Research, v. 23, no. 1, p. 220–237, https://doi.org/10.1016/j.gr.2012.02.016.

Maboko, A.H., and Nakamura, E., 1996, Nd and Sr isotopic mapping of the Archaean-Proterozoic boundary in southeastern Tanzania using granites as probes for crustal growth: Precambrian Research, v. 77, p. 105–115, https://doi.org/10.1016/0301-9268(95)00048-8.

Macfarlane, A., 1963, Geological map of Itumba: Geological Survey of Tanzania, Geological map of Tanzania, Quarter Degree Sheet 258 and 258 S.

Macfarlane, A., 1965, Geological map of Gua: Geological map, Geological Survey of Tanzania, Quarter Degree Sheet 208.

Macfarlane, A., 1966, Geological map of Itumba: Geological Survey of Tanzania, Geological map of Tanzania, Quarter Degree Sheet 258.

Macfarlane, A., Mudd, G.C., and Orridge, G.R., 1962, Geological map of Makongolosi: Geological Survey of Tanzania, Geological map of Tanzania, Quarter Degree Sheet 228.

Macfarlane, A., Macdonald, A.S., and Grantham, D.R., 1964, Geological map of Luika: Geological Survey of Tanzania, Geological map of Tanzania, Quarter Degree Sheet 227.

Maier, W.D., Peltonen, P., and Livesey, T., 2007, The ages of the Kabanga north and Kapalagulu intrusions, western Tanzania: A reconnaissance study: Economic Geology and the Bulletin of the Society of Economic Geologists, v. 102, no. 1, p. 147–154, https://doi.org/10.2113/gsecongeo.102.1.147.

Maier, W.D., Barnes, S.J., Bandyayera, D., Livesey, T., Li, C., and Ripley, E., 2008, Early Kibaran rift-related mafic-ultramafic magmatism in western Tanzania and Burundi: Petrogenesis and ore potential of the Kapalagulu and Musongati layered intrusions [rift related Magmatism.]: Lithos, v. 101, no. 1, p. 24–53, https://doi.org/10.1016/j.lithos.2007.07.015.

Manya, S., 2011, Nd-isotopic mapping of the Archaean–Proterozoic boundary in southwestern Tanzania: Implication for the size of the Archaean Tanzania Craton: Gondwana Research, v. 20, p. 325–334, https://doi.org/10.1016/j.gr.2011.01.002.

Manya, S., 2013, Geochemistry and U-Pb zircon dating of the high-K calc-alkaline basaltic andesitic lavas from the Buanji Group, south-western Tanzania: Journal of African Earth Sciences, v. 86, p. 107–118, https://doi.org/10.1016/j.jafrearsci.2013.06.011.

Manya, S., and Maboko, M.A., 2016, Generation of Palaeoproterozoic tonalites and associated high-K granites in southwestern Tanzania by partial melting of underplated mafic crust in an intracontinental setting: Constraints from geochemical and isotopic data: Lithos, v. 260, p. 120–133, https://doi.org/10.1016/j.lithos.2016.05.011.

Maruyama, S., Liou, J.G., and Terabayashi, M., 1996, Blueschists and eclogites of the World and their exhumation: International Geology Review, v. 38, no. 6, p. 485–594, https://doi.org/10.1080/00206819709465347.

McConnell, R., 1950, Outline of the Geology of Ufipa and Ubende: Geological Survey of Tanganyika Bulletin 19, 62 p.

McConnell, R., 1967, The East African rift system: Nature, v. 215, no. 5101, p. 578–581, https://doi.org/10.1038/215578a0.

Meert, J.G., 2003, A synopsis of events related to the assembly of eastern Gondwana, *in* MacNiocaill, C., Torsvik, T., and van der Pluijm, B.A., eds., Paleomagnetism Applied to Tectonics: A Tribute to Rob Van der Voo: Amsterdam, Netherlands, Elsevier, v. 362, no. 1–4, p. 1–40, https://doi.org/10.1016/S0040-1951(02)00629-7.

Meert, J.G., Hargraves, R.B., Van der Voo, R., Hall, C.M., and Halliday, A.N., 1994, Paleomagnetic and $^{40}Ar/^{39}Ar$ studies of late Kibaran intrusives in Burundi, east Africa; Implications for late Proterozoic supercontinents: The Journal of Geology, v. 102, p. 621–637, https://doi.org/10.1086/629708.

Meinhold, K., 1970, Petrographie, Metamorphose, Tektonik und stratigraphische Stellung der Konse-Serie in Zentral-Tanzania (Östafrica), Beihefte zum: Geologisches Jahrbuch, v. 91, p. 1–137.

Mints, M.V., Dokukina, K.A., and Konilov, A.N., 2014, The Meso-Neoarchaean Belomorian eclogite province: Tectonic position and geodynamic evolution: Gondwana Research, v. 25, no. 2, p. 561–584, https://doi.org/10.1016/j.gr.2012.11.010.

Miyashev, M., Pentelkov, V., Emilyanov, S., Chuklanov, B., and Stepnov, E., 1970, Geological map of Usevya: Geological Survey of Tanzania, Geological map of Tanzania, Quarter Degree Sheet 188. (Map reproduced in 1997 by F.N.S. Petro, F. Moses, B. Troöng, B. Eriksson, and E.B. Temu.)

Mnali, S., 2002, Tectonic setting of gabbroic rocks in the western part of the Lupa gold field, south-west Tanzania: Tanzania Journal of Science, v. 28, p. 99–113, https://doi.org/10.4314/tjs.v28i1.18322.

Möller, A., Appel, P., Mezger, K., and Schenk, V., 1995, Evidence for a 2 Ga subduction zone: eclogites in the Usagaran Belt of Tanzania: Geology, v. 23, p. 1067–1070, https://doi.org/10.1130/0091-7613(1995)023<1067:EFAGSZ>2.3.CO;2.

Möller, A., Mezger, K., and Schenk, V., 2000, U-Pb dating of metamorphic minerals: Pan-African metamorphism and prolonged slow cooling of high-pressure granulites in Tanzania, East Africa: Precambrian Research, v. 104, p. 123–146, https://doi.org/10.1016/S0301-9268(00)00086-3.

Mori, K., Tsujimori, T., and Boniface, N., 2018, Finding of talc-and kyanite-bearing amphibolite from the Paleoproterozoic Usagaran belt, Tanzania: Journal of Mineralogical and Petrological Sciences, v. 113, p. 316–321, https://doi.org/10.2465/jmps.180713.

Morris, H.R., 1952, Geological reconnaissance of the Magnetite-bearing belt of Ukinga and Upangwa areas, SW Njombe district: Geological Survey of Tanganyika unpublished report.

Mruma, A.H., 1989, Stratigraphy, Metamorphism and Tectonic Evolution of the Early Proterozoic Usagaran Belt, Tanzania [Ph.D. thesis]: University of Oulu, Finland.

Mruma, A.H., 1995, Stratigraphy and palaeodepositional environment of the Palaeoproterozoic volcano-sedimentary Konse Group in Tanzania: Journal of African Earth Sciences, v. 21, no. 2, p. 281–290, https://doi org/10.1016/0899-5362(95)00065-2.

Mudd, G.C., 1962, Geological map of Ngualla: Dodoma, Geological Survey of Tanzania, Quarter degree geological map sheet series 209, 1:125,000.

Muhongo, S., Tuisku, P., Mnali, S., Temu, E., Appel, P., and Stendal, H., 2002, High-pressure granulite-facies metagabbros in the Ubendian belt of SW Tanzania: Preliminary petrography and P-T estimates, *in* 18th colloquium of African Geology: Oxford, United Kingdom, Pergamon, v. 34, no. 3–4, p. 279–285.

Nanyaro, J.T., Basu, N.K., Muhongo, S.M., Mruma, A.H., Djare, S.A., Mduma, I., Mudiguza, K.M., Van, S.P., and Klerkx, J., 1981, Structural evolution of the Ubendian Belt: preliminary results of a traverse between Karema and Mpanda (Tanzania): Rapport Annuel—Musee Royal de l'Afrique Centrale, v. 1981–1982, p. 147–152.

Nanyaro, J.T., Ishihara, S., Hirano, H., and Sasaki, A., 1983, Precambrian granitoids from two areas in western Tanzania: the Archean Bukoli pluton and the Proterozoic Kate batholith: Bulletin of the Geological Survey of Japan, v. 34, no. 11, p. 535–551.

Newton, R.C., and Perkins, D.I., 1982, Thermodynamic calibration of geobarometers based on the assemblages garnet-plagioclase-orthopyroxene (clinopyroxene)-quartz: The American Mineralogist, v. 67, no. 3–4, p. 203–222.

Orridge, G.R., 1962, Geological map of Kipembawe: Dodoma, Geological Survey of Tanzania, Quarter degree geological map sheet series 210, 1:125,000.

Pinna, P., Muhongo, S., Mcharo, B.A., Le Goff, E., Deschamps, Y., Ralay, F., and Milesi, J.P., 2004, Geology and Mineral map of Tanzania: Bureau de recherches géologiques et minières (BRGM) 1:2,000,000.

Powell, R., and Holland, T.J.B., 1988, An internally consistent dataset with uncertainties and correlations: 3, applications to geobarometry, worked examples and a computer program: Journal of Metamorphic Geology, v. 6, no. 2, p. 173–204, https://doi.org/10.1111/j.1525-1314.1988.tb00415.x.

Priem, H.N.A., Boelrijk, N.A.I.M., Hebeda, E.H., Verdurmen, E.A.Th., Verschure, R.H., Oen, I.S., and Westra L., 1979, Isotopic age determinations on granitic and gneissic rocks from the Ubendian-Usagaran system in southern Tanzania: Precambrian Research, v. 9, p. 227–239, https://doi.org/10.1016/0301-9268(79)90004-4.

Ramadhani, H., and Kamihanda, G., 2014a, Geological map of Lupila: Geological Survey of Tanzania, Geological map, Quarter Degree Sheet 273.

Ramadhani, H.S., and Kamihanda, G., 2014b, Geological map of Kasumulu: Geological Survey of Tanzania, Geological map, Quarter Degree Sheet 272 and 272 W.

Ramadhani, H.S., Kamihanda, G., and Boniface, N., 2015, Explanatory notes of the geology of Kasumulu of QDS 272 and 272W: Geological Survey of Tanzania, 48 p.

Ray, G.E., 1974, The structural and metamorphic geology of northern Malawi: Journal of the Geological Society, v. 130, p. 427–440, https://doi.org/10.1144/gsjgs.130.5.0427.

Reddy, S.M., Collins, A.S., and Mruma, A., 2003, Complex high-strain deformation in the Usagaran Orogen, Tanzania: structural setting of Palaeoproterozoic eclogites: Tectonophysics, v. 375, p. 101–123, https://doi.org/10.1016/S0040-1951(03)00335-4.

Ring, U., 2014, The East African Rift System: Mitteilungen der Österreichischen Geologischen Gesellschaft, v. 107, no. 1, p. 132–146.

Ring, U., Kroener, A., and Toulkeridis, T., 1997, Palaeoproterozoic granulite-facies metamorphism and granitoid intrusions in the Ubendian-Usagaran Orogen of northern Malawi, east-central Africa: Precambrian Research, v. 85, no. 1–2, p. 27–51, https://doi.org/10.1016/S0301-9268(97)00028-4.

Ring, U., Kröner, A., Buchwaldt, R., Toulkeridis, T., and Layer, P.W., 2002, Shear-zone patterns and eclogite-facies metamorphism in the Mozambique Belt of northern Malawi, east-central Africa: implications for the assembly of Gondwana: Precambrian Research, v. 116, no. 1–2, p. 19–56, https://doi.org/10.1016/S0301-9268(01)00233-9.

Rossetti, F., Cozzupoli, D., and Phillips, D., 2008, Compressional reworking of the East African Orogen in the Uluguru Mountains of eastern Tanzania at c. 550 Ma: implications for the final assembly of Gondwana: Terra Nova, v. 20, no. 1, p. 59–67, https://doi.org/10.1111/j.1365-3121.2007.00787.x.

Rubatto, D., 2002, Zircon trace element geochemistry: partitioning with garnet and the link between U-Pb ages and metamorphism: Chemical Geology, v. 184, no. 1–2, p. 123–138, https://doi.org/10.1016/S0009-2541(01)00355-2.

Schandelmeier, H., 1983, The Geochronology of post Ubendian granitoids and dolerites from the Mambwe Area, Northern Province, Zambia: Institute Geological Sciences Report 83/1.

Schenk, V., Boniface, N., and Loose, D., 2006, Paleoproterozoic subduction zones at the margins of the Tanzania and Congo Cratons: Evidence from eclogites with MORB-type chemistry in the Usagaran Ubendian Belts of Tanzania and the Nyong complex of Cameroon, *in* Proceedings, IGCP 509, 9–21 September 2006, Bahia/Minas Gerais, Brazil [abs.]: International Geological Correlation Programme, p. 102–103.

Semyanov, A., Kireev, A., Doronkin, I., and Gavrilov, G., 1970, Geological map of Mpanda: Dodoma, Geological Survey of Tanzania, Geological map of Tanzania, Quarter Degree Sheet 153.

Semyanov, A., Shulyatin, O., and Vaganov, V., 1972a, Geological map of Ninde: Geological Survey of Tanzania, Geological map of Tanzania, Quarter Degree Sheet 205 (remapped in 1988 by B. Troöng and F.N. Makyao).
Semyanov, A., Shulyatin, O., Vaganov, V., Emilyanov, S., and Doronkin, I., 1972b, Geological map of Nkundi: Geological Survey of Tanzania, Geological map of Tanzania, Quarter Degree Sheet 206 (compiled and edited by B. Troöng and F.N. Makyao 1988).
Semyanov, A., Shulyatin, O., Vaganov, V., Emilyanov, S., and Doronkin, I., 1972c, Geological map of Sumbawanga: Dodoma, Geological Survey of Tanzania, Geological map of Tanzania, Quarter Degree Sheet 207.
Sklyarov, E.V., Theunissen, K., Melnikov, A.I., Klerkx, J., Gladkochub, D.P., and Mruma, A., 1998, Paleoproterozoic eclogites and garnet pyroxenites of the Ubende Belt (Tanzania): Schweizerische Mineralogische und Petrographische Mitteilungen, v. 78, p. 257–271.
Smirnov, V., Shulyatin, O., Tolochko, V., Zhukov, S., and Mwakisunga, M., 1970, Geological map of Katuma: Geological Survey of Tanzania, Geological map of Tanzania, Quarter Degree Sheet 152.
Smirnov, V., Shulyatin, O., Tolochko, V., and Zhukov, S., 1971a, Geological map of Karema: Geological Survey of Tanzania, Geological map of Tanzania, Quarter Degree Sheet 169W.
Smirnov, V., Shulyatin, O., Tolochko, V., Zhukov, S., and Mwakisunga, M., 1971b, Geological map of Mwese: Geological Survey of Tanzania, Geological map of Tanzania, Quarter Degree Sheet 151.
Smirnov, V., Pentelkov, V., Tolochko, V., Trifan, M., and Zhukov, S., 1973, Geology and minerals of the central part of the western Rift: Dodoma, Geological Survey of Tanzania, Geological Mapping, Mineral and Resource Division, unpublished report.
Sommer, H., Kröner, A., Muhongo, S., and Hauzenberger, C., 2005, SHRIMP zircon ages for post-Usagaran granitoid and rhyolitic rocks from the Palaeoproterozoic terrain of southwestern Tanzania: South African Journal of Geology, v. 108, p. 247–256, https://doi.org/10.2113/108.2.247.
Stendal, H., Frei, R., Muhongo, S., Rasmussen, T.M., Mnali, S., Petro, F., and Temu, E.B., 2004, Gold potential of the Mpanda Mineral Field, SW Tanzania: evaluation based on geological, lead isotopic and aeromagnetic data: Journal of African Earth Sciences, v. 38, no. 5, p. 437–447, https://doi.org/10.1016/j.jafrearsci.2004.04.005.
Stern, R.J., Tsujimori, T., Harlow, G., and Groat, L.A., 2013, Plate tectonic gemstones: Geology, v. 41, no. 7, p. 723, https://doi.org/10.1130/G34204.1.
Stockley, G.M., 1948, Geology of north, west and central Njombe District, Southern Highlands Province: Geological Survey of Tanganyika Bulletin 18.
Sutton, J., and Watson, J., 1959, Metamorphism in deep-seated zones of transcurrent movement at Kungwe Bay, Tanganyika Territory: The Journal of Geology, v. 67, p. 1–13, https://doi.org/10.1086/626555.
Sutton, J., Watson, J., and James, T., 1954, A Study of the Metamorphic Rocks of Karema and Kungwe Bay, Western Tanganyika: Geological Survey of Tanganyika Bulletin 22.
Tack, L., Liégois, J.P., Deblond, A., and Duchesne, J.C., 1994, Kibaran A-type granitoids and mafic rocks generated by two mantle sources in a late orogenic setting (Burundi): Precambrian Research, v. 68, no. 3–4, p. 323–356, https://doi.org/10.1016/0301-9268(94)90036-1.
Tack, L., Wingate, M.T.D., De Waele, B., Meert, J., Belousova, E., Griffin, B., Tahon, A., and Fernandez-Alonso, M., 2010, The 1375 Ma Kibaran event in Central Africa: Prominent emplacement of bimodal magmatism under extensional regime: Precambrian Research, v. 180, p. 63–84, https://doi.org/10.1016/j.precamres.2010.02.022.
Tamaini, A., Lavreau, J., Lavreau, J., Nanyaro, J., and Yanda, P., 1988, Regional metallogenic analysis in western Tanzania: Mineralization during the first stages of the Lower Proterozoic, *in* Lavreau, J., and Cardinet, C., eds., The UNESCO-IUGS GARS Program in Africa: Image analysis, geological control and radiometric survey of Landsat TM data in Tanzania: Royal Museum for Central Africa, Tervuren, Belgium, v. 96, p. 43–62.
Teale, E., Spurr, A., Harkin, D., and Brown, P., 1958, Geological map of Mbeya: Dodoma, Geological Survey of Tanzania, Geological map of Tanzania, Quarter Degree Sheet 244.
Tenczer, V., Hauzenberger, C.A., Fritz, H., Whitehouse, M.J., Mogessie, A., Wallbrecher, E., Muhongo, S.M., and Hoinkes, G., 2006, Anorthosites in the eastern granulites of Tanzania—New SIMS zircon U-Pb age data, petrography and geochemistry: Precambrian Research, v. 148, p. 85–114, https://doi.org/10.1016/j.precamres.2006.03.004.
Thatcher, E., 1974, The geology of the Nyika area: Geological Survey of Malawi Bulletin 40.
Theunissen, K., Lenoir, J.L., Liegeois, J.P., Delvaux, D., and Mruma, A., 1992, Major Pan-African imprint in the Ubendian Belt of SW Tanzania: U-Pb zircon geochronology and structural context [Empreinte panafricaine majeure dans la chaine ubendienne de Tanzanie sud-occidentale: geochronologie U-Pb sur zircon et contexte structural]: Comptes Rendus Académie des Sciences, Serie II, v. 314, no. 12, p. 1355–1362.
Theunissen, K., Klerkx, J., Melnikov, A., and Mruma, A., 1996, Mechanisms of inheritance of rift faulting in the western branch of the East African Rift, Tanzania: Tectonics, v. 15, p. 776–790, https://doi.org/10.1029/95TC03685.
Thomas, R.J., Spencer, C., Bushi, A.M., Baglow, N., Boniface, N., de Kock, G., Horstwood, M.S., Hollick, L., Jacobs, J., Kajara, S., Kamihanda, G., Key, R.M., Maganga, Z., Mbawala, F., McCourt, W., Momburi, P., Moses, F., Mruma, A., Myambilwa, Y., Roberts, N.M., Saidi, H., Nyanda, P., Nyoka, K., and Millar, I., 2016, Geochronology of the central Tanzania Craton and its southern and eastern orogenic margins: Precambrian Research, v. 277, p. 47–67, https://doi.org/10.1016/j.precamres.2016.02.008.
Thomas, R.J., Jacobs, J., Elburg, M.A., Mruma, A., Kamihanda, G., Kankila, A., Masanja, A., and Saidi, H., 2018, New U-Pb-Hf zircon isotope data for the Paleoproterozoic Ubendian belt in the Chimala area, SW Tanzania. Geoscience Frontiers, v. 10, p. 1993–2006, https://doi.org/10.1016/j.gsf.2018.05.010.
Tolochko, V., Smirnov, V., Zhukov, S., and Stepnov, E., 1972, Geological map of Kasoje: Geological Survey of Tanzania, Geological map of Tanzania, Quarter Degree Sheet 150.
Trifan, M., Beysenov, S., Pentelov, V., Korotkov, V., and Gavrilov, G., 1972, Geological map of Igalukilo: Geological Survey of Tanzania, Geological map of Tanzania, Quarter Degree Sheet 189 (remapped in 1998 by B. Troöng and F.N.S. Petro).
Tsujimori, T., and Ernst, W.G., 2014, Lawsonite blueschists and lawsonite eclogites as proxies for paleo-subduction zone processes: A review: Journal of Metamorphic Geology, v. 32, no. 5, p. 437–454, https://doi.org/10.1111/jmg.12057.
Tulibonywa, T., Manya, S., and Maboko, M.A., 2015, Palaeoproterozoic volcanism and granitic magmatism in the Ngualla area of the Ubendian Belt, SW Tanzania: Constraints from SHRIMP U-Pb zircon ages, and Sm–Nd isotope systematics: Precambrian Research, v. 256, p. 120–130, https://doi.org/10.1016/j.precamres.2014.11.003.
Tulibonywa, T., Manya, S., Torssander, P., and Maboko, M.A., 2017, Geochemistry of the Palaeoproterozoic volcanic and associated potassic granitic rocks of the Ngualla area of the Ubendian Belt, SW Tanzania: Journal of African Earth Sciences, v. 129, p. 291–306, https://doi.org/10.1016/j.jafrearsci.2017.01.022.
Unrug, R., 1984, The Mid-Proterozoic Mporokoso Group of northern Zambia: Stratigraphy, sedimentation and regional position: Precambrian Research, v. 24, no. 2, p. 99–121, https://doi.org/10.1016/0301-9268(84)90053-6.
van Loenen, R., and Kabengele, M., 1962, Geological map of Mkulwe: Dodoma, Geological Survey of Tanzania, Geological map of Tanzania, Quarter Degree Sheet 242 and 242 S.
van Loenen, R., and Kennerley, J., 1962a, Geological map of Kamsamba: Dodoma, Geological Survey of Tanzania, Geological map of Tanzania, Quarter Degree Sheet 226.
van Loenen, R., and Kennerley, J., 1962b, Geological map of Mpui: Dodoma, Geological Survey of Tanzania, Geological map of Tanzania, Quarter Degree Sheet 225.
Van Straaten, V., 1984, Gold mineralization in Tanzania a review, *in* Proceedings, Gold82: The geology, geochemistry and genesis of gold deposits, May 1982: University of Zimbabwe, p. 673–685.
Viola, G., Henderson, I.H.C., Bingen, B., Thomas, R.J., Smethurst, M.A., and de Azavedo, S., 2008, Growth and collapse of a deeply eroded orogen: Insights from structural, geophysical, and geochronological constraints on the Pan-African evolution of NE Mozambique: Tectonics, v. 27, no. 5, TC5009.
Vogt, M., Kröner, A., Poller, U., Sommer, H., Muhongo, S., and Wingate, M., 2006, Archaean and Palaeoproterozoic gneisses reworked during a Neoproterozoic (Pan-African) high-grade event in the Mozambique belt of East Africa: Structural relationships and zircon ages from the Kidatu area, central Tanzania: Journal of African Earth Sciences, v. 45, no. 2, p. 139–155, https://doi.org/10.1016/j.jafrearsci.2006.01.012.
Volodichev, O.I., Slabunov, A.I., Bibikova, E.V., Konilov, A.N., and Kuzenko, T.I., 2004, Archean eclogites in the Belomorian mobile belt, Baltic Shield: Petrology, v. 12, p. 540–560.

Vrána, S., Kachlík, V., Kröner, A., Marheine, D., Seifert, A., Žáček, V., and Babůrek, J., 2004, Ubendian basement and its late Mesoproterozoic and early Neoproterozoic structural and metamorphic overprint in northeastern Zambia: Journal of African Earth Sciences, v.38, no. 1, p. 1–21.

Wadsworth, W.J., Dunham, A.C., and Almohandis, A.A., 1982, Cryptic variation in the Kapalagulu layered intrusion, western Tanzania: Mineralogical Magazine, v. 45, p. 227–236, https://doi.org/10.1180/minmag.1982.045.337.26.

Wakita, K., and Metcalfe, I., 2005, Ocean plate stratigraphy in East and Southeast Asia: Journal of Asian Earth Sciences, v. 24, p. 679–702, https://doi.org/10.1016/j.jseaes.2004.04.004.

Whitney, D.L., and Evans, B.W., 2010, Abbreviations for names of rock-forming minerals: The American Mineralogist, v. 95, p. 185–187, https://doi.org/10.2138/am.2010.3371.

Whittingham, J.K., 1959, Geological map and a brief explanation of the geology of QDS 215, Geological map, Geological Survey Division, Dodoma.

Wilhelmij, H., and Cabri, L., 2016, Platinum mineralization in the Kapalagulu Intrusion, western Tanzania: Mineralium Deposita, v. 51, no. 3, p. 343–367, https://doi.org/10.1007/s00126-015-0603-2.

Windley, B.F., 1995, The Evolving Continents, 3rd edition: New York, Chichester, John Wiley and Sons, 526 p.

Windley, B.F., 1998, Tectonic development of Early Precambrian orogens, *in* Origin and Evolution of Continents: Proceedings of the International Symposium: Tokyo, Japan, Memoirs of the National Institute of Polar Research, Special Issue v. 53, p. 8–28.

Manuscript Accepted by the Society 2 April 2021
Manuscript Published Online xx Month 2021

Printed in the USA